

ABSTRACT

Title of Document: MECHANISTIC-EMPIRICAL DESIGN OF
FLEXIBLE PAVEMENTS: A SENSITIVITY STUDY

Regis L. Carvalho, Master of Science, 2006

Thesis directed by: Dr. Charles W. Schwartz
Department of Civil and Environmental Engineering

Pavement structural design is a daunting task. Traffic loading is a heterogeneous mix of vehicles, axle types and loads with distributions that vary daily and over the pavement design life. Pavement materials respond to these loads in complex ways influenced by stress state and magnitude, temperature, moisture, loading rate, and other factors. Environment exposure adds further complications. It should be no wonder the profession has resorted to largely empirical methods. Developments over recent decades offered an opportunity for more rational and rigorous pavement design procedures. The latest of these accomplishments is the development of the mechanistic-empirical pavement design procedure in NCHRP Project 1-37A. This study presents a comparison of flexible pavement designs between the 1993 AASHTO guide and the NCHRP 1-37A methodology and a sensitivity analysis of the NCHRP 1-37A's input parameters. Recommendations for future studies involving the application and implementation of the new mechanistic-empirical pavement design guide concludes the study.

MECHANISTIC-EMPIRICAL DESIGN OF FLEXIBLE PAVEMENTS: A
SENSITIVITY STUDY

By

Régis Luis Equal de Carvalho

Thesis submitted to the Faculty of the Graduate School of the
University of Maryland, College Park, in partial fulfillment
of the requirements for the degree of
Master of Science
2006

Advisory Committee:

Dr. Charles W. Schwartz, Chair
Professor Deborah J. Goodings
Dr. Dimitrios G. Goulias

©Copyright by

Regis L. Carvalho

2006

DEDICATION

To Ana, my unconditional and inspirational love.

ACKNOWLEDGEMENTS

I would like to acknowledge Dr. Charles Schwartz for his valuable guidance and continuous encouragement throughout this first phase of my graduate studies and for keeping me motivated for the challenges ahead.

I would also like to express my gratitude to Professor Deborah Goodings and Dr. Dimitrios Goulias for serving as committee members and for their support and help. I wish to extend my gratitude to Dr. Ahmet Aydilek and Professor Sherif Aggour for their valuable advices.

I would like to express my sincere appreciation to my friend Mr. Nelson Gibson for his support, especially during the earlier stages of my graduate studies; our friendship extends beyond school boundaries. I am also grateful to Mr. Mehmet Melih Demirkan, Dr. Emin Kutay, and Mr. Haejin Kim for their friendship, for sharing valuable geotechnical discussions and laughs at the geotech/pavements graduate student offices.

Finally, I would like to express my endless gratitude to my family, my brother Arthur, my sisters Nathalia and Lele, and my mother Vitória Regia for their love and support, and especially to my father eng. Luiz Antônio Carvalho, who always encouraged me to pursue my dreams.

TABLE OF CONTENTS

List of Tables.....	v
List of Figures.....	vi
Chapter 1 : Introduction.....	1
Chapter 2 : Review of Flexible Pavement Design Principles.....	4
Chapter 3 : Pavement Design Procedures.....	11
3.1. 1993 AASHTO Guide.....	12
3.1.1. The AASHTO Road Test and Previous Versions of the Guide.....	12
3.1.2. Current Design Equation.....	19
3.1.3. Input Variables.....	21
3.1.4. Reliability.....	26
3.1.5. Considerations and Comments Found in the Literature.....	28
3.2. NCHRP 1-37A Design Procedure.....	31
3.2.1. Design process.....	32
3.2.2. Inputs.....	35
3.2.3. Pavement Response Models.....	43
3.2.4. Empirical Performance Models.....	50
3.2.5. Reliability.....	64
3.2.6. Remarks.....	66
Chapter 4 : Comparative Study between the 1993 AASHTO Guide and the NCHRP 1-37A Procedure.....	67
4.1. Conceptual Differences between 1993 AASHTO Guide and NCHRP 1-37A.....	68
4.2. Description of Pavement Sections.....	73
4.3. General Inputs.....	74
4.4. 1993 AASHTO Designs.....	78
4.5. NCHRP 1-37A Analysis.....	80
4.5.1. Traffic.....	80
4.5.2. Environment.....	80
4.5.3. Material Properties.....	81
4.5.4. Performance Models and Criteria.....	86
4.6. Results.....	87
Chapter 5 : NCHRP 1-37A Performance Prediction Sensitivity to Parameters.....	97
5.1. Thickness.....	97
5.2. Traffic.....	104
5.3. Environment.....	108
5.4. Material Properties.....	111
5.4.1. Asphalt Concrete.....	112
5.4.2. Unbound Materials.....	121
5.5. Empirical Performance Model Calibration.....	125
5.6. Service Life.....	133
Chapter 6 : Case Study: Maryland Designs.....	142
Chapter 7 : Conclusions.....	154
7.1. Summary.....	154
7.2. Principal Findings.....	154
7.3. Implementation Issues.....	160
Chapter 8 : References.....	162

LIST OF TABLES

Table 3.1. Recommended values for Regional Factor R (AASHTO, 1972).....	16
Table 3.2. Ranges of structural layer coefficients (AASHTO, 1972).....	17
Table 3.3. Recommended drainage coefficients for unbound bases and subbases in flexible pavements (Huang, 1993).	26
Table 3.4. Suggested levels of reliability for various highway classes (AASHTO, 1993).....	27
Table 3.5. Z_R values for various levels of reliability (Huang, 1993).	28
Table 3.6. Material inputs requirement for flexible pavements.	39
Table 4.1. Locations and climate conditions.....	74
Table 4.2. Number of axle per truck class and vehicle distribution by traffic level.	77
Table 4.3. Traffic volume.	78
Table 4.4. Base layer coefficient and subgrade resilient modulus.	78
Table 4.5. 1993 AASHTO designs.	79
Table 4.6. Location of designs and environmental data.	81
Table 4.7. Asphalt concrete properties.....	83
Table 4.8. Binder grade by state for low traffic case.	83
Table 4.9. Binder grade by state for moderate and high traffic cases.....	84
Table 4.10. Granular base resilient modulus calculated from the 1993 AASHTO's structural layer coefficient.....	84
Table 4.11. Granular aggregate base properties.....	84
Table 4.12a. Subgrade properties.....	85
Table 5.1. AC mix properties.....	117
Table 6.1. Traffic data for case study.....	144
Table 6.2. I-95 structural designs.....	152
Table 6.3. US-219 structural designs.....	153
Table 6.4. ICC structural designs.....	153

LIST OF FIGURES

Figure 3.1. General procedure for computing thickness.....	20
Figure 3.2. Chart for estimating layer coefficient for asphalt concrete based on elastic modulus (AASHTO, 1993).....	24
Figure 3.3. M-E flexible pavement design flow chart.....	34
Figure 3.4. Summary of schematics for horizontal location of critical response predictions (NCHRP, 2004).....	44
Figure 4.1. Pavement structure.....	73
Figure 4.2. States selected for comparison study.....	73
Figure 4.3. Distribution mass function of single axle loads by vehicle class type.....	75
Figure 4.4. Distribution mass function of tandem axle loads by vehicle class type.....	76
Figure 4.5. Distribution mass function of tridem axle loads by vehicle class type.....	76
Figure 4.6. Granular base thickness design.....	88
Figure 4.7. Asphalt concrete thickness design.....	89
Figure 4.8. NCHRP 1-37A predictions for low traffic scenario.....	91
Figure 4.9. NCHRP 1-37A predictions for moderate traffic scenario.....	91
Figure 4.10. NCHRP 1-37A predictions for high traffic scenario.....	92
Figure 4.11. Summary of 1-37A predictions.....	93
Figure 4.12. “Alligator” fatigue cracking predictions range.....	94
Figure 4.13. Permanent deformation predictions range.....	95
Figure 5.1. Sensitivity to base thickness.....	98
Figure 5.2. MLET calculated horizontal tensile strain versus base thickness.....	99
Figure 5.3. MLET calculated vertical compressive strain versus pavement depth: (a) along the total thickness of the pavement; and (b) only base thickness, in percentage of total base thickness.....	101
Figure 5.4. NCHRP 1-37A rutting predictions versus base thickness.....	102
Figure 5.5. Sensitivity to AC thickness.....	103
Figure 5.6. NCHRP 1-37A rutting predictions versus AC thickness.....	103
Figure 5.7. Rutting performance sensitivity to traffic load type at 15 years.....	105
Figure 5.8. Effect of traffic load type on AC rutting (Basyouny et al., 2005).....	106
Figure 5.9. Fatigue cracking performance sensitivity to traffic load type at 15 years.....	106
Figure 5.10. Class 5 and class 9 percentages for different vehicle distribution scenarios.....	107
Figure 5.11. Performance for different vehicle class distributions.....	108
Figure 5.12. Sensitivity to local climate conditions.....	110
Figure 5.13. Sensitivity to ground water table.....	111
Figure 5.14. Sensitivity of predicted dynamic modulus to mixture inputs. (Schwartz et al., 2006 – in preparation).....	113
Figure 5.15. Sensitivity to binder grade.....	114
Figure 5.16. Sensitivity to effective binder content (% by volume).....	116
Figure 5.17. Sensitivity to air voids.....	116
Figure 5.18. (a) Year seasonal variation of predicted $ E^* $; (b) Sensitivity to AC dense graded mixture type.....	118
Figure 5.19. (a) Sensitivity to AC dense graded mixture and SMA; (b) year seasonal variation of predicted $ E^* $	120
Figure 5.20. Sensitivity to granular base resilient modulus.....	122
Figure 5.21. Multi-layer linear elastic computation of vertical compressive strains versus base M_R	123

Figure 5.22. Multi-layer linear elastic computation of horizontal tensile strain at the bottom of AC layer versus base M_R .	123
Figure 5.23. Sensitivity to subgrade resilient modulus.	124
Figure 5.24. Sensitivity to subgrade type.	125
Figure 5.25. Sensitivity to AC rutting model calibration coefficients.	129
Figure 5.26. Sensitivity to base layer rutting model calibration coefficient.	130
Figure 5.27. Sensitivity to fatigue cracking model calibration coefficients.	132
Figure 5.28. Service life sensitivity to design criterion for different AC thickness: (a) rutting; (b) fatigue cracking.	135
Figure 5.29. Service life sensitivity to design criterion for vehicle distribution: (a) rutting; (b) fatigue cracking.	136
Figure 5.30. Service life sensitivity to design criterion for MD climate conditions: (a) rutting; (b) fatigue cracking.	137
Figure 5.31. Service life sensitivity to design criterion for different binder grade: (a) rutting; (b) fatigue cracking.	138
Figure 5.32. Service life sensitivity to design criterion for different base resilient modulus: (a) rutting; (b) fatigue cracking.	139
Figure 5.33. Service life sensitivity to design criterion for different subgrade resilient modulus: (a) rutting; (b) fatigue cracking.	140
Figure 6.1. M-E flexible pavement design flow chart.	143
Figure 6.2. Vehicle distribution by project.	145
Figure 6.3. Load distribution for the I-95 project.	145
Figure 6.4. Load distribution for the US-219 project.	146
Figure 6.5. Load distribution estimated for the ICC project.	146
Figure 6.6. I-95 project performance predictions.	150
Figure 6.7. US-219 project performance predictions.	151
Figure 6.8. ICC project performance predictions.	151

Chapter 1: Introduction

Pavement structural design is a daunting task. Although the basic geometry of a pavement system is quite simple, everything else is not. Traffic loading is a heterogeneous mix of vehicles, axle types, and axle loads with distributions that vary with time throughout the day, from season to season, and over the pavement design life. Pavement materials respond to these loads in complex ways influenced by stress state and magnitude, temperature, moisture, time, loading rate, and other factors. Exposure to harsh environmental conditions ranging from subzero cold to blistering heat and from parched to saturated moisture states adds further complications. It should be no wonder, then, that the profession has resorted to largely empirical methods like the American Association of State Highway and Transportation Officials (AASHTO) guides for pavement design (AASHTO, 1993).

Several developments over recent decades have offered an opportunity for more rational and rigorous pavement design procedures. Advances in computational mechanics and in the computers available for performing the calculations have greatly improved our ability to predict pavement response to load and climate effects. Improved material characterization and constitutive models make it possible to incorporate nonlinearities, rate effects, and other realistic features of material behavior. Large databases now exist for traffic characteristics, site climate conditions, pavement material properties, and historical performance of in-service pavement sections. These and other assets provided the technical infrastructure that made possible the development of the mechanistic-empirical pavement design procedure in NCHRP Project 1-37A (NCHRP, 2004).

The objectives of this study are (1) to compare flexible pavement designs and performance between the empirical 1993 AASHTO pavement design guide and the mechanistic-empirical NCHRP 1-37A methodology and (2) to perform a sensitivity analysis of the NCHRP 1-37A methodology's input parameters. The comparisons span a range of locations within the United States, each with its own climate, subgrade and other material properties, and local design preferences. Particular emphasis is devoted to the influence of traffic and reliability levels on the comparisons. The sensitivity study is performed for several key input variables. A design exercise consisting of three Maryland projects is presented, from which inferences regarding appropriate design criteria for rutting and bottom-up fatigue cracking are also drawn.

This thesis is divided in seven chapters. The first chapter presents an introduction, the objective of the research, and the description of the chapters.

The second chapter is the literature review of the most relevant pavement design methods. The methods are grouped in two categories, empirical and mechanistic-empirical, attempting to maintain the focus at the research objectives.

The third chapter describes the 1993 AASHTO pavement design guide and the new mechanistic-empirical NCHRP 1-37A procedure, currently under evaluation for adoption as the new standard AASHTO Guide.

The fourth chapter discusses the differences between pavement designs in the 1993 AASHTO guide and the NCHRP 1-37A methodology. Typical 1993 AASHTO designs for five different regions in the U.S. and three traffic levels are analyzed using the latest version of the NCHRP 1-37A software. Comparisons are made based on fatigue

cracking and permanent deformation predictions from the mechanistic-empirical procedure.

The fifth chapter describes the results of the NCHRP 1-37A sensitivity study. The sensitivity study is a parametric evaluation of key inputs and their analysis of reasonableness and consistency with expected field results. The sensitivity is performed for fatigue cracking, permanent deformation and the impact on service life.

The sixth chapter presents application examples of Maryland designs obtained from the Maryland State Highway Administration (MDSHA). Three 1993 AASHTO designs are evaluated using the NCHRP 1-37A methodology.

The seventh chapter presents a summary of conclusions, final remarks and recommendations for future studies involving the application and implementation of the new mechanistic-empirical pavement design guide.

Chapter 2: Review of Flexible Pavement Design Principles

Before the 1920s pavement design consisted basically of defining thicknesses of layered materials that would provide strength and protection to a soft, weak subgrade. Pavements were designed against subgrade shear failure. Engineers used their experience based on successes and failures of previous projects. As experience evolved, several pavement design methods based on subgrade shear strength were developed.

Since then, traffic volume has increased and the design criteria have changed. As important as providing subgrade support, it was equally important to evaluate pavement performance through ride quality and other surface distresses that increase the rate of deterioration of pavement structures. Performance became the focus point of pavement designs. Methods based on serviceability (an index of the pavement service quality) were developed based on test track experiments. The AASHO Road Test in 1960s was a seminal experiment from which the AASHTO design guide was developed.

Methods developed from laboratory test data or test track experiment where model curves are fitted to data are typical examples of empirical methods. Although they may exhibit good accuracy, empirical methods are valid only for the material selection and climate condition in which they were developed.

Meanwhile, new materials started to be used in pavement structures that provided better subgrade protection, but with their own failure modes. New design criteria were required to incorporate such failure mechanisms (e.g., fatigue cracking and permanent deformation in the case of asphalt concrete). The Asphalt Institute method (Asphalt Institute, 1982, 1991) and the Shell method (Claussen et al., 1977; Shook et al., 1982) are

examples of procedures based on asphalt concrete's fatigue cracking and permanent deformation failure modes. These methods were the first to use linear-elastic theory of mechanics to compute structural responses (in this case strains) in combination with empirical models to predict number of loads to failure for flexible pavements.

The dilemma is that pavement materials do not exhibit the simple behavior assumed in isotropic linear-elastic theory. Nonlinearities, time and temperature dependency, and anisotropy are some examples of complicated features often observed in pavement materials. In this case, advanced modeling is required to mechanistically predict performance. The mechanistic design approach is based on the theories of mechanics to relate pavement structural behavior and performance to traffic loading and environmental influences. Progress has been made in recent years on isolated pieces of the mechanistic performance prediction problem. But the reality is that fully mechanistic methods are not yet available for practical pavement design.

The mechanistic-empirical approach is the consolidation of the two sides. Empirical models are used to fill in the gaps that exist between the theory of mechanics and the performance of pavement structures. Simple mechanistic responses are easy to compute with assumptions and simplifications (i.e., homogeneous material, small strain analysis, static loading as typically assumed in linear elastic theory), but they by themselves cannot be used to predict performance directly; some type of empirical model is required to make the appropriate correlation. Mechanistic-empirical methods are considered an intermediate step between empirical and fully mechanistic methods.

The objective of this section is to review briefly some of these advancements in pavement design focusing on flexible pavements. The nomenclature in the literature often

shows several groups of different pavement design methods, mostly according to their origin and development techniques. For simplification, pavement design methods in this study are grouped as empirical and mechanistic-empirical.

Empirical Methods

An empirical design approach is one that is based solely on the results of experiments or experience. Observations are used to establish correlations between the inputs and the outcomes of a process--e.g., pavement design and performance. These relationships generally do not have a firm scientific basis, although they must meet the tests of engineering reasonableness (e.g., trends in the correct directions, correct behavior for limiting cases, etc.). Empirical approaches are often used as an expedient when it is too difficult to define theoretically the precise cause-and-effect relationships of a phenomenon.

The first empirical methods for flexible pavement design date to the mid-1920s when the first soil classifications were developed. One of the first to be published was the Public Roads (PR) soil classification system (Hogentogler & Terzaghi, 1929, after Huang, 2004). In 1929, the California Highway Department developed a method using the California Bearing Ratio (CBR) strength test (Porter, 1950, after Huang, 2004). The CBR method related the material's CBR value to the required thickness to provide protection against subgrade shear failure. The thickness computed was defined for the standard crushed stone used in the definition of the CBR test. The CBR method was improved by U.S. Corps of Engineers (USCE) during the World War II and later became the most popular design method. In 1945 the Highway Research Board (HRB) modified

the PR classification. Soils were grouped in 7 categories (A-1 to A-7) with indexes to differentiate soils within each group. The classification was applied to estimate the subbase quality and total pavement thicknesses.

Several methods based on subgrade shear failure criteria were developed after the CBR method. Barber (1946, after Huang 2004) used Terzaghi's bearing capacity formula to compute pavement thickness, while McLeod (1953, after Huang 2004) applied logarithmic spirals to determine bearing capacity of pavements. However, with increasing traffic volume and vehicle speed, new materials were introduced in the pavement structure to improve performance and smoothness and shear failure was no longer the governing design criterion.

The first attempt to consider a structural response as a quantitative measure of the pavement structural capacity was measuring surface vertical deflection. A few methods were developed based on the theory of elasticity for soil mass. These methods estimated layer thickness based on a limit for surface vertical deflection. The first one published was developed by the Kansas State Highway Commission, in 1947, in which Boussinesq's equation was used and the deflection of subgrade was limited to 2.54 mm. Later in 1953, the U.S. Navy applied Burmister's two-layer elastic theory and limited the surface deflection to 6.35 mm. Other methods were developed over the years, incorporating strength tests. More recently, resilient modulus has been used to establish relationships between the strength and deflection limits for determining thicknesses of new pavement structures and overlays (Preussler and Pinto, 1984). The deflection methods were most appealing to practitioners because deflection is easy to measure in the

field. However, failures in pavements are caused by excessive stress and strain rather than deflection.

After 1950 experimental tracks started to be used for gathering pavement performance data. Regression models were developed linking the performance data to design inputs. The empirical AASHTO method (AASHTO, 1993), based on the AASHO Road Test (1960s), is the most widely used pavement design method today. The AASHTO design equation is a relationship between the number of load cycles, pavement structural capacity, and performance, measured in terms of serviceability. The concept of serviceability was introduced in the AASHTO method as an indirect measure of the pavement's ride quality. The serviceability index is based on surface distresses commonly found in pavements.

The biggest disadvantage of regression methods is the limitation on their application. As any empirical method, regression methods can be applied only to the conditions at the road test site in which they were developed. The AASHTO method, for example, was adjusted several times over the years to incorporate extensive modifications based on theory and experience that allowed the design equation to be used under conditions other than those of the AASHO Road Test.

Regression equations can also be developed using performance data from existing pavements, such as the COPES (Darter et al., 1985) and EXPEAR (Hall et al., 1989) systems. Although these models can represent and explain the effects of several factors on pavement performance, their limited consideration of materials and construction data result in wide scatter and many uncertainties. Their use as pavement design tools is therefore very limited.

Mechanistic-Empirical Methods

Mechanistic-Empirical methods represent one step forward from empirical methods. The induced state of stress and strain in a pavement structure due to traffic loading and environmental conditions is predicted using theory of mechanics. Empirical models link these structural responses to distress predictions. Kerkhoven & Dormon (1953) first suggested the use of vertical compressive strain on the top of subgrade as a failure criterion to reduce permanent deformation. Saal & Pell (1960) published the use of horizontal tensile strain at the bottom of asphalt layer to minimize fatigue cracking. Dormon & Metcalf (1965) first used these concepts for pavement design. The Shell method (Claussen et al., 1977) and the Asphalt Institute method (Shook et al., 1982; AI, 1992) incorporated strain-based criteria in their mechanistic-empirical procedures.

Several studies over the past fifteen years have advanced mechanistic-empirical techniques. Most of work, however, was based on variants of the same two strain-based criteria developed by Shell and the Asphalt Institute. The Departments of Transportation of the Washington State (WSDOT), North Carolina (NCDOT) and Minnesota (MNDOT), to name a few, developed their own M-E procedures. The National Cooperative Highway Research Program (NCHRP) 1-26 project report, *Calibrated Mechanistic Structural Analysis Procedures for Pavements* (1990), provided the basic framework for most of the efforts attempted by state DOTs. WSDOT (Pierce et al., 1993; WSDOT, 1995) and NCDOT (Corley-Lay, 1996) developed similar M-E frameworks incorporating environmental variables (e.g., asphalt concrete temperature to determine stiffness) and cumulative damage model using Miner's Law with the fatigue cracking criterion.

MNDOT (Timm et al., 1998) adopted a variant of the Shell's fatigue cracking model developed in Illinois (Thompson, 1985) and the Asphalt Institute's rutting model.

The NCHRP 1-37A project (NCHRP, 2004) delivered the most recent M-E-based method that incorporates nationally calibrated models to predict distinct distresses induced by traffic load and environmental conditions. The NCHRP 1-37A methodology also incorporates vehicle class and load distributions in the design, a step forward from the Equivalent Single Axle Load (ESAL) used in the AASHTO design equation and other methods. The performance computation is done on a seasonal basis to incorporate the effects of climate conditions on the behavior of materials.

The NCHRP 1-37A methodology is the main focus of this study. A complete description of its components, key elements, and use is presented in Chapter 3. Chapter 3 also includes a complete review of the 1993 AASHTO Guide and its previous versions. The comparison of the empirical 1993 AASHTO Guide and the mechanistic-empirical NCHRP 1-37A procedure, which is one of the objectives of this study, is presented in Chapter 4.

Chapter 3: Pavement Design Procedures

The current 1993 AASHTO Guide and the new mechanistic-empirical NCHRP 1-37A procedure for flexible pavements are described in this chapter. The 1993 AASHTO is the latest version of AASHTO Guide for pavement design and analysis, which is based primarily on the AASHO Road Test conducted in the late 1950s. Over the years adjustments and modifications have been made in an effort to upgrade and expand the limits over which the AASHTO guide is valid (HRB, 1962; AASHTO, 1972, 1986, 1993).

The Federal Highway Administration's 1995-1997 National Pavement Design Review found that some 80 percent of states use one of the versions of the AASHTO Guide. Of the 35 states that responded to a 1999 survey by Newcomb and Birgisson (1999), 65 percent reported using the 1993 AASHTO guide for both flexible and rigid pavement designs.

A 1996 workshop meant to develop a framework for improving the 1993 Guide recommended instead the development of a new guide based as much as possible on mechanistic principles. The NCHRP 1-37A procedure is the result of this effort. Following independent reviews and validations that have been ongoing since its initial release in April, 2004, the NCHRP 1-37A procedure is expected to be adopted by AASHTO as the new national pavement design guide.

This chapter is divided in two sections. The first describes the AASHTO Guide and its revisions since its first edition dated 1961, with the original empirical equations

derived from the AASHO Road Test, to its latest dated 1993¹ (HRB, 1961, 1962; AASHTO, 1972, 1986, 1993). The second part explains in some detail the new mechanistic-empirical NCHRP 1-37A pavement design procedure (NCHRP, 2004).

3.1. 1993 AASHTO Guide

The 1993 AASHTO Guide is the latest version of the AASHTO Interim Pavement Design Guide, originally released in 1961. The evolution of the AASHTO Guide is outlined, followed by a description of the current design equation and input variables. At the end of this section, a summary of recent evaluation studies of the AASHTO guide is also presented.

3.1.1. The AASHO Road Test and Previous Versions of the Guide

After two successful road projects, the Road Test One-MD and the WASHO Road Test (Western Association of State Highway Officials), in 1955 the Highway Research Board (HRB) approved the construction of a new test track project located in Ottawa, Illinois. This test facility was opened to traffic in 1958. Traffic operated on the pavement sections until November, 1960, and a little more than 1 million axle loads were applied to the pavement and bridges. (HRB, 1961)

¹ The supplement of the 1993 AASHTO Guide, released in 1998 (AASHTO, 1998), substantially modified the rigid pavement design procedure, based on recommendations from NCHRP Project 1-30 and studies conducted using the LTPP database. However this supplement is not addressed in this thesis because it is solely related to rigid pavements.

The main objective of the AASHO Road Test was to determine the relation between the number of repetitions of specified axle loads (different magnitudes and arrangements) and the performance of different flexible and rigid pavement structures.

The test track consisted of 6 loops, each with a segment of four-lane divided highway (two lanes per direction) whose parallel roadways were connected with a turnaround at both ends. Five loops were trafficked and loop 1 received no traffic during the entire experiment. Test sections were located only on tangents separated by a short transition lengths. The inner and outer lane had identical pavement sections. Each lane had its own assigned traffic level. The subgrade was identified as a fine grained silty clay (A-6 or A-7-6 according to the AASHTO soil classification). For uniformity purposes, the top 3 ft of the embankment consisted of a borrowed A-6 soil from areas along the right-of-way of the project. The climate was temperate (average summer temperature of 76 °F and 27 °F in winter, annual precipitation of 34 inches) with frost/thaw cycles during the winter/spring months. (HRB, 1962)

The Concept of Serviceability and Structural Number

The performance of various pavements is a function of their relative ability to serve traffic over a period of time. This definition of “relative” performance was stated in Appendix F of the HRB Special Report 61E that described the findings of the pavement research at the AASHO Road Test (HRB, 1962). It goes further stating: “At the time, there were no widely accepted definitions of performance and therefore, a “relative” performance definition should be used instead.”

The concept of serviceability is supported by five fundamental assumptions: (1) highways are for the comfort of the traveling user; (2) the user's opinion as to how a highway should perform is highly subjective; (3) there are characteristics that can be measured and related to user's perception of performance; (4) performance may be expressed by the mean opinion of all users; and (5) performance is assumed to be a reflection of serviceability with increasing load applications.

Based on these assumptions the definition of present serviceability is: "The ability of a specific section of pavement to serve high speed, high volume, and mixed traffic in its existing condition." (HRB, 1962) The Present Serviceability Ratio (PSR) is the average of all users' ratings of a specific pavement section on a scale from 5 to 0 (being 5 very good and 0 very poor). The mathematical correlation of pavement distresses observed during visual surveys and profile measurements (roughness) with PSR is termed the Present Serviceability Index (PSI); PSI is the measure of performance in the AASHTO design equation. The correlation between PSI and typical flexible pavement distresses observed during the AASHTO Road Test is represented by the following equation (HRB, 1962):

$$PSI = 5.03 - 1.91 \cdot \log(1 + \overline{SV}) - 1.38 \overline{RD}^2 - 0.01 \sqrt{C + P} \quad (3.1)$$

in which:

SV = mean of slope variance in the wheelpaths

RD = mean rut depth (in)

C = cracking (ft²/1000 ft²)

P = patching (ft²/1000 ft²)

1961 Interim Guide

The first results from data collected at the AASHO Road Test were released in the form of Highway Research Board reports (HRB, 1961, 1962). The original design equation was empirically developed for the specific subgrade type, pavement materials and environmental conditions at the location of the AASHO Road Test as follows:

$$\log(W_{18}) = 9.36 \cdot \log(SN + 1) - 0.20 + \frac{\log(4.2 - p_t)/(4.2 - 1.5)}{0.4 + 1094/(SN + 1)^{5.19}} \quad (3.2)$$

in which:

W_{18} = accumulated 18 kip equivalent single axle load for the design period

p_t = terminal serviceability at the end of design life

SN = structural number

The structural number (SN) is the parameter that represents the pavement structural strength. It is given as the sum of the product of each layer thickness by its structural layer coefficient, which is an empirical coefficient representing each layer's relative contribution to the pavement strength:

$$SN = a_1 D_1 + a_2 D_2 + a_3 D_3 \quad (3.3)$$

in which:

a_1, a_2, a_3 = structural layer coefficients for surface, base, and subbase

D_1, D_2, D_3 = thicknesses for surface, base, and subbase

The Equation (3.2) is solved for the structural number for a given traffic and terminal serviceability criterion. The layer thicknesses are determined from Equation (3.3). Note that there is not a unique solution for the layer thicknesses.

1972 Interim Guide

The 1972 Interim Design Guide was the first attempt to extend the empirical relationships developed at the AASHO Road Test to a broader range of materials and environmental conditions. This version also included the first step towards an overlay design procedure. Some of the added features for flexible pavement designs are described below.

An empirical soil support (S_i) scale was developed to reflect the influence of different local subgrade soils in Equation (3.2). The scale ranged from 1 to 10, with 10 corresponding to crushed stone materials and 1 to highly plastic clays. The A-6 subgrade soil at the AASHO Road Test was defined as S_i value of 3. All other values were to be set by local agency experience, but there were no guidelines on how to determine these values.

There was also a new regional factor R for adjusting the structural number for local environment, estimated from serviceability loss rates in the AASHO Road Test. These values varied between 0.2 and 5.0, with an annual average of about 1.0. Table 3.1 summarizes the recommended values for R.

Table 3.1. Recommended values for Regional Factor R (AASHTO, 1972).

Roadbed material condition	R
Frozen to depth of 5'' or more (winter)	0.2 – 1.0
Dry (summer and fall)	0.3 – 1.5
Wet (spring thaw)	4.0 – 5.0

The 1972 Interim Guide also specified ranges for structural layer coefficients applicable to materials other than those used during the AASHO Road Test. The values were based on a survey of state highway agencies that were using the 1961 Interim Guide. Table 3.2 summarizes these values for different layer applications.

Table 3.2. Ranges of structural layer coefficients (AASHTO, 1972).

Coefficient	Range
a ₁ (surface course)	0.17 – 0.45
a ₂ (untreated base)	0.05 – 0.18
a ₃ (subbase)	0.05 – 0.14

Equation (3.2) was modified to account for the new input terms:

$$\log(W_{18}) = 9.36 \cdot \log(SN + 1) - 0.20 + \frac{\log(4.2 - p_t)/(4.2 - 1.5)}{0.4 + 1094/(SN + 1)^{5.19}} + \log \frac{1}{R} + 0.372(S_i - 3) \quad (3.4)$$

in which:

R = regional factor

S_i = soil support value

and other terms are as previously defined

1986 and 1993 Guides

The 1986 revision of the 1972 Interim Guide added more features to the design procedure. The focus was on four important issues: (1) better characterization of the subgrade and unbound materials, (2) incorporation of pavement drainage, (3) better consideration of environmental effects, and (4) incorporation of reliability as a factor into the design equation.

In the 1986 version of the AASHTO Guide, the subgrade was for the first time characterized by its resilient modulus M_R , a fundamental engineering material property. The structural layer coefficients for unbound materials were also related quantitatively to resilient modulus by empirical equations.

Drainage quality was incorporated in the design process by introducing empirical drainage coefficients into the structural number equation. Equation (3.3) becomes:

$$SN = a_1D_1 + a_2D_2m_2 + a_3D_3m_3 \quad (3.5)$$

in which:

m_2, m_3 = drainage coefficients for base and subbase

and other terms are as previously defined

Recommended values for the drainage coefficients are defined based on the quality of drainage and period of exposure to moisture levels near saturation.

Environmental effects were also considered in two additional distinct ways: (1) separation of total serviceability losses into traffic and environmental components, and (2) estimation of an effective subgrade resilient modulus that reflects seasonal variations due primarily to moisture susceptibility. The loss in serviceability ΔPSI was decomposed into three components:

$$\Delta PSI = \Delta PSI_{TR} + \Delta PSI_{SW} + \Delta PSI_{FH} \quad (3.6)$$

in which:

$\Delta PSI_{TR}, \Delta PSI_{SW}, \Delta PSI_{FH}$ = components attributed to traffic, swelling and frost heave, respectively

Appendix G in the 1986 AASHTO Guide describes in more detail the methods for evaluating these environmental losses, which depend on the swell/frost heave rate, probability of swell/frost heave, and maximum potential serviceability loss.

Reliability was introduced into the 1986 AASHTO Guide to account for the effects of uncertainty and variability in the design inputs. Although it represents the

uncertainty of all inputs, it is very simply incorporated in the design equation through factors that modify the allowable design traffic (W_{18}).

There were few changes to the flexible pavement design procedure between the 1986 version and the current 1993 version. Most of the enhancements were geared towards rehabilitation, the use of nondestructive testing for evaluation of existing pavements, and backcalculation of layer moduli for determination of the layer coefficients. The design equation did not change from the 1986 to 1993 version. The complete description of the 1993 AASHTO Guide is presented in the following subsections.

3.1.2. Current Design Equation

The 1993 AASHTO Guide specifies the following empirical design equation for flexible pavements:

$$\log(W_{18}) = Z_R \cdot S_0 + 9.36 \cdot \log(SN + 1) - 0.20 + \frac{\log(\Delta PSI)/(4.2 - 1.5)}{0.4 + 1094/(SN + 1)^{5.19}} + 2.32 \cdot \log(MR) - 8.07 \quad (3.7)$$

in which:

W_{18} = accumulated 18 kip equivalent single axle load for the design period

Z_R = reliability factor

S_0 = standard deviation

SN = structural number

ΔPSI = initial PSI – terminal PSI

M_R = subgrade resilient modulus (psi)

The solution of Equation (3.7) follows the same procedure described before for the previous versions of the Guide. Given all the inputs Equation (3.7) is solved for the structural number (SN) and then the layer thicknesses can be computed. The solution is not unique and different combination of thicknesses can be found. Additional design constraints, such as costs and constructability, must also be considered to determine the optimal final design. The 1993 Guide recommends the top-to-bottom procedure in which each of the upper layers is designed to provide adequate protection to the underlying layers. Figure 3.1 illustrates the procedure for a 3-layer flexible pavement. The steps in this case are as follows:

- Calculate SN_1 required to protect the base, using E_2 as M_R in Equation (3.7), and compute the thickness of layer 1 as:

$$D_1 \geq \frac{SN_1}{a_1} \quad (3.8)$$

- Calculate SN_2 required to protect the subgrade, using Equation (3.7), now with the subgrade effective resilient modulus as M_R . The thickness of the base is computed as:

$$D_2 \geq \frac{SN_2 - a_1 D_1}{a_2 m_2} \quad (3.9)$$

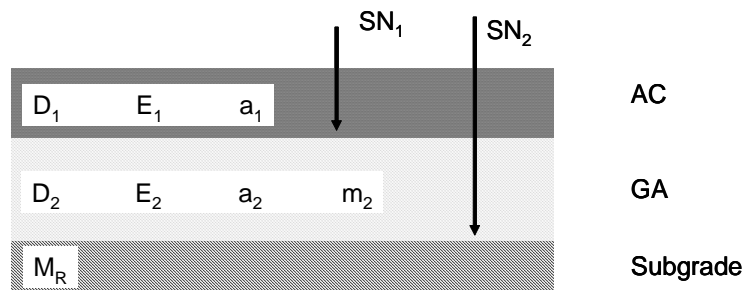


Figure 3.1. General procedure for computing thickness.

3.1.3. Input Variables

The input variables required for the 1993 AASHTO guide are summarized in this section and the most important recommendations are described. Additional guidance can be found in the literature (AASHTO, 1993; Huang, 2004).

Design period and serviceability loss are the initial inputs to be defined. Serviceability loss is defined as the difference between initial and terminal serviceability. Initial serviceability is the condition immediately after pavement construction. The conventional value is 4.2 (the average initial serviceability value at the AASHO Road Test). Terminal serviceability is the value at which the pavement is no longer capable of providing adequate service and major rehabilitation is required. Most state agencies have their own specification, although the 1993 AASHTO Guide recommends a terminal PSI of 2.5 for major highways and 2.0 for low volume roads, unless otherwise specified.

The other input variables are separated into three groups: (a) traffic, (b) material properties, and (c) environmental effects.

Traffic

Vehicle and load distributions grouped by axle type are used to transform mixed traffic into a unified traffic parameter that can be used in the design equation. The mixed traffic is converted into one parameter called the Equivalent Single Axle Load (ESAL). ESAL is defined as the number of 18-kip single axles that causes the same pavement damage as caused by the actual mixed axle load and axle configuration traffic. The damage associated with the equivalent axle can be defined in numerous ways; in the 1993 AASHTO Guide it is defined in terms of serviceability. The 18-kip single axle load was

chosen because it was the maximum legal load permitted in many states at the time of the AASHO Road Test (Zhang et al., 2000).

The first step in calculating ESALs for mixed traffic is to establish first the load equivalent factor (LEF) of every axle of the traffic distribution. In the 1993 AASHTO Guide, LEFs were developed based on empirical data obtained from the AASHO Road Test. The AASHTO LEFs consider the following variables:

- Axle load
- Axle configuration (e.g., single, tandem, etc.)
- Structural number (for flexible pavements)
- Terminal serviceability

The computation of LEFs for flexible pavements is based on the following equations (Huang, 2004):

$$LEF = \frac{W_{t18}}{W_{tx}} \quad (3.10a)$$

$$\log\left(\frac{W_{tx}}{W_{t18}}\right) = 4.79 \log(18+1) - 4.79 \log(L_x - L_2) + 4.33 \log L_2 + \frac{G_t}{\beta_x} - \frac{G_t}{\beta_{18}} \quad (3.10b)$$

$$G_t = \log\left(\frac{4.2 - p_t}{4.2 - 1.5}\right) \quad (3.10c)$$

$$\beta_x = 0.40 + \frac{0.081(L_x + L_2)^{3.23}}{(SN + 1)^{5.19} L_2^{3.23}} \quad (3.10d)$$

in which:

W_{tx} = number of x-axle load applications applied over the design period

W_{t18} = number of equivalent 18-kip (80 kN) single axle load applications

over the design period

L_x = load on one single axle, or a set of tandem or tridem, in kip

L_2 = axle code (1 for single axle, 2 for tandem, and 3 for tridem)

SN = structural number of the designed pavement

p_t = terminal serviceability

$\beta_{18} = \beta_x$ for $L_x = 18$ kip and $L_2 = 1$

With LEF calculated for every load group, the second step is to compute the truck factor T_f as follows:

$$T_f = \sum_i (p_i \times LEF_i) \times A \quad (3.11)$$

in which:

p_i = percentage of repetitions for i^{th} load group

LEF_i = LEF for the i^{th} load group (e.g., single-12kip, tandem-22kip, etc.)

A = average number of axles per truck

The number of *ESALs* is calculated as follows:

$$ESAL = AADT \times T \times T_f \times G \times D \times L \times 365 \times Y \quad (3.12)$$

in which:

$AADT$ = annual average daily traffic

T = percentage of trucks

G = growth factor

D = trucks in design direction (%)

L = trucks in design lane (%)

Y = design period

Material properties

The fundamental material property in the 1993 AASHTO Guide is the resilient modulus. Since the framework was constructed based upon structural layer coefficients, empirical relationships were developed to correlate resilient modulus with structural layer coefficient. Figure 3.2 summarizes the relationship for the layer coefficient a_1 for asphalt concrete. Figure 3.2 summarizes the relationship for the layer coefficient a_1 for asphalt concrete.

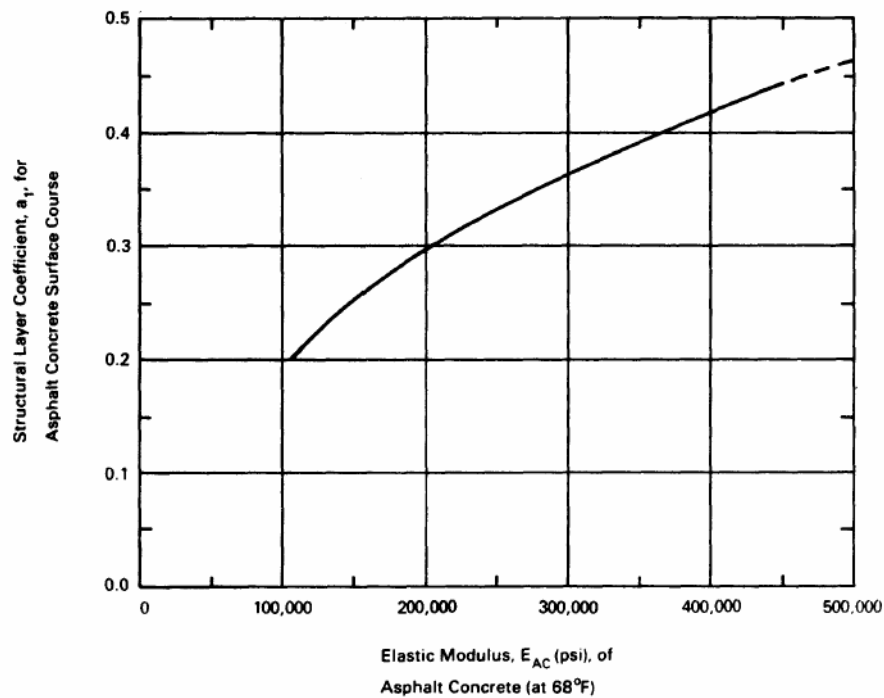


Figure 3.2. Chart for estimating layer coefficient for asphalt concrete based on elastic modulus (AASHTO, 1993)

The layer coefficient a_2 for nonstabilized base materials is given by:

$$a_2 = 0.249 \log E_2 - 0.977 \quad (3.13)$$

and the layer coefficient a_3 for nonstabilized subbase materials is given by:

$$a_3 = 0.227 \log E_3 - 0.839 \quad (3.14)$$

in which:

E_2 = resilient modulus of unbound base layer materials

E_3 = resilient modulus of unbound subbase layer materials

The layer coefficients in the AASHO Road Test were assumed equal to 0.44 for asphalt concrete, which corresponds to a $M_R = 450,000$ psi; 0.14 for the granular base, corresponding to $M_R = 30,000$ psi; and 0.11 for the subbase, equivalent to $M_R = 15,000$ psi.

The subgrade is characterized solely by its resilient modulus in Equation (3.7). There are also several correlations between M_R and other soil properties that can be found in the literature. Most of them relate M_R to CBR or R-Value (Heukelom and Klomp, 1962; Asphalt Institute, 1982; Van Til et al., 1972 – after Huang, 1993; NCHRP, 2004).

Environmental Effects

Environmental effects (other than swelling and frost heave) are accounted for in two input parameters in the 1993 AASHTO Guide, the seasonally-adjusted subgrade resilient modulus and the drainage coefficient m_i applied to the structural number in Equation (3.5).

It is recommended that an effective subgrade resilient modulus be used to represent the effect of seasonal variations, especially for moisture-sensitive fine-grained soils or for locations with significant freeze-thaw cycles (AASHTO, 1993). The effective resilient modulus is the equivalent modulus that would result in the same damage to the pavement as if seasonal modulus were used. The relative damage u_r is describe by the following empirical relationship:

$$u_r = 1.18 \times 10^8 M_R^{-2.32} \quad (3.15)$$

The average relative damage (u_f) is computed by taking the average of u_r of all seasons. The effective subgrade resilient modulus is then given by:

$$M_R = 3015 \cdot u_f^{-0.431} \quad (3.16)$$

The drainage coefficient is related to the material's permeability and the amount of time that the material is expected to be at near saturation conditions. Table 3.3 shows recommended drainage coefficients for unbound materials. However, in practice it is difficult to assess the quality of drainage or the percentage of time the material is exposed to near saturation conditions, and most agencies use drainage coefficient values of 1.0, relying mostly on the effective subgrade resilient modulus as the climatic-sensitive input parameter².

Table 3.3. Recommended drainage coefficients for unbound bases and subbases in flexible pavements (Huang, 1993).

Quality of drainage		Percentage of time pavement structure exposed to moisture levels approaching saturation			
Rating	Water removed within	Less than 1%	1-5%	5-25%	Greater than 25%
Excellent	2 hours	1.40-1.35	1.35-1.30	1.30-1.20	1.20
Good	1 day	1.35-1.25	1.25-1.15	1.15-1.00	1.00
Fair	1 week	1.25-1.15	1.15-1.05	1.00-0.80	0.80
Poor	1 month	1.15-1.05	1.05-0.80	0.80-0.60	0.60
Very poor	Never drain	1.05-0.95	0.95-0.75	0.75-0.40	0.40

3.1.4. Reliability

There are many sources for uncertainties in pavement design problems – e.g., traffic prediction, material characterization and behavior modeling, environmental

² In the survey done with 5 states for the sensitivity analysis presented in Chapter 4, all of them responded that their drainage coefficient were equal to 1.0.

conditions, etc. – as well as variability during construction and maintenance. The uncertainty comes not only from data collection, but also from the lack of input parameters required to better characterize traffic, materials and environmental conditions. The reliability factor was introduced in the design equation to account for these uncertainties.

Reliability is defined as the probability that the design pavement will achieve its design life with serviceability higher than or equal to the specified terminal serviceability. Although the reliability factor is applied directly to traffic in the design equation, it does not imply that traffic is the only source of uncertainty.

Table 3.4 suggests appropriate levels of reliability for various highway classes. There is some guidance on how reliability is considered. High volume and high speed highways have higher reliability factors than minor roads and local routes. The standard deviation (S_0) and reliability factor (Z_R) parameters in the design equation are respectively defined as the standard deviation of uncertainties and the area under a normal distribution curve for $p \leq$ reliability. The parameter Z_R can be retrieved from Table 3.5. The 1993 AASHTO Guide recommends values for S_0 between 0.35 and 0.45 for flexible pavements.

Table 3.4. Suggested levels of reliability for various highway classes (AASHTO, 1993).

Functional classification	Recommended level of reliability	
	Urban	Rural
Interstate and freeways	85-99.9	80-99.9
Principal arterials	80-99	75-95
Collectors	80-95	75-95
Locals	50-80	50-80

Table 3.5. Z_R values for various levels of reliability (Huang, 1993).

Reliability	Z_R	Reliability	Z_R
50	0.000	93	-1.476
60	-0.253	94	-1.555
70	-0.524	95	-1.645
75	-0.674	96	-1.751
80	-0.841	97	-1.881
85	-1.037	98	-2.054
90	-1.282	99	-2.327
91	-1.340	99.9	-3.090
92	-1.405	99.99	-3.750

3.1.5. Considerations and Comments Found in the Literature

Several researchers have studied the AASHTO Guide in all its versions. This section summarizes the relevant findings gathered from the literature that discuss conflicting issues such as traffic, material properties, environmental conditions, and parametric sensitivity of the design equation.

Serviceability cannot be directly measured in the field. A panel of users is required to provide subjective assessments of serviceability. This value is the Present Serviceability Ratio (PSR). The correlation of PSR with measured distresses is the Present Serviceability Index (PSI). PSI is the input parameter of the design equation, not the PSR, because determining PSR is very subjective, not to mention expensive and time consuming. Alternative approaches are available correlating PSI with roughness, which is a more reliable, and more easily measured parameter than the recommended distresses given in Equation (3.1) (Al-Omari and Darter, 1994; Gulen et al., 1994).

Traffic has been a controversial parameter in the 1993 AASHTO Guide and its earlier versions. The fact that it relies on a single value to represent the overall traffic spectrum is questionable. The method used to convert the traffic spectra into ESALs by

applying LEFs is also questionable. The AASHTO LEFs consider serviceability as the damage equivalency between two axles. Zhang et al. (2000) have found that Equations 3.10, used to determine LEFs, are also capable of capturing damage in terms of equivalent deflection, which is easier to measure and validate. However quantifying damage equivalency in terms of serviceability or even deflections is not enough to represent the complex failure modes of flexible pavements.

Several studies were conducted to investigate effects of different load types and magnitudes on damage of pavement structures using computed mechanistic pavement responses (Sebaaly and Tabatabaee, 1992; Zaghoul and White, 1994). Hajek (1995) proposed a general axle load equivalent factor – independent from pavement-related variables and axle configurations, based only on axle load – suitable for use in pavement management systems and simple routine design projects.

Today it is widely accepted that load equivalency factors are a simple technique for incorporating mixed traffic into design equations and are well suited for pavement management systems. However pavement design applications require more comprehensive procedures. Mechanistic-empirical design procedures take a different approach for this problem; different loads and axle geometrics are mechanistically analyzed to determine directly the most critical structural responses that are significant to performance predictions, avoiding the shortcut of load equivalency factors.

Layer coefficients have also been of interest to those developing and enhancing pavement design methods. Several studies have been conducted to find layer coefficients for local and new materials (Little, 1996; Richardson, 1996; MacGregor et al., 1999). Coree and White (1990) presented a comprehensive analysis of layer coefficients and

structural number. They showed that the approach was not appropriate for design purposes. Baladi and Thomas (1994), through a mechanistic evaluation of 243 pavement sections designed with the 1986 AASHTO guide, demonstrated that the layer coefficient is not a simple function of the individual layer modulus, but a function of all layer thicknesses and properties.

There are several studies in the literature of the environmental influences in the AASHTO method. There are two main environmental factors that impact service life of flexible pavements: moisture and temperature. The effect of moisture on subgrade strength has been well documented in past years and uncountable publications about temperature effects on asphalt concrete are available. Basma and Al-Suleiman (1991) suggested using empirical relations between moisture content and resilient modulus directly in the design Equation (3.7). The variation of the structural number with moisture content was defined as ΔSN and was used to adjust the calculated SN . Basma and Al-Suleiman (1991) also suggested using a nomograph containing binder and mixture properties to determine the layer coefficient for asphalt concrete layer. Noureldin et al. (1996) developed an approach for considering temperature effects in the 1993 AASHTO design equation. In their approach, the mean annual pavement temperature is used to compute temperature coefficients that modify the original asphalt concrete layer coefficient used to compute the structural number.

The 1993 AASHTO Guide and its earlier versions were developed based on results from one test site trafficked over two years with a total of slightly over one million ESALs. From this test track, which was built with the same materials varying only thicknesses, the design equation was developed. Studies have shown that despite of the

adjustments made over the years to the design equation in attempts to expand its suitability to different climate regions and materials, the design of flexible pavements still lacks accuracy in performance predictions and in ability to include different materials and their complex behavior.

3.2. NCHRP 1-37A Design Procedure

The NCHRP 1-37A procedure is a mechanistic-empirical (M-E) method for designing and evaluating pavement structures. Structural responses (stresses, strains and deflections) are mechanistically calculated based on material properties, environmental conditions, and loading characteristics. These responses are used as inputs in empirical models to compute distress performance predictions.

The NCHRP 1-37A procedure was developed under a research project funded by the National Cooperative Highway Research Program (NCHRP) and released in draft form in April, 2004 (NCHRP, 2004).

The NCHRP 1-37A still depends on empirical models to predict pavement performance from calculated structural responses and material properties. The accuracy of these models is a function of the quality of the input information and the calibration of empirical distress models to observed field performance. Two types of empirical models are used in the NCHRP 1-37A. One type predicts the magnitude of the distress accumulation directly (e.g., rutting model for flexible pavements, and faulting for rigid); the other type predicts first the number of load applications to failure (i.e., given a specific load and climate condition) which is then empirically related to the distress

accumulation (e.g., fatigue cracking for flexible pavements, and transverse cracking for rigid).

This section briefly describes the NCHRP 1-37A procedure. A description of the design process is provided, followed by information about the components of the design procedure: inputs (design criteria, traffic, material properties, and environmental conditions), pavement response models (mechanistic structural computational tools and climate model), empirical performance models, and reliability.

3.2.1. Design process

The NCHRP 1-37A design process is not as straightforward as the 1993 AASHTO guide, in which the structure's thicknesses are obtained directly from the design equation. Instead an iterative process is used in which predicted performance of selected pavement structure is compared against the design criteria as shown in Figure 3.3. The structure and/or material selection are adjusted until a satisfactory design is achieved. A step-by-step description is as follows:

- Definition of a trial design for specific site conditions: subgrade support, material properties, traffic loading, and environmental conditions;
- Definition of design criteria for acceptable pavement performance at the end of the design period (i.e., acceptable levels of rutting, fatigue cracking, thermal cracking, and roughness);
- Selection of reliability level for each one of the distresses considered in the design;

- Calculation of monthly traffic loading and seasonal climate conditions (temperature gradients in asphalt concrete layers, moisture content in unbound granular layers and subgrade);
- Modification of material properties in response to environmental conditions;
- Computation of structural responses (stresses, strains and deflections) for each axle type and load and for each time step throughout the design period;
- Calculation of predicted distresses (e.g., rutting, fatigue cracking) at the end of each time step throughout the design period using the calibrated empirical performance models;
- Evaluation of the predicted performance of the trial design against the specified reliability level. If the trial design does not meet the performance criteria, the design (thicknesses or material selection) must be modified and the calculations repeated until the design is acceptable.

The NCHRP 1-37A procedure is implemented in software in which all of above steps are performed automatically, except for the pavement structure and material selection.

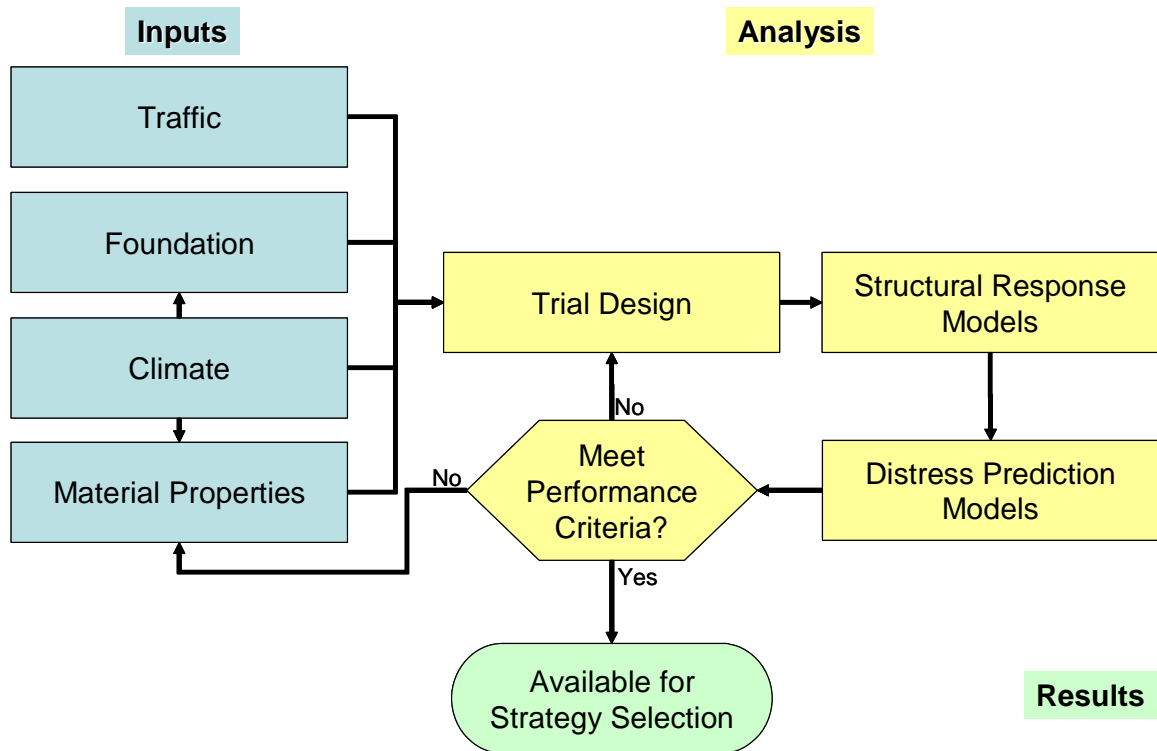


Figure 3.3. M-E flexible pavement design flow chart.

The NCHRP 1-37A has a hierarchical approach for the design inputs, defined by the quality of data available and importance of the project. There are three levels:

- Level 1 – Laboratory measured material properties are required (e.g., dynamic modulus master curve for asphalt concrete, nonlinear resilient modulus for unbound materials). Project-specific traffic data is also required (e.g., vehicle class and load distributions);
- Level 2 – Inputs are obtained through empirical correlations with other parameters (e.g., resilient modulus estimated from CBR values);
- Level 3 – Inputs are selected from a database of national or regional default values according to the material type or highway class (e.g., soil

classification to determine the range of resilient modulus, highway class to determine vehicle class distribution).

According to the NCHRP 1-37A report, level 1 is recommended for heavily trafficked highways where premature failure is economically undesirable. Level 2 can be used for intermediate projects, while level 3 is recommended for minor projects, usually low traffic roads. In addition, level 3 may be appropriate for pavement management programs widely implemented in highway state agencies.

The NCHRP 1-37A methodology uses the Multi-Layer Linear Elastic Theory (MLET) to predict mechanistic responses in the pavement structure. When level 1 nonlinear stiffness inputs for unbound material are selected, MLET is not appropriate and a nonlinear Finite Element Method (FEM) is used instead.

Level 3 was used throughout this study because (a) at present there are rarely level 1 input data to be used on a consistent basis, and (b) the final version of the NCHRP 1-37A software was calibrated using level 3.

3.2.2. Inputs

The hierarchical level defines what type of input parameter is required. This section describes the input variables required for level 3.

Design Criteria

The design criteria are defined as the distress magnitudes at the minimum acceptable level of service. The design criteria are agency-defined inputs that may vary by roadway class, location, importance of the project, and economics.

The distresses considered for flexible pavements are: permanent deformation (rutting), “alligator” fatigue cracking (bottom-up), “longitudinal” cracking (top-down), thermal cracking, and roughness. The only functional distress predicted is roughness. Friction is not considered in the NCHRP 1-37A methodology. Among all these distresses, roughness is the only one not predicted entirely from mechanistic responses. Roughness predictions also include other non-structural distresses and site factors. Design criteria must be specified for each of these distresses predicted in the NCHRP 1-37A methodology.

Traffic

The NCHRP 1-37A methodology uses the concept of load spectra for characterizing traffic. Each axle type (e.g., single, tandem) is divided in a series of load ranges. Vehicle class distributions, daily traffic volume, and axle load distributions define the number of repetitions of each axle load group at each load level. The specific traffic inputs consist of the following data:

- Traffic volume – base year information:
 - Two-way annual average daily truck traffic (AADTT)
 - Number of lanes in the design direction
 - Percent trucks in design direction
 - Percent trucks in design lane
 - Vehicle (truck) operational speed
- Traffic volume adjustment factors:
 - Vehicle class distribution factors

- Monthly truck distribution factors
- Hourly truck distribution factors
- Traffic growth factors
- Axle load distribution factors
- General traffic inputs:
 - Number axles/trucks
 - Axle configuration
 - Wheel base
 - Lateral traffic wander

Vehicle class is defined using the FHWA classification (FHWA, 2001).

Automatic Vehicle Classification (AVC) and Weigh-in-Motion (WIM) stations can be used to provide data. The data needs to be sorted by axle type and vehicle class to be used in the NCHRP 1-37A procedure. In case site-specific data are not available, default values are recommended in the procedure.

The use of load spectra enhances pavement design. It allows mixed traffic to be analyzed directly, avoiding the need for load equivalency factors. Additional advantages of the load spectra approach include: the possibility of special vehicle analyses, analysis of the impact on performance of overloaded trucks, and analysis of weight limits during critical climate conditions (e.g., spring thawing).

Environment

The environmental conditions are predicted by the Enhanced Integrated Climatic Model (EICM). The following data are required:

- Hourly air temperature
- Hourly precipitation
- Hourly wind speed
- Hourly percentage sunshine
- Hourly relative humidity

These parameters can be obtained from weather stations close to the project location. The NCHRP 1-37A software includes a library of weather data for approximately 800 weather stations throughout the U.S.

Additional environmental data are also required:

- Groundwater table depth
- Drainage/surface properties:
 - Surface shortwave absorptivity
 - Infiltration
 - Drainage path length
 - Cross slope

The climate inputs are used to predict moisture and temperature distributions inside the pavement structure. Asphalt concrete stiffness is sensitive to temperature variations and unbound material stiffness is sensitive to moisture variations. The EICM is described later in Section 3.2.3.

Material Properties

The NCHRP 1-37A methodology requires a large set of material properties. Three components of the design process require material properties: the climate model, the pavement response models, and the distress models.

Climate-related properties are used to determine temperature and moisture variations inside the pavement structure. The pavement response models use material properties (corrected as appropriate for temperature and moisture effects) to compute the state of stress/strain at critical locations in the structure due to traffic loading and temperature changes. These structural responses are used by the distress models along with complementary material properties to predict pavement performance.

Only flexible pavements were studied in this research and therefore only material properties for asphalt concrete and unbound materials are described. Table 3.6 summarizes the flexible pavement material properties required by the NCHRP 1-37A procedure. (Recall that measured properties are level 1 inputs, correlations with other parameters are level 2, and default values selected from typical ranges are level 3.)

Table 3.6. Material inputs requirement for flexible pavements.

Material Category	Material inputs required		
	Climatic models	Response models	Distress models
Asphalt concrete	<ul style="list-style-type: none"> - <u>mixture</u>: surface shortwave absorptivity, thermal conductivity, and heat capacity - <u>asphalt binder</u>: viscosity (stiffness) characterization 	<ul style="list-style-type: none"> - time-temperature dependent dynamic modulus (E*) of HMA mixture - Poisson's ratio 	<ul style="list-style-type: none"> - tensile strength, - creep compliance - coefficient of thermal expansion
Unbound materials	<ul style="list-style-type: none"> - plasticity index - gradation parameters - effective grain sizes - specific gravity - saturated hydraulic conductivity - optimum moisture content - parameters to define the soil-water characteristic curve 	<ul style="list-style-type: none"> - resilient modulus (Mr) at optimum density and moisture content - Poisson's ratio - unit weight - coefficient of lateral pressure 	<ul style="list-style-type: none"> - gradation parameters

Two material properties required in the NCHRP 1-37A methodology are considered innovative for pavement design methods, the dynamic modulus for asphalt concrete and the nonlinear stiffness model for unbound materials. Time- and temperature-dependency of asphalt mixtures is characterized by the dynamic modulus, $|E^*|$. The dynamic modulus master curve describes the variation of asphalt concrete stiffness due to rate of loading and temperature variation (hardening with low temperature/high frequency and softening with high temperature/low frequency). The nonlinear elastic behavior of unbound granular materials is modeled by a stress-dependent resilient modulus included as level 1 input.

Asphalt Concrete

The complex dynamic modulus $|E^*|$ is the principal material property input for asphalt concrete. It is a function of mixture characteristics (binder, aggregate gradation, and volumetrics), rate of loading, temperature, and age. For level 1 inputs, the dynamic modulus master curve is constructed based on time-temperature superposition principles (Huang, 2004; Pellinen et al., 2004) by shifting laboratory frequency sweep test data. Binder viscosity measured using the dynamic shear rheometer (DSR) is also a required level 1 input. Aging effects on binder viscosity are simulated using the Global Aging System, which considers short term aging from mix/compaction and long term aging from oxidation (NCHRP 1-37A report, appendix CC-4, 2004).

For level 2 and 3 inputs, the dynamic modulus master curve is obtained via an empirical predictive equation. The $|E^*|$ predictive equation is an empirical relationship between $|E^*|$ and mixture properties:

$$\log E^* = 3.750063 + 0.02932 \cdot \rho_{200} - 0.001767 \cdot (\rho_{200})^2 - 0.002841 \cdot \rho_4 - 0.058097 \cdot V_a$$

$$- 0.802208 \cdot \left(\frac{V_{beff}}{V_{beff} + V_a} \right) + \frac{3.871977 + 0.0021 \cdot \rho_4 + 0.003958 \cdot \rho_{38} - 0.000017 \cdot (\rho_{38})^2 + 0.005470 \cdot \rho_{34}}{1 + e^{(-0.603313 - 0.313351 \cdot \log(f) - 0.393532 \cdot \log(\eta))}}$$

(3.17)

in which:

- E^* = dynamic modulus, 10^5 psi
- η = binder viscosity, 10^6 Poise
- f = loading frequency, Hz
- V_a = air void content, %
- V_{beff} = effective binder content, % by volume
- ρ_{34} = cumulative % retained on the 19-mm sieve
- ρ_{38} = cumulative % retained on the 9.5-mm sieve
- ρ_4 = cumulative % retained on the 4.75-mm sieve
- ρ_{200} = % passing the 0.075-mm sieve

The binder's viscosity at any temperature is given by the binder's viscosity-temperature relationship:

$$\log \log \eta = A + VTS \cdot \log T_R \quad (3.18)$$

in which:

- η = bitumen viscosity, cP
- T_R = temperature, Rankine ($T_R = T_{\text{Fahrenheit}} + 460$)
- A = regression intercept
- VTS = regression slope of viscosity temperature susceptibility

For level 2 asphalt concrete inputs, binder parameters A and VTS are determined from DSR testing. For level 3, default A and VTS values are based on the binder grading (e.g., Superpave performance grade, penetration grade, or viscosity grade).

Additional asphalt concrete material properties are required to predict thermal cracking: (1) tensile strength, (2) creep compliance, (3) coefficient of thermal expansion, (4) surface shortwave absorptivity, and (5) thermal conductivity and heat capacity. The last two properties are also required for the climatic model (EICM). Tensile strength and creep compliance are determined in the laboratory using the indirect tensile test for level 1 and 2 inputs. At level 3, these properties are correlated with other material parameters.

Unbound Materials

Resilient modulus is the principal unbound material property required for the structural response model. Level 1 resilient modulus values are determined from laboratory test data as fitted to the stress-dependent stiffness model:

$$M_R = k_1 p_a \left(\frac{\theta}{p_a} \right)^{k_2} \left(\frac{\tau_{oct}}{p_a} \right)^{k_3} \quad (3.19)$$

in which:

M_R = resilient modulus

θ = bulk stress = $\sigma_1 + \sigma_2 + \sigma_3$

σ_1 = major principal stress

σ_2 = intermediate principal stress = σ_3 for M_R test on cylindrical specimens

σ_3 = minor principal stress/confining pressure

τ_{oct} = octahedral shear stress = $\frac{1}{3} \sqrt{(\sigma_1 - \sigma_2)^2 + (\sigma_1 - \sigma_3)^2 + (\sigma_2 - \sigma_3)^2}$

p_a = atmospheric pressure (used to normalize the equation)

k_1, k_2, k_3 = regression constants determined from the laboratory tests

At level 2 the resilient modulus is correlated with other parameters (e.g., California Bearing Ratio (CBR), R-value, AASHTO layer coefficient). At level 3 the resilient modulus can be selected from a range of default values that are typical for the material type and/or soil classification. The input resilient modulus data at all levels are assumed to be at optimum moisture content and density; this value is adjusted by the EICM for seasonal climate variations. There is also an option for direct entry of a best estimate for the seasonally-adjusted unbound resilient modulus, in which case the EICM is bypassed.

Poisson's ratio is also required for the structural response model. It can be determined from laboratory testing, correlations with other properties, or estimated from ranges of typical values. The Atterberg limits, gradation, hydraulic conductivity, maximum dry unit weight, specific gravity, optimum moisture, and degree of saturation are additional unbound material inputs used for determining the effect of seasonal climate variations on resilient modulus.

3.2.3. Pavement Response Models

The NCHRP 1-37A procedure utilizes three models to predict pavement structural responses (stresses, strains, and displacements). Multi-Layer Elastic Theory (MLET) and the Finite Element Model (FEM) are used to compute responses due to traffic loading and the Enhanced Integrated Climate Model (EICM) is used to predict temperature and moisture histories throughout the pavement structure. When non-linear behavior of

unbound materials is desired—i.e., for level 1 inputs—the FEM is chosen; otherwise the load-related analysis is done with MLET.

The load-related structural responses are predicted at critical locations based on maximum damage. The response at each point is evaluated at various depths and afterward the most critical is used to predict pavement distress performance. Figure 3.4 shows in plan view the location of possible critical points for single, tandem, and tridem axles. If a single axle is being analyzed, line Y1 of points is used; if tandem, lines Y2 and Y3; and if tridem, lines Y2, Y3, Y6 and Y7 (NCHRP, 2004).

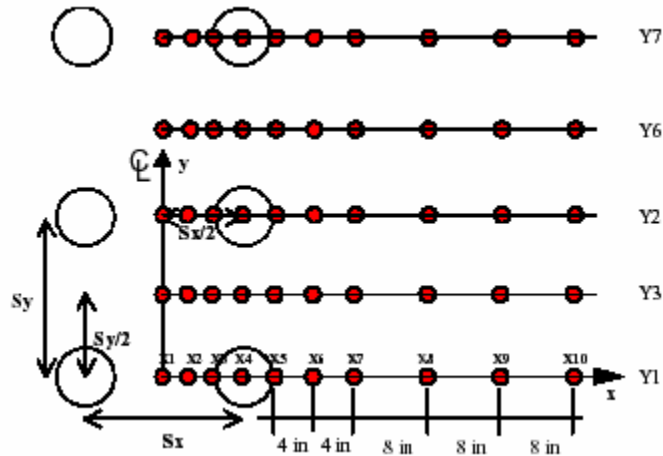


Figure 3.4. Summary of schematics for horizontal location of critical response predictions (NCHRP, 2004)

The depths at which the calculations are performed depend on the distress type:

- Fatigue cracking
 - at surface (top-down cracking)
 - 0.5 inches from the surface (top-down cracking)
 - at the bottom of the asphalt concrete layer (bottom-up cracking)
- Rutting
 - mid-depth of each layer/sublayer
 - top of subgrade

- 6 inches below the top of subgrade

Each pavement layer is divided into thin sublayers so that properties varying in the vertical direction are represented better (e.g., asphalt concrete layer is divided and different dynamic moduli are assigned depending on the temperature in each sublayer).

For flexible pavements, the sublayering is determined as follows:

- The first 1 inch of asphalt concrete (AC) is divided into two 0.5-inch sublayers. The remaining AC thickness is divided into 1-inch sublayers until 4 inches of total depth from the surface is achieved. The remaining thickness, if there is any, is considered the final AC sublayer.
- The unbound base is divided into $a + nb$ sublayers, in which a has half the thickness of b . The number of remaining sublayers is determined by: $n = \text{int}[(h_{\text{base}} - 2)/4]$. Therefore, the total number of sublayers is $n + 1$. This procedure is valid for base thickness exceeding 6 inches.
- The subgrade is divided into 3 sublayers of equal thickness until the total depth of the pavement structure reaches 8 feet. From this point on there is no more sublayering and the remaining subgrade is treated as an infinite layer.

Multi-layer Linear Elastic Theory

The first attempt to calculate displacements due to loading on an elastic half-space, such as the surface of an homogeneous material with infinite area and depth, was made by Kelvin in 1868 (Croney and Croney, 1997). Later, Boussinesq's solution (1885) for a concentrated load became a fundamental tool to compute stress, strain and deflection. The solution could be integrated to obtain responses due to a general surface

load, including a circular loaded area (Huang, 1993). The concept of multi-layer analysis has its roots in the Burmister two-layer and three-layer solutions (Burmister, 1945); charts and tables summarizing these solutions were developed later (Foster and Alvin, 1954; Burmister, 1958; Jones, 1962; Huang, 1969, and 1973).

Burmister's layered theory can be applied to a multi-layer system of linear elastic materials structured on top of a half space subgrade following the basic assumptions (Huang, 1994):

- Each layer is homogeneous, isotropic, and linearly elastic, characterized by Young's modulus of elasticity, E , and Poisson's ratio, ν .
- The material is weightless and horizontally infinite
- The thickness of each layer is finite, and the subgrade is considered as infinite layer.
- The load is uniformly applied on the surface over a circular area.
- Continuity conditions are satisfied at the layer interfaces.

In the NCHRP 1-37A procedure, the MLET is implemented in a modified version of the JULEA algorithm (NCHRP, 2004). Using the principle of superposition, single wheels can be combined spatially into multi-wheel axles to simulate different axle configurations.

The small set of input parameters required by MLET facilitates its implementation and use. The only inputs required are the layer thicknesses, the elastic properties (Young's modulus of elasticity and Poisson's ratio) for each layer, the tire pressure, and the tire contact area. The main disadvantage of MLET is its inability to consider nonlinearities often exhibited by pavement materials.

Finite Element Method

The Finite Element Method (FEM) allows structural modeling of a multi-layer pavement section having material properties that can vary both vertically and horizontally throughout the profile. It is a versatile tool capable of considering three dimensional geometries, non-linear material behavior, large strain effects, dynamic loading and other features. It is well suitable for structural evaluation and response prediction of pavements. Although its robustness permits solving more complex problems, the longer computational time compared to MLET represents a significant disadvantage.

The general idea of finite element technique is the partitioning of the problem into small discrete elements (mesh), formulating an approximation to the stress and strain variations across each individual element, and then applying equilibrium requirements to combine the individual elements to get the formulation for the global problem in terms of a set of simultaneous linear equations. The solution is therefore a piecewise approximation to the true solution. In the NCHRP 1-37A methodology, the FEM was implemented with the following features:

- Linearly elastic behavior for asphalt concrete
- Nonlinearly elastic behavior (stress-dependent stiffness model) with tension cut-off for unbound materials
- Fully bonded, full slip, and intermediate interface conditions between layers

The asphalt concrete layer is modeled as a linearly elastic material with stiffness given by the mixture dynamic modulus master curve. The stress dependence of unbound material is expressed by the stiffness model described in section 3.2.2 as:

$$M_R = k_1 p_a \left(\frac{\theta}{p_a} \right)^{k_2} \left(\frac{\tau_{oct}}{p_a} \right)^{k_3} \quad (3.20)$$

in which the parameters are as previously described. The tension cut-off feature is triggered whenever tensile principal stresses are calculated in the unbound layers (the excess tensile stress is distributed over neighboring elements in an iterative process). The load is applied in small increments, and the stress/strain output from each increment provides the initial condition for the next stage (NCHRP, Appendix RR, 2004).

EICM Environmental Model

EICM is a mechanistic model of one dimensional heat and moisture flow that simulates changes in the behavior and characteristics of pavement and subgrade materials induced by environmental factors (NCHRP, 2004). Daily and seasonal variations of temperature and moisture within the pavement structure are induced by the weather history at the project site.

Different material types have different responses to climatic variations. Unbound materials are affected by moisture change and by freeze-thaw cycles during winter and spring seasons. Asphalt concrete responds to temperature variations, which affects directly the dynamic modulus of the mixture. Temperature is also the cause of thermal cracks, either from a single thermal variation or from repetitive cycles of warm/cool temperatures.

The EICM consists of three major components (NCHRP, 2004):

- The Climatic-Materials-Structural Model (CMS Model) originally developed at the University of Illinois (Dempsey *et al.*, 1985)

- The CRREL Frost Heave and Thaw Settlement Model (CRREL Model) originally developed at the United States Army Cold Regions Research and Engineering Laboratory (CRREL) (Guymon *et al.*, 1986)
- The Infiltration and Drainage Model (ID Model) originally developed at Texas A&M University (Lytton *et al.*, 1990)

In the case of flexible pavements, three major environmental effects are of particular interest:

- Temperature variations for the asphalt concrete. The dynamic modulus of asphalt concrete mixtures is very sensitive to temperature. Temperature distributions in asphalt concrete layers are predicted and then used to define the stiffness of the mixture throughout the sublayers. Temperature distributions are also used as inputs for the thermal cracking prediction model.
- Moisture variation for subgrade and unbound materials. The resilient modulus input of unbound materials is defined as being at optimum density and moisture content. A correction factor is defined to adjust the resilient modulus based on predicted moisture content.
- Freezing and thawing for subgrade and unbound materials. The resilient modulus of unbound materials located within the freezing zone increases during freezing periods and decrease during thawing periods. The EICM predicts the formation of ice lenses and defines the freezing zone.

3.2.4. Empirical Performance Models

This section presents a description of empirical models for predicting performance of flexible pavements in the NCHRP 1-37A procedure. The models described here are the following: “alligator” or bottom-up fatigue cracking, longitudinal or top down fatigue cracking, thermal cracking, rutting and roughness. The calibration of these models was done using the Long Term Pavement Performance (LTPP) database with sections distributed all over the U.S. This calibration effort is defined in the NCHRP 1-37A methodology as the national calibration.

The national calibration was a task undertaken by the NCHRP 1-37A project team to determine calibration coefficients for the empirical distress models that would be representative of the wide range of materials available in the U.S. for pavement construction. The LTPP database was used as primary source of data for this purpose. Permanent deformation, longitudinal (top-down), alligator (bottom-up) and thermal cracking were calibrated for flexible pavement sections. According to the NCHRP 1-37A report, the roughness model was developed directly using the LTPP data and therefore required no additional calibration.

The importance of calibration is evident. Pavement structures behave in different ways and the current state-of-the-art mechanistic models are not capable of fully predicting the behavior of pavement structures. The empirical models are not sufficient to stand alone and capture the wide possibilities of failure mechanism. In addition, most of these models were developed from laboratory test data and laboratory-field shifting factors are required.

Alligator Fatigue Cracking

“Alligator” fatigue cracking develops from mechanical failure caused by tensile strains at the bottom of asphalt concrete layers and once developed propagates upwards. It is also known as bottom-up cracking. Stiffer mixtures or thin layers are more likely to exhibit bottom-up fatigue cracking problems, which makes it a problem often aggravated by cold weather. It is also noted that the supporting layers are important for the development of fatigue cracking. Soft layers placed immediately below the asphalt concrete layer increase the tensile strain magnitude at the bottom of the asphalt concrete and consequently increase the probability of fatigue crack development.

Fatigue cracking is evaluated by first predicting damage and then converting damage into cracked area. The model used in the NCHRP 1-37A procedure was adopted from the Asphalt Institute (Asphalt Institute, 1991) and calibrated based on 82 LTPP section data in 24 states across the country (NCHRP, 2004). The number of repetitions to failure for a given load magnitude is computed as follows:

$$N_f = k_t \left[\beta_1 k_1 C (\varepsilon_t)^{-\beta_2 k_2} (E)^{-\beta_3 k_3} \right] \quad (3.21)$$

in which:

N_f = number of repetitions of a given load to failure

k_t = thickness correction factor

$\beta_1, \beta_2, \beta_3$ = field calibration coefficients

k_1, k_2, k_3 = material properties determined from regression analysis

laboratory test data

C = laboratory to field adjustment factor

ε_t = tensile strain at the critical location within asphalt concrete layer

E = asphalt concrete stiffness at given temperature

The calibration of the model using the LTPP database resulted in the following values: $k_1 = 0.00432$, $k_2 = 3.9492$, $k_3 = 1.281$. The β_i field calibrations coefficients were assumed to be equal to 1 for this calibration. This set of calibration coefficients is referred to in the NCHRP 1-37A methodology as the national calibration.

The thickness correction factor is determined as follows:

$$k_t = \frac{1}{0.000398 + \frac{0.003602}{1 + e^{(11.02 - 3.49 * h_{AC})}}} \quad (3.22)$$

in which:

h_{AC} = total AC thickness

The laboratory-field adjustment factor is given by:

$$C = 10^M \quad (3.23a)$$

$$M = 4.84 \left(\frac{V_{beff}}{V_a + V_{beff}} - 0.69 \right) \quad (3.23b)$$

in which:

V_{beff} = effective binder content (% of volume)

V_a = air voids (%)

The damage resulted from a given load is then computed from the number of repetitions using Miner's Law:

$$D = \sum_{i=1}^T \frac{n_i}{N_{fi}} \quad (3.24)$$

in which:

D = damage

T = total number of seasonal periods

n_i = actual traffic for period i

N_{fi} = traffic repetitions of a given load to cause failure at period i

The last step is to convert damage into cracked area as follows:

$$FC = \left(\frac{C_4}{1 + e^{(C_1 C_1' + C_2 C_2' \log(D-100))}} \right) \cdot \left(\frac{1}{60} \right) \quad (3.25a)$$

$$C_2' = -2.40874 - 39.748(1 + h_{AC})^{-2.856} \quad (3.25b)$$

$$C_1' = -2C_2' \quad (3.25c)$$

in which:

FC = “alligator” fatigue cracking (% of lane area)

C_1, C_2, C_4 = constants

D = damage

h_{AC} = total AC thickness

The calibration using the LTPP database resulted in the following values for the regression constants: $C_1 = 1$, $C_2 = 1$ and $C_4 = 6000$. Equation (3.25a) is of a convenient sigmoidal form that models the two end-conditions of the damage-cracked area relationship. At 0% damage the percentage of cracked area is equal to zero. At the other end, at 100% damage, an assumption was adopted that only half of the area would be cracked. Therefore when damage is 100%, cracked area is equal to 50% or 3000 ft² over a 500 ft lane length (the total lane area considered in the NCHRP 1-37A methodology is 12 ft x 500 ft = 6000 ft²). The statistics for the “alligator” fatigue cracking model after calibration using 461 observations from the LTPP database standard error (Se) = 6.2%, and Se/Sy = 0.947.

Longitudinal Cracking

Longitudinal cracking develops at the surface and propagates downward (top-down cracking). Longitudinal crack formation in flexible pavements is conceptually similar to “alligator” fatigue cracking. Tensile strains at the top of the surface asphalt concrete layer induced by traffic loading cause the appearance of cracks.

The NCHRP 1-37A model for longitudinal cracking follows the same formulation as for alligator cracking. The difference is in the damage-crack relationship. Equation (3.21) is used to calculate the number of applications to failure for a given load. Damage is computed using Miner’s Law, Equation (3.24). Cracking, in units of foot/mile, is then given by:

$$FC = \left(\frac{C_4}{1 + e^{(C_1 - C_2 \cdot \log(D-100))}} \right) \cdot 10.56 \quad (3.26)$$

in which:

FC = longitudinal cracking (foot/mile)

C_1, C_2, C_4 = calibration coefficients

D = damage

The calibration using the LTPP database resulted in the following values for the regression constants: $C_1 = 7$, $C_2 = 3.5$ and $C_4 = 1000$. The sigmoidal form model was used to model the damage-crack length relationship. The two end-conditions are satisfied. At 0% damage the model predicts no cracking, and at 100% damage, 500 ft of longitudinal cracking per 500 ft of pavement (assumed only 50% of the lane with cracks on both wheel paths: 2 x 250 ft). The statistics for the longitudinal cracking calibration based on 414 field measurements are $Se = 1242.25$ feet/mile and $Se/Sy = 0.977$.

Thermal Cracking

Thermal cracking is a consequence of heating/cooling cycles occurring in the asphalt concrete. The pavement surface cools down faster and with more intensity than the core of the pavement structure, which causes thermal cracking to occur at the surface of flexible pavements. Thermal cracks extend in the transverse direction across the full width of the pavement.

The thermal cracking model used in the NCHRP 1-37A procedure is an enhanced version of the TCMODEL developed under the SHRP A-005 research contract. This model has a robust theoretical background and is the most fully mechanistic of the distress prediction components in the NCHRP 1-37A procedure.

The main improvement from the SHRP A-005 model was the incorporation of an advanced analysis technique to convert data directly from the Superpave Indirect Tensile Test into viscoelastic properties, specifically the creep compliance function that is further converted to the relaxation modulus. The relaxation modulus is coupled with the temperature data from the EICM to predict thermal stresses. The growth behavior of the thermal crack is calculated from the thermal stresses.

The crack propagation is computed using Paris's law:

$$\Delta C = A \cdot \Delta K^n \quad (3.27)$$

in which:

ΔC = change in crack depth for each thermal cycle

ΔK = change in stress intensity factor during thermal cycle

A, n = fracture parameters for the asphalt concrete mixture

The master creep compliance function is expressed as a power law:

$$D(\xi) = D_0 + D_1 (\xi)^m \quad (3.28)$$

in which:

ξ = reduced time

D_0, D_1, m = compliance coefficients

Given the compliance function model expressed by Equation (3.28), the values of n and A can be calculated as follows:

$$n = 0.8 \left(1 + \frac{1}{m} \right) \quad (3.29)$$

$$A = 10^{\beta \cdot (4.389 - 2.52 \cdot \log(E \cdot \sigma_m \cdot n))} \quad (3.30)$$

in which:

m = power coefficient in the compliance function

β = calibration coefficient

E = mixture stiffness

σ_m = undamaged mixture tensile strength

The calibration of Equation (3.30) depends upon knowing the creep compliance function from indirect tensile testing. For level 1 and 2 inputs laboratory data are required (creep compliance and tensile strength) and for level 3 input a set of correlation equations are used to predict the creep compliance function from mixture properties (NCHRP 1-37A report, appendix HH, 2004). The calibration coefficient β varied with the input level: 5 (level 1), 1.5 (level 2), and 3 (level 3).

The length of thermal cracking is then predicted based on an assumed relationship between the crack depth and percentage of cracking in the pavement:

$$C_f = \beta_1 \cdot N\left(\frac{\log C/h_{ac}}{\sigma}\right) \quad (3.31)$$

in which:

C_f = predicted thermal cracking, ft/500ft

β_1 = field calibration coefficient

$N()$ = standard normal distribution at ()

C = crack depth

σ = standard deviation of the log of crack depth

h_{ac} = asphalt concrete thickness

The calibration of the thermal cracking model was based on data from the LTPP database, the Canadian C-SHRP program, MnROAD, and one section in Peoria, IL. The value of the calibration coefficient β_1 was found equal to 400.

Rutting

Permanent deformation or rutting is a load-related distress caused by cumulative applications of loads at moderate to high temperatures, when the asphalt concrete mixture has the lowest stiffness. It can be divided into 3 stages. Primary rutting develops early in the service life and it is caused predominantly by densification of the mixture (compaction effort by passing traffic) and with decreasing rate of plastic deformations. In the secondary stage, rutting increments are smaller at a constant rate, and the mixture is mostly undergoing plastic shear deformations. The tertiary stage is when shear failure occurs, and the mixture flows to rupture. Usually the tertiary stage is not reached in in-service pavements – preventive maintenance and rehabilitation are required by agencies long before this stage is achieved.

Permanent deformation is predicted using empirical models. Only primary and secondary stages are modeled. For asphalt concrete materials the model is an enhanced version of Leahy's model (Leahy, 1989), modified by Ayres (1997) and then by Kaloush (2001). The model for unbound materials is based on Tseng and Lytton's model (Tseng and Lytton, 1989), which was modified by Ayres and later on by El-Basyouny and Witczak (NCHRP, 2004).

Total permanent deformation is the summation of rut depths from all layers:

$$RD_{\text{total}} = RD_{\text{AC}} + RD_{\text{Base}} + RD_{\text{subgrade}} \quad (3.32)$$

Asphalt concrete model

The asphalt concrete layer is subdivided into sublayers and the total predicted rut depth for the layer is given by:

$$RD_{\text{AC}} = \sum_{i=1}^N (\varepsilon_p)_i \cdot \Delta h_i \quad (3.33)$$

in which:

RD_{AC} = rut depth at the asphalt concrete layer

N = number of sublayers

$(\varepsilon_p)_i$ = vertical plastic strain at mid-thickness of layer i

Δh_i = thickness of sublayer i

The vertical plastic strain (ε_p) at each sublayer is calculated as:

$$\frac{\varepsilon_p}{\varepsilon_r} = \beta_{\sigma 3} \left[\beta_1 10^{k_1} T^{k_2 \beta_2} N^{k_3 \beta_3} \right] \quad (3.34)$$

in which:

ε_r = computed vertical resilient strain at mid-thickness of

sublayer i for a given load

$\beta_{\sigma 3}$ = depth correction factor

k_1, k_2, k_3 = regression coefficients derived from laboratory repeated

load permanent deformation test data

$\beta_1, \beta_2, \beta_3$ = field calibration coefficients

T = temperature

N = number of repetitions for a given load

The depth correction factor is a function of asphalt layer thickness and depth to computational point (mid-thickness of sublayer i) that adjusts the computed plastic strain for the confining pressure at different depths. The depth correction factor is computed as follows:

$$\beta_{\sigma 3} = (C_1 + C_2 \cdot depth) \cdot 0.328196^{depth} \quad (3.35a)$$

$$C_1 = -0.1039 \cdot h_{AC}^2 + 2.4868 \cdot h_{AC} - 17.342 \quad (3.35b)$$

$$C_2 = 0.0172 \cdot h_{AC}^2 - 1.7331 \cdot h_{AC} + 27.428 \quad (3.35c)$$

in which:

$depth$ = depth to the point of strain calculation

h_{AC} = thickness of the asphalt layer

After the calibration using the national LTPP database, the regression coefficients are $k_1 = -3.4488$, $k_2 = 1.5606$, $k_3 = 0.4791$, and the assumed β_i 's are equal to 1. A total of 387 observed rut points from the 88 LTPP sections were used in the calibration effort.

The goodness-of-fit statistics for the calibration are $R^2 = 0.643$, standard error $S_e = 0.055$ in for the wide range mixture types in the LTPP calibration sections.

Unbound materials

The NCHRP 1-37A methodology divides all unbound granular materials into sublayers, and the total rutting for each layer is the summation of the permanent deformation of all sublayers. The permanent deformation at any given sublayer is computed as:

$$\delta_i = \beta_1 k_1 \left(\frac{\varepsilon_0}{\varepsilon_r} \right) e^{-\left(\frac{\rho}{N}\right)^\beta} \varepsilon_v h_i \quad (3.36)$$

in which:

δ_i = permanent deformation for sublayer i

β_1 = field calibration coefficient

k_1 = regression coefficient determined from laboratory permanent deformation test data

$\varepsilon_0/\varepsilon_r, \beta, \rho$ = material properties

N = number of repetitions of a given load

ε_v = computed vertical resilient strain at mid-thickness of sublayer i for a given load

h_i = thickness of sublayer i

The model described in Equation (3.36) is a modification of the original Tseng and Lytton's model (Tseng and Lytton, 1989). The material properties $\varepsilon_0/\varepsilon_r, \beta, \rho$ are derived from other properties according to the following relationships:

$$\log \beta = -0.61119 - 0.017638 W_c \quad (3.37a)$$

$$\log \left(\frac{\varepsilon_0}{\varepsilon_r} \right) = \frac{\left(e^{(\rho)^\beta} \times 1.094 \times 10^{-18} E_r^{3.52} \right) + \left(e^{(\rho/10^7)^\beta} \times 0.0316 E_r^{0.5} \right)}{2} \quad (3.37b)$$

$$\rho = 10^7 \left[\frac{C_o}{(1 - (10^7)^\beta)} \right]^{\frac{1}{\beta}} \quad (3.37c)$$

in which:

W_c = water content (%)

E_r = resilient modulus of the layer/sublayer, psi

The parameter C_o is determined by:

$$C_o = \ln \left[\frac{(1.094 \times 10^{-18} E_r^{3.52})}{(0.0316 E_r^{0.5})} \right] \quad (3.38)$$

The water content can be empirically related to the ground water table depth and the resilient modulus:

$$W_c = 51.712 \left[\left(\frac{E_r}{2555} \right)^{\frac{1}{0.64}} \right]^{-0.3586 * GW^{0.1192}} \quad (3.39)$$

The subgrade is modeled as a semi-infinite layer in the structural response models (MLET or FEM). An adjustment on the permanent deformation models is therefore required for computing the plastic strains in a semi-infinite layer. The plastic strain at different depths in the subgrade can be computed by:

$$\varepsilon_p(z) = (\varepsilon_{p0}) e^{-\alpha z} \quad (3.40)$$

in which:

$\varepsilon_p(z)$ = plastic vertical strain at depth z (measured from the top of the subgrade)

ε_{p0} = plastic vertical strain at the top of the subgrade ($z = 0$)

z = depth measured from the top of the subgrade

α = regression coefficient

In Equation (3.36), plastic strain is given by the term δ_i/h_i . Given two points in the subgrade (NCHRP 1-37A procedure uses top of subgrade, $z=0$, and $z=6$ inches below the top), plastic strains are computed and the regression coefficient α is determined from Equation (3.40). The total subgrade permanent deformation then is computed by integrating Equation (3.40) over the depth of subgrade until bedrock:

$$\delta_{SG} = \varepsilon_{p0} \int_0^{h_{bedrock}} e^{-\alpha z} dz = \left(\frac{1 - e^{-\alpha h_{bedrock}}}{\alpha} \right) \varepsilon_{p0} \quad (3.41)$$

in which, $h_{bedrock}$ = depth to bedrock, and the other terms are as defined previously.

A total of 88 LTPP sections were used for calibration of the permanent deformation model for unbound materials for both base/subbase and subgrade. The regression coefficient k_1 for base/subbase and subgrade are respectively 1.673 and 1.35. The goodness-of-fit statistics are $R^2 = 0.62$ and $Se = 0.014$ in for the base/subbase model, and $R^2 = 0.19$ and $Se = 0.056$ in for the subgrade model.

Roughness

Roughness is generally acknowledged as the distress most representative of the overall serviceability of a pavement section. A rough pavement directly affects the ride quality. Any incremental increase in surface distress causes surface roughness to increase (NCHRP, 2004).

The NCHRP 1-37A project found that permanent deformations, thermal cracking, and fatigue cracking were the most dominant distresses affecting roughness. It was also noted that local environmental conditions and the base type supporting the surface layer were also important factors. The calibration effort considered over 350 sections having

good quality data in the LTPP database. Three models were developed for flexible pavements with different base layers: granular base, asphalt-treated base, and cement-stabilized base. The roughness model for conventional flexible pavements with granular base, is as follows:

$$IRI = IRI_0 + 0.0463SF \left(e^{\frac{age}{20}} - 1 \right) + 0.00119TC_L + 0.1834COV_{RD} + 0.00736BC + 0.00115LC \quad (3.42)$$

in which:

IRI_0 = initial IRI expected within six months after construction, m/km

SF = site factor

TC_L = total length of transverse cracks, m/km

COV_{RD} = rut depth coefficient of variation, %

FC_T = total area of fatigue cracking, percent of total lane area

BC_T = total area of block cracking, percent of total lane area

LC = length of sealed longitudinal cracks outside the wheel path, m/km

Age = age after construction, years

The flexible pavement roughness models for the other base types have a similar form. The structural distresses required as inputs for the roughness model are obtained from the predictions made with the distress models discussed previously. The site factor (SF) is given by:

$$SF = \left(\frac{(R_{SD})(P_{0.075} + 1)(PI)}{2 \times 10^4} \right) + \left(\frac{\ln(FI + 1)(P_{0.02} + 1)(\ln(R_m + 1))}{10} \right) \quad (3.43)$$

in which:

R_{SD} = standard deviation in the monthly rainfall, mm

R_m = average annual rainfall, mm

$P_{0.075}$ = percent passing the 0.075 mm sieve

$P_{0.02}$ = percent passing the 0.02 mm sieve

PI = plasticity index

FI = average annual freezing index

The LTPP sections used for calibration provided 353 data points for this model.

The goodness-of-fit statistics are $R^2 = 0.62$ and standard error $Se = 0.387$ m/km (NCHRP, 2004).

3.2.5. Reliability

Pavement design inputs have large uncertainties. The design is often based on the mean values of the input parameters. In the NCHRP 1-37A, the key outcomes are the individual distresses, considered as the random variables of interest. The distress distribution is considered to be normal with a mean predicted value and a corresponding standard deviation. The standard deviation of the distribution is estimated based on the model's calibration error. The predicted distress considering reliability is given by the general formulation:

$$D_{reliability} = D_{mean} + S_D \times z_R \quad (3.44)$$

in which $D_{reliability}$ is the distress prediction with reliability, D_{mean} is the mean distress value from the performance model, S_D is the computed standard deviation for the distress type (D), and z_R is the standard normal deviate from the normal distribution for the level of reliability selected.

The formulation in Equation (3.44) for the NCHRP 1-37A procedure models reliability in the same way as the general reliability factor in the 1993 AASHTO Guide. Recall in the 1993 AASHTO Guide, reliability is included in the design equation via the product of the overall standard deviation and the reliability factor ($S_0 \times Z_R$).

The estimates of error are obtained from the calibration (predicted versus measured data). They include a combined input variability from the input uncertainties, construction variability, and model error. Therefore, the model's error becomes a key factor in the reliability – the smaller the error, the smaller is the gap between a design with a reliability factor (higher than 50%) and one at the mean value (reliability = 50%).

Based on the national calibration results, the default standard error (Se) for permanent deformations is defined for each individual layer as follows:

$$Se_{AC} = 0.1587 \times RD_{AC}^{0.4579} \quad (3.45a)$$

$$Se_{GB} = 0.1169 \times RD_{GB}^{0.5303} \quad (3.45b)$$

$$Se_{SG} = 0.1724 \times RD_{SG}^{0.5516} \quad (3.45c)$$

in which AC represents asphalt concrete, GB , granular base, and SG , subgrade. RD is the rut depth at any given sublayer.

The standard error for alligator and longitudinal cracking are defined as follows:

$$(Se)_{alligator} = 0.5 + 12 / (1 + e^{1.308 - 2.949 \cdot \log D}) \quad (3.46a)$$

$$(Se)_{longitudinal} = 200 + 2300 / (1 + e^{1.072 - 2.1654 \cdot \log D}) \quad (3.46b)$$

in which D is damage computed as the primary variable in the cracking model.

There were data available for all three input levels for the calibration of the mechanistic thermal cracking model. Standard error equations were developed for each input level as follows:

$$\text{Level 1: } Se_{thermal-1} = 0.2474 \times C_{thermal} + 10.619 \quad (3.47a)$$

$$\text{Level 2: } Se_{thermal-2} = 0.3371 \times C_{thermal} + 14.468 \quad (3.47b)$$

$$\text{Level 3: } Se_{thermal-3} = 0.6803 \times C_{thermal} + 29.197 \quad (3.47c)$$

It is important to notice in Equations (3.47) the reduction in error estimate as input level goes from 3 to 1. Level 1 input requires more laboratory data to better characterize the material behavior which in turn reduces the predicted standard error.

3.2.6. Remarks

The M-E approach for designing and evaluating flexible pavements represents a major step forward from purely empirical methods. Mechanistic models are employed for predicting pavement responses and climatic effects on material behavior. The pavement distresses are too complex to be modeled by mechanistic models only. Empirical models are employed to overcome these limitations of theory; the empirical models establish a connection between structural responses and performance prediction. Calibration of the empirical distress models is a critical requirement for quality performance predictions.

Chapter 4: Comparative Study between the 1993 AASHTO Guide and the NCHRP 1-37A Procedure

The advent of M-E pavement performance modeling allows more realistic features to be included in pavement analysis and design. Improvements in traffic and material characterization are among the more important of these enhanced features. Although most of those enhancements have been available as research-oriented design and evaluation tools in the past, routine design is still done using empirical methods, the state-of-practice followed by most agencies.

The benefits of M-E procedures require engineers to improve the design process in several key areas ranging from data collection to interpretation of results. Additional effort and resources must be expended to better characterize materials, improve traffic data quality, and effectively use environmental conditions. Implementation is also a costly, time consuming task that agencies must be willing to undertake. Initial studies are necessary to evaluate the benefits of M-E versus empirical design and to help agencies assess the sensitivity of M-E approach to their local conditions. Although these studies alone are insufficient for justifying the investments required for an agency to implement a new pavement design process, they nevertheless are an essential first step of an implementation process.

The objectives of the sensitivity study in this research are as follows: (1) to compare pavement designs using the empirical 1993 AASHTO guide and those using the NCHRP 1-37A M-E procedure; and (2) to evaluate the sensitivity of pavement design and performance to each of the parameters required by the NCHRP 1-37A procedure.

The first objective is subject of this Chapter. The second objective is reported in Chapter 5 and is intended not only to provide a better understanding of the NCHRP 1-37A procedure and its nuances but also to provide information on research needs for local implementation and calibration.

Three pavement design case studies are also presented in Chapter 6. In these case studies, designs done with the 1993 AASHTO Guide were evaluated with the NCHRP 1-37A procedure for different performance criteria. The results were analyzed in the context of design limits, required pavement structure, and service life.

4.1. Conceptual Differences between 1993 AASHTO Guide and NCHRP 1-37A

The comparison between the 1993 AASHTO Guide and the NCHRP 1-37A procedure is an important step to understand the differences between the two approaches. As mentioned before, the key conceptual differences can be summarized as follows:

- The 1993 AASHTO guide designs pavements to a single performance criterion, the present serviceability index (PSI), while the NCHRP 1-37A procedure simultaneously considers multiple performance criteria (e.g., rutting, cracking, and roughness – for flexible pavements).
- The 1993 AASHTO guide directly computes the layer thicknesses. The NCHRP 1-37A is an iterative procedure. A trial section is defined and evaluated by its predicted performance against the design criteria. If the result is not satisfactory, the section is modified and reanalyzed until an acceptable design is reached.

- The NCHRP 1-37A approach requires more input parameters, especially environmental and material properties. It also employs a hierarchical concept in which one may choose different quality levels of input parameters depending upon the level of information and resources available, technical issues, and the importance of the project.
- The 1993 AASHTO guide was developed based on limited field test data from only one location (Ottawa, IL). The seasonally adjusted subgrade resilient modulus and the layer drainage coefficients are the only variables that account to some extent for environmental conditions. NCHRP 1-37A utilizes a set of project-specific climate data (air temperature, precipitation, wind speed, relative humidity, etc.) to adjust material properties for temperature and moisture influences.
- The 1993 AASHTO guide uses the concept of ESALs to define traffic levels, while the NCHRP 1-37A adopts the more detailed load spectra concept. Pavement materials respond differently to traffic pattern, frequency and loading. Traffic loading in different seasons of the year also has different effects on the response of the pavement structure. These factors can be most effectively considered using the load spectra concept.

Although these differences seem clear, their impacts on performance prediction are more obscure. The different ways that the two procedures define performance makes direct comparisons difficult. The 1993 AASHTO guide predicts pavement condition as a function of distresses translated into one single index (PSI). The NCHRP 1-37A

procedure predicts directly the structural distresses observed in the pavement section and the PSI concept is no longer employed.

PSI was based originally on subjective assessment of pavement condition by a road testing panel. The pavement quality rating is based on distresses observed on the pavement surface. The PSI equation developed in the AASHO Road Test correlates PSI with the individual distresses of slope variance (roughness), cracking and patching. The strongest correlation is with roughness, the performance measure most closely linked to road users' perception of pavement ride quality. However the conditions in the AASHO Road Test in the early 1960's (e.g., traffic volume, vehicle characteristics, travel speeds, materials) were quite different from the conditions in highways today. Users' perceptions of serviceability may also have changed throughout these years, possibly demanding better quality with continuous improvements in highway and vehicle standards. Therefore, converting pavement distresses into serviceability for comparison purposes is unlikely to produce useful results.

Another area that requires careful attention when making comparisons between the two approaches is traffic data. As mentioned before, the NCHRP 1-37A procedure does not use ESALs to define traffic. Instead, traffic is defined by vehicle class and load distributions in terms of traffic load spectra. In the M-E methodology each load application is analyzed individually to compute pavement responses. These responses are used to predict distresses and damage increments that are accumulated over load applications and time.

For these and other reasons, the comparison of results from the two design approaches seems incompatible. The option chosen here to overcome this problem was to

design pavement structures (thicknesses) using the 1993 AASHTO guide and then analyze their predicted performance using the NCHRP 1-37A procedure. Using the NCHRP 1-37A predicted performance as the basis for comparison assumes implicitly that the NCHRP 1-37A predictions are closer to “correct” values. Given this assumption, if the 1993 AASHTO guide predicts performance correctly, then the NCHRP 1-37A predictions of distresses for pavements designed using the 1993 AASHTO guide should also be consistent, regardless of location of the project or traffic conditions.

In summary, the method of comparison employed in this study followed the following sequence: (1) pavements were designed using the 1993 AASHTO guide; (2) performance of the pavement sections were then evaluated using the NCHRP 1-37A software; (3) performance results were grouped by traffic level and location, and compared. The main purpose of grouping is to identify trends in performance behavior for different traffic levels and environmental conditions.

The main focus of this study was evaluation of permanent deformation and classical bottom-up or “alligator” fatigue cracking. Thermal cracking, top-down longitudinal cracking, and roughness were not evaluated. Thermal cracking is a concern only in locations susceptible to freezing temperatures. In such conditions the asphalt concrete becomes stiff and brittle, loses tensile strength, and cracks in response to thermal contractions. However, thermal cracking is not a factor in all the locations to be studied here.

Longitudinal cracking or top-down cracking was not considered in this study because the existing models for this distress incorporated in the NCHRP 1-37A procedure are immature and did not appear to produce reasonable predictions. Longitudinal

cracking predictions were up to 5 times higher than the recommended limit at the end of the design period and were considered above reasonable values. Improvements to top-down longitudinal cracking models are the focus of a new NCHRP study currently underway (NCHRP Project 1-42A).

The NCHRP 1-37A roughness models are based on empirical relationships between pavement distresses and IRI (International Roughness Index). In this case the structural distresses – predicted with other NCHRP 1-37A models (e.g., rutting and fatigue cracking) – are coupled with nonpredicted distresses that are dependent on environmental and location conditions. Roughness was originally intended for evaluation in this study but preliminary results for predicted IRI, although within reasonable ranges, were surprisingly insensitive to structural distresses and more dependent on location and climate conditions. For this reason roughness was dropped from this comparison study.

All of the analyses in this study were performed with the April 2004 Version 0.700 of the NCHRP 1-37A software and field calibration coefficients. This is the final version submitted at the end of the NCHRP Project 1-37A. However, refinements to the software and calibrations continue to the present day.

All of the pavement structures considered in this study were simple three layer flexible structures, as shown in Figure 4.1, consisting of an asphalt concrete mixture (AC) on top of a granular aggregate base (GB) and subgrade. The NCHRP 1-37A predictions considered in this study are for rutting and fatigue cracking at the end of the design period.



Figure 4.1. Pavement structure

4.2. Description of Pavement Sections

The objective of this portion of the sensitivity study is to evaluate designs developed using the empirical 1993 AASHTO guide against performance predictions from the mechanistic-empirical NCHRP 1-37A procedure.

Figure 4.2 shows five different states that were selected to represent most of the climate conditions observed in the country. The stars in the figure represent the approximate design location in each state selected. Table 4.1 summarizes the locations and the typical weather conditions. Local pavement design parameters (e.g., effective subgrade resilient modulus, base layer and drainage coefficient) were obtained from a survey of DOT personnel in each of the five states.

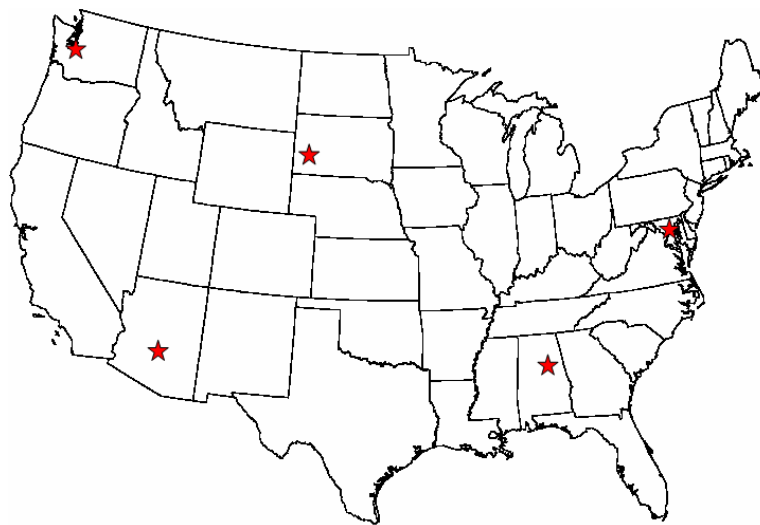


Figure 4.2. States selected for comparison study.

Table 4.1. Locations and climate conditions.

Location	Temperature	Precipitation
Alabama	High	High
Arizona	High	Low
Maryland	Moderate	Moderate
South Dakota	Low	Low
Washington State	Moderate	High

Three traffic levels were considered. Traffic levels were defined in terms of ESALs as the designs were done using the 1993 AASHTO guide. The target values for low, moderate and high traffic levels were 3.8, 15, and 55 Million ESALs, respectively. The low traffic level represents local routes and minor collectors, the moderate traffic level represents minor arterials, and the high traffic level represents principal arterials or interstates.

In order to make the 1993 AASHTO and NCHRP 1-37A comparisons as compatible as possible, the vehicle class and load distributions used in the 1993 AASHTO ESAL calculations were the same as the default distributions used to determine the traffic load spectra for each road functional class in the NCHRP 1-37A software.

The pavement sections designed with the 1993 AASHTO guide were then evaluated using the NCHRP 1-37A procedure and comparisons were made using the predicted rutting and fatigue cracking performance.

4.3. General Inputs

General inputs common to both methods include traffic data and the subgrade and base properties. In the 1993 AASHTO guide, the calculations of the number of ESALs were carried out following all the steps described in Section 3.1.3 – load equivalent factors were calculated from the vehicle class distribution and load spectrum, followed by

computation of truck factor, and finally ESALs. In the NCHRP 1-37A procedure, traffic load spectrum data were used directly to compute pavement structural responses. It is important to emphasize that using the input traffic data gave equivalent loading conditions for each method, therefore allowing for reasonable comparisons between them.

Figure 4.3 to Figure 4.5 show the vehicle load distribution data in the form of cumulative distribution functions by vehicle class. The same load distribution was used for all traffic levels – this means that only the daily volume and the vehicle class distribution were varied to achieve the required number of ESALs. The load distribution were varied to achieve the required number of ESALs. The load distribution used consisted of the NCHRP 1-37A’s default values.

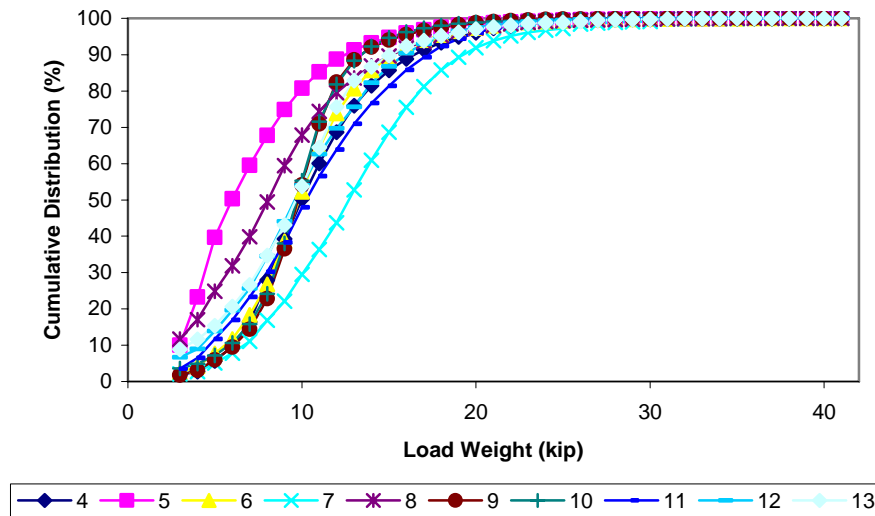


Figure 4.3. Distribution mass function of single axle loads by vehicle class type.

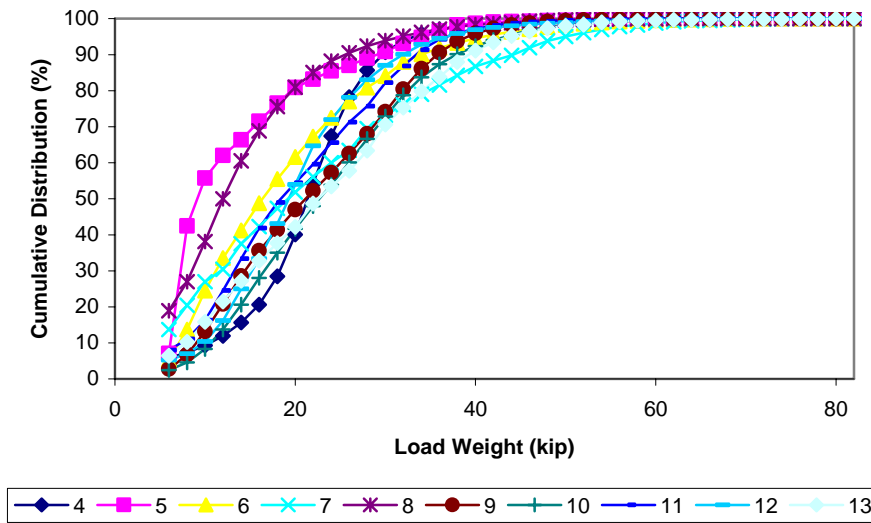


Figure 4.4. Distribution mass function of tandem axle loads by vehicle class type.

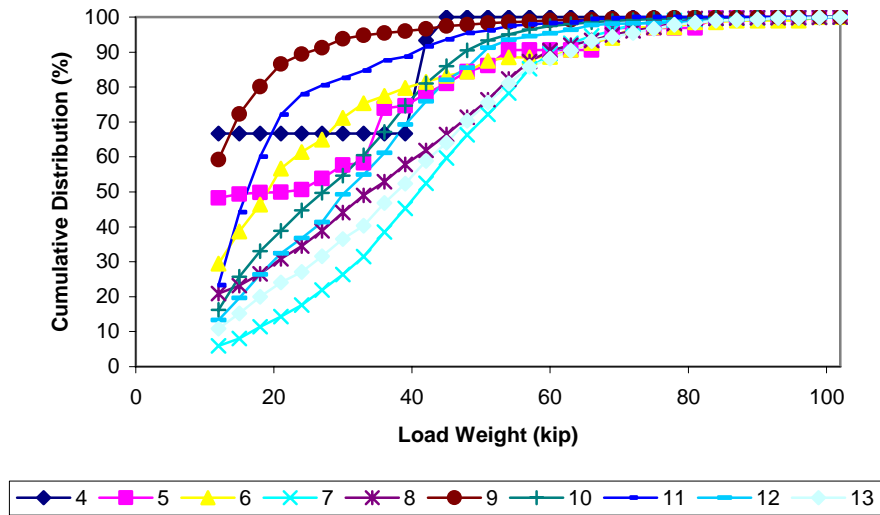


Figure 4.5. Distribution mass function of tridem axle loads by vehicle class type.

Vehicle distribution is likely to be different between low, moderate, and high volume highways. Low volume roads are characterized by higher volume of class 5 trucks (single axle, small size trucks) and high volume roads by higher volume of class 9 trucks (typically the 18-wheelers) in their distribution. The three vehicle distributions

considered in this study were taken as the NCHRP 1-37A default values³ for their specific road functional class, as summarized in Table 4.2. Moderate traffic level was taken as an intermediate condition between the extremes. Table 4.2 also shows the NCHRP 1-37A default distribution of axles by vehicle class, also adopted in this study.

Table 4.2. Number of axle per truck class and vehicle distribution by traffic level.

Vehicle Class	Axle type			Distribution by traffic ^a		
	Single	Tandem	Tridem	Low	Moderate	High
Class 4	1.62	0.39	0.00	3.9%	3.3%	1.3%
Class 5	2.00	0.00	0.00	40.8%	34.0%	8.5%
Class 6	1.02	0.99	0.00	11.7%	11.7%	2.8%
Class 7	1.00	0.26	0.83	1.5%	1.6%	0.3%
Class 8	2.38	0.67	0.00	12.2%	9.9%	7.6%
Class 9	1.13	1.93	0.00	25.0%	36.2%	74.0%
Class 10	1.19	1.09	0.89	2.7%	1.0%	1.2%
Class 11	4.29	0.26	0.06	0.6%	1.8%	3.4%
Class 12	3.52	1.14	0.06	0.3%	0.2%	0.6%
Class 13	2.15	2.13	0.35	1.3%	0.3%	0.3%

^a NCHRP 1-37A default road functional classes: Low (TTC 12), Moderate (TTC 9), and High (TTC 1)

The remaining required traffic data were: Annual Average Daily Traffic (AADT), the percentage of trucks – and consequently Annual Average Daily Truck Traffic (AADTT), and the percentage of trucks in the design direction and in the design lane.

Table 4.3 shows the traffic volume characteristics for all three conditions. These numbers were adjusted to achieve the target traffic levels in terms of ESALs.

The resilient modulus of the subgrade and the structural layer coefficient for the base as obtained from the DOT survey for the 1993 AASHTO designs were used in the NCHRP 1-37A calculations. The resilient modulus of the base layer was calculated using Equation (3.13). Table 4.4 presents the values obtained from the DOT survey.

³ According to the NCHRP 1-37A report (NCHRP, 2004), these default values were defined based on data from state DOTs and the LTPP database for different highway classes and vehicle distributions.

Table 4.3. Traffic volume.

	Low	Moderate	High
AADT	12,000	50,000	180,000
Trucks	15%	15%	12%
AADTT	1,800	7,500	21,600
Trucks design dir.	50%	50%	50%
Trucks design lane	90%	80%	70%
Calculated ESALs	3.8 Million	15 Million	55 Million

Table 4.4. Base layer coefficient and subgrade resilient modulus.

	Alabama	Arizona	Maryland	South Dakota	Washington
Subgrade type	A-6	A-7-5	A-7-6	A-7-6	A-7-6
Subgrade M_R (psi)	7,500	12,000	5,000	7,500	10,000
Base layer coeff.	0.17	0.17	0.11	0.10	0.13
Base M_R (psi) – calculated	40,000	40,000	23,000	21,000	28,000

Curiously the survey asked for the asphalt concrete layer coefficient and granular base drainage coefficient; all the answers were equal to 0.44 and 1.0 respectively – a demonstration that the “default” values from the AASHO Road Test continue to be used today regardless the location and environmental conditions.

4.4. 1993 AASHTO Designs

The design period for all cases was 15 years, which is typical of most agencies’ standards for flexible pavements. Local pavement design parameters (summarized in Table 4.4) reflected typical material properties and environmental conditions for each state. The remaining design parameters were fixed for all designs and assumed as follows:

- initial serviceability = 4.5
- terminal serviceability = 2.5

- design period = 15 years
- reliability = 95%
- standard deviation (S_o) = 0.45
- annual growth rate = 2% linear for all axle types, which gives a growth rate factor value $G = 1.15$

The AASHTO design equation – Equation (3.7) – was used to calculate the structural number required for each traffic level. Using the input parameters given above, the design thicknesses were computed following the procedure described in Section 3.1.2. The final designs are summarized in Table 4.5. It is important to notice that none of the design thicknesses were rounded as they would be in a practical design, as rounding would cloud the comparisons between the different designs.

Table 4.5. 1993 AASHTO designs.

		Traffic level		
		Low	Moderate	High
Alabama	Asphalt Concrete (AC)	5.5	6.8	8.3
	Granular Base (GB)	11.5	13.5	15.5
	AC/GB ratio	0.48	0.50	0.54
Arizona	AC	5.5	6.8	8.3
	GB	7.7	9.2	10.5
	AC/GB ratio	0.71	0.74	0.79
Maryland	AC	6.7	8.3	10.0
	GB	18.6	21.3	24.3
	AC/GB ratio	0.36	0.39	0.41
South Dakota	AC	6.9	8.5	10.3
	GB	13.3	15.5	17.5
	AC/GB ratio	0.52	0.55	0.59
Washington	AC	6.2	7.7	9.4
	GB	9.5	11.0	12.4
	AC/GB ratio	0.65	0.70	0.76

4.5. NCHRP 1-37A Analysis

The NCHRP 1-37A M-E procedure was used to evaluate all the structures in Table 4.5. The additional required input parameters are described in this section.

4.5.1. Traffic

In addition to the traffic inputs used to calculate the number of ESALs in the 1993 AASHTO designs, other minor traffic variables required for the NCHRP 1-37A procedure were assumed as follows:

- Vehicle operational speed
 - Low traffic cases: 45 MPH
 - Moderate traffic cases: 55 MPH
 - High traffic cases: 65 MPH
- Mean wheel location = 18 inches from the lane marking
- Traffic wander standard deviation = 10 inches
- Average axle width = 8.5 ft from edge to edge
- Average axle spacing = 51.6 (tandem) and 49.2 (tridem), inches
- Dual tire spacing = 12 inches
- Tire pressure = 120 psi

4.5.2. Environment

The environmental conditions are simulated by EICM, as described earlier in Chapter 3. This study used data from weather stations of the NCHRP 1-37A software database. Key locations in each state were selected as most representative of local climate

conditions. Table 4.6 summarizes the geographical location and elevation of the assumed project location in each state, as well as the number of months of weather data available. The geographical location was used in the EICM tool to generate the climatic data by interpolation of the three closest weather stations accessible in the NCHRP 1-37A software database.

Table 4.6. Location of designs and environmental data.

	Alabama	Arizona	Maryland	South Dakota	Washington
Latitude (deg.min)	33.34	33.26	39.1	44.03	47.28
Longitude (deg.min)	-86.45	-111.59	-76.41	-103.03	-122.19
Elevation (ft)	636	1103	193	3150	447
Appr. Location	Birmingham	Tempe	Annapolis	Rapid City	Seattle
Num. months	40	66	66	66	63

The groundwater table is an important parameter to define variations in material properties due to moisture dependency – especially the subgrade and intermediate unbound layers – as well as in the mechanistic prediction of pavement responses. The groundwater table depth in this comparative study was kept constant at 15 ft below the pavement surface for all analyses for consistency. The effect of varying the groundwater table depth is part of the input parameters sensitivity study, described later in Chapter 5.

4.5.3. Material Properties

One of the greatest differences between NCHRP 1-37A procedure and the 1993 AASHTO guide is the material properties required. In the 1993 AASHTO guide, there are only a few parameters identified as material properties: the structural layer coefficients, the layer drainage coefficients, and the subgrade resilient modulus. These parameters are not enough to describe complex material behavior such as stress-

dependent stiffness of unbound materials and time- and temperature-dependent response of asphalt mixtures.

The NCHRP 1-37A procedure requires engineering properties of layer materials for a mechanistic analysis of pavement responses (either using elastic theory or the finite element method). In the case of flexible pavements, these properties are (1) dynamic modulus for asphalt mixtures, and (2) resilient modulus for unbound materials. These properties are also environment-dependent, and seasonal variations in temperature and moisture affect their values. The EICM predicts variations of temperature and moisture throughout the seasons and within the pavement structure that are used to adjust the material property for that particular environmental condition.

As mentioned before, the hierarchical input approach provides three input levels depending on the quality of the data. For example, level 1 for asphalt concrete is based on laboratory-measured dynamic modulus while levels 2 and 3 rely on predicted dynamic modulus based on binder properties, mixture gradation, and volumetric properties (Section 0 describes in more detail the dynamic modulus predictive equation). Level 3 material property inputs were used in this study. These are judged to be most consistent with the quality of material inputs used in the 1993 AASHTO procedure. It also represents the expected input level to be used by most agencies at the beginning of the NCHRP 1-37A implementation.

A set of typical material properties was selected for the asphalt concrete and granular base. The same asphalt concrete volumetrics and gradation were used with all cases, with the exception of binder type. The LTPPBIND[®] software (LTPPBIND[®], version 2.1, 1999) was used to determine the optimal binder grade at each geographical

location and traffic volume. For each state, the typical subgrade soil type was provided by the agencies as part of the survey, along with the resilient modulus.

The NCHRP 1-37A procedure requires the subgrade resilient modulus at optimum moisture and density. Alabama and Maryland’s DOT indicated in the survey that they do not seasonally adjust subgrade resilient modulus. Arizona and South Dakota did not provide this information, and Washington uses the effective or seasonally adjusted resilient modulus for subgrade materials. All values used in this study were taken as at optimum moisture and density because they were within expected ranges typical of their soil type found in the literature as well as in the NCHRP 1-37A software. The material properties used for the NCHRP 1-37A analyses in this study are summarized in Table 4.7 through Table 4.12.

Table 4.7. Asphalt concrete properties.

General properties	
Reference temperature (°F)	70
Poisson’s ratio	0.35
Volumetrics	
Effective binder content (%)	9
Air voids (%)	6.2
Total unit weight (pcf)	148
Gradation	
Cumulative % Retained 3/4 inch sieve	4
Cumulative % Retained 3/8 inch sieve	27
Cumulative % Retained #4 sieve	56
% Passing #200 sieve	6
Thermal properties	
Thermal conductivity asphalt (BTU/hr-ft-F°)	0.67
Heat capacity asphalt (BTU/lb-F°)	0.23

Table 4.8. Binder grade by state for low traffic case.

	Alabama	Arizona	Maryland	South Dakota	Washington
Binder grade	PG 70-16	PG 76-10	PG 64-22	PG 64-28	PG 64-22
A (correlated)	10.6410	10.0590	10.9800	10.3120	10.9800
VTS (correlated)	-3.5480	-3.3310	-3.6800	-3.4400	-3.6800

Table 4.9. Binder grade by state for moderate and high traffic cases.

	Alabama	Arizona	Maryland	South Dakota	Washington
Binder grade	PG 76-16	PG 82-10	PG 70-22	PG 70-28	PG 70-22
A (correlated)	10.0150	9.5140	10.2990	9.7150	10.2990
VTS (correlated)	-3.3150	-3.1280	-3.4260	-3.2170	-3.4260

Table 4.10. Granular base resilient modulus calculated from the 1993 AASHTO's structural layer coefficient.

	Resilient modulus (psi)
Alabama	40,000
Arizona	40,000
Maryland	23,000
South Dakota	21,000
Washington	28,000

Table 4.11. Granular aggregate base properties.

Strength properties	
Poisson's ratio	0.35
Coeff. of lateral pressure, Ko	0.5
Gradation and Plasticity Index	
Plasticity Index, PI	1
Passing #200 sieve (%)	10
Passing #4 sieve (%)	80
D60 (mm)	2
Calculated/derived parameters (level 3)	
Maximum dry unit weight (pcf)	122.3
Specific gravity of solids, Gs	2.67
Saturated hydraulic conductivity (ft/hr)	37
Optimum gravimetric water content (%)	11.2
Calculated degree of saturation (%)	82.8
Soil water characteristic curve parameters	
a, b, c	11.4; 1.72; 0.518
Hr	371

Table 4.12a. Subgrade properties.

	Alabama	Arizona	Maryland
AASHTO classification of soil	A-6	A-7-5	A-7-6
Strength properties			
Poisson's ratio	0.35	0.35	0.35
Coeff. of lateral pressure, K_0	0.5	0.5	0.5
Resilient modulus (psi)	7,500	12,000	5,000
Gradation and Plasticity Index			
Plasticity Index, PI	25	30	40
Passing #200 sieve (%)	80	85	90
Passing #4 sieve (%)	95	99	99
D60 (mm)	0.01	0.01	0.01
Calculated/derived parameters (level 3)			
Maximum dry unit weight (pcf)	100.8	97.1	91.3
Specific gravity of solids, G_s	2.75	2.75	2.77
Saturated hydraulic conductivity (ft/hr)	3.25×10^{-5}	3.25×10^{-5}	3.25×10^{-5}
Optimum gravimetric water content (%)	22.6	24.8	28.8
Calculated degree of saturation (%)	88.5	88.9	89.4
Soil water characteristic curve parameters			
a, b, c	174; 1.05; 0.707	301; 0.995; 0.732	750; 0.911; 0.772
Hr	8190	15700	47500

Table 4.12b. Subgrade properties. (cont.)

	South Dakota	Washington
AASHTO classification of soil	A-7-6	A-7-6
Strength properties		
Poisson's ratio	0.35	0.35
Coefficient of lateral pressure, K_o	0.5	0.5
Resilient modulus (psi)	7,500	7,500
Gradation and Plasticity Index		
Plasticity Index, PI	40	40
Passing #200 sieve (%)	90	90
Passing #4 sieve (%)	99	99
D60 (mm)	0.01	0.01
Calculated/derived parameters (level 3)		
Maximum dry unit weight (pcf)	91.3	91.3
Specific gravity of solids, G_s	2.77	2.77
Saturated hydraulic conductivity (ft/hr)	3.25×10^{-5}	3.25×10^{-5}
Optimum gravimetric water content (%)	28.8	28.8
Calculated degree of saturation (%)	89.4	89.4
Soil water characteristic curve parameters		
a, b, c	750; 0.911; 0.772	750; 0.911; 0.772
Hr	47500	47500

4.5.4. Performance Models and Criteria

Permanent deformation and “alligator” fatigue cracking are the distresses chosen to be evaluated in this study. The national calibration coefficients for the empirical distress models determined for these distresses at the end of NCHRP 1-37A were used in all cases. They are:

- Permanent deformation model
 - Asphalt concrete:
 - $k_1 = -3.4488$
 - $k_2 = 1.5606$
 - $k_3 = 0.4791$

- Granular base:
 - $k_1 = 1.6730$
- Subgrade:
 - $k_1 = 1.3500$
- “Alligator” fatigue cracking
 - $k_1 = 0.00432$
 - $k_2 = 3.9492$
 - $k_3 = 1.2810$

4.6. Results

The 1993 AASHTO designs are based on loss of serviceability. All structures were designed to have the same terminal serviceability equal to 2.0. The goal of the NCHRP 1-37A analyses was to evaluate how predictions of individual structural distresses varied in relation to traffic and environmental conditions for the selected states. The expectation is that the predicted distress magnitudes would be similar in all cases if the 1993 AASHTO guide correctly incorporates the influence of traffic level and environmental conditions. (The implicit assumption here is that the more sophisticated NCHRP 1-37A predictions represent the “correct” results.)

Subgrade resilient modulus and structural layer coefficients are responsible for incorporating the influence of environmental conditions in the 1993 AASHTO design method (other than for frost heave and/or swelling soils, which are treated separately in the procedure and are not considered here). The 1993 AASHTO guide recommends the use of a seasonally adjusted subgrade resilient modulus to reflect the effects of seasonal

variations in subgrade moisture content, winter freezing strengthening and spring thaw weakening. Most agencies surveyed did not report using an adjusted resilient modulus. There is also the drainage coefficient, which quantifies the layer's capacity for draining moisture. All 5 states surveyed reported a value of 1.0 – i.e., no modification of layer properties because of drainage – although some states implicitly include the effects of drainage in their unbound layer coefficients.

The influence of subgrade stiffness and base structural layer coefficient reflects directly on the base thickness design, as seen on Figure 4.6. The weakest subgrade case (Maryland) had the highest base thickness while the strongest subgrade case (Arizona) had the smallest base thickness. For the same subgrade conditions (Alabama and South Dakota), a higher base structural layer coefficient led to thinner layers, as expected.

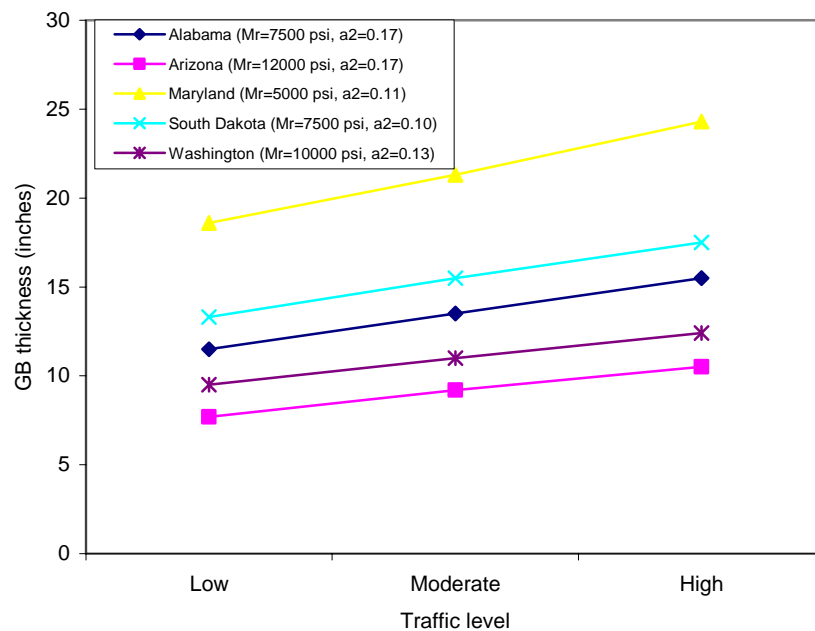


Figure 4.6. Granular base thickness design.

The designed asphalt concrete thicknesses vary over a significant smaller range, as summarized in Figure 4.7. The asphalt concrete thickness is influenced only by the

structural layer coefficients of the base and surface layers. The subgrade stiffness has no impact at all on the determination of the surface layer thickness at least when following strictly the 1993 AASHTO guide recommended procedure for computing layer thicknesses, described in Section 3.1.2. As an example, Alabama has a weak subgrade ($M_R=7,500$ psi) and Arizona a strong one ($M_R=12,000$ psi), but both have the same layer coefficients for the base and asphalt materials; as shown in Figure 4.7 the two cases have the same asphalt concrete thickness. However, the base layer in the Alabama design is thicker to compensate for the poorer subgrade support.

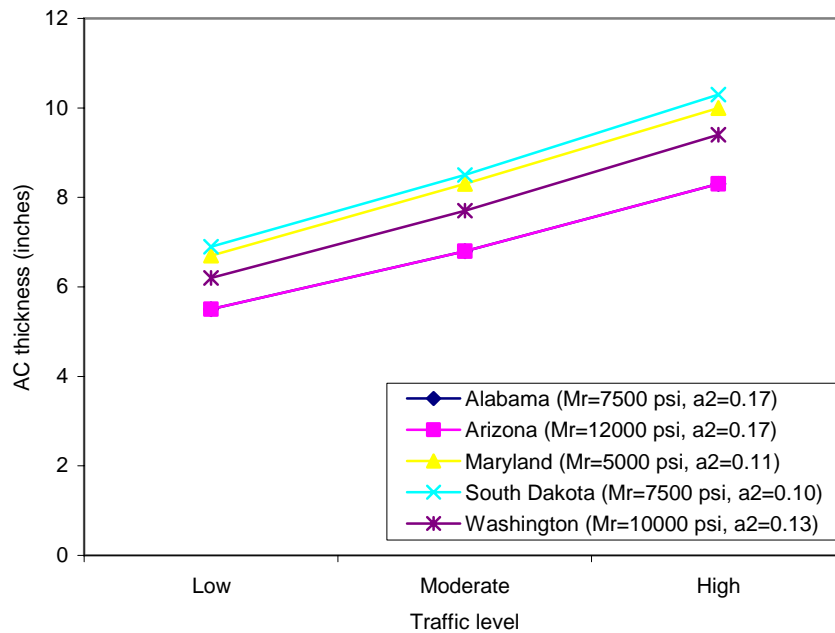


Figure 4.7. Asphalt concrete thickness design.

Figure 4.6 and Figure 4.7 illustrate that the base layer thickness is the only parameter in the 1993 AASHTO design solution that is sensitive to local subgrade condition. The calculation of asphalt concrete thickness is a function of the base layer characteristics only, regardless the subgrade stiffness. This design scheme assumption is not valid in all situations. Pavement sections with thick asphalt concrete or granular base

layers presumably have less interaction between the asphalt layer and the subgrade. However pavement sections with thin asphalt or granular base layers are likely to have more interaction between the layers and the subgrade stiffness in this case would be expected to strongly influence the required asphalt layer thickness.

Although all of the designs were based on the same Δ PSI, the individual distress predictions from the NCHRP 1-37A methodology showed much more variable behavior for rutting and fatigue cracking performance. Figure 4.8 through Figure 4.10 show that the NCHRP 1-37A performance predictions for each state were considerably different, considering the same traffic level and the same design performance. The variability of the predictions increased for moderate and high traffic levels. It can also be noted that the group of warm region states (Alabama and Arizona) had higher distress level predictions compared to the states in moderate to cold regions (Maryland, South Dakota and Washington). The expectation was that the NCHRP 1-37A predictions would have small variations in predicted performance if the 1993 AASHTO and NCHRP 1-37A design methodologies are compatible.

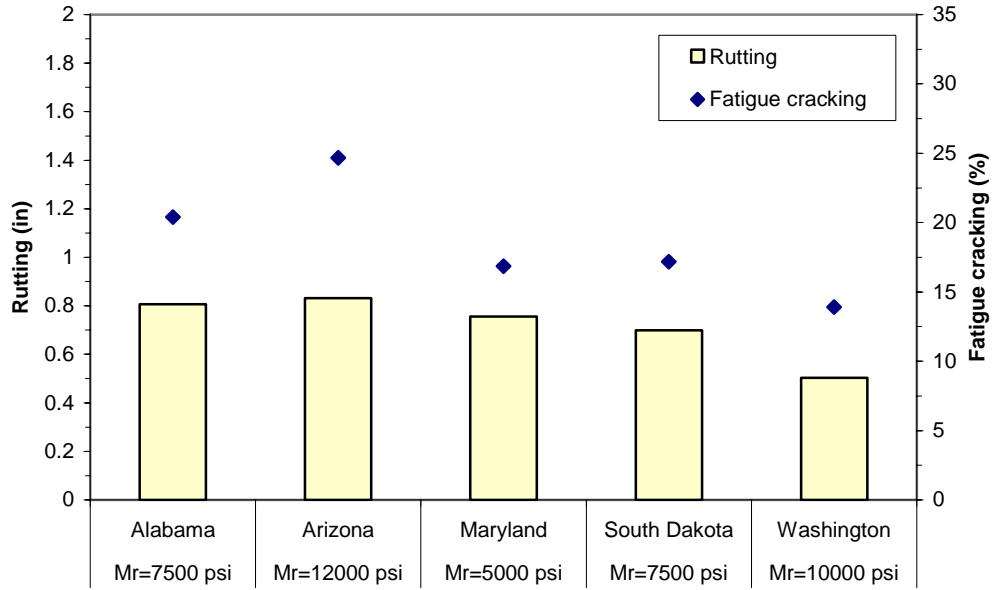


Figure 4.8. NCHRP 1-37A predictions for low traffic scenario.

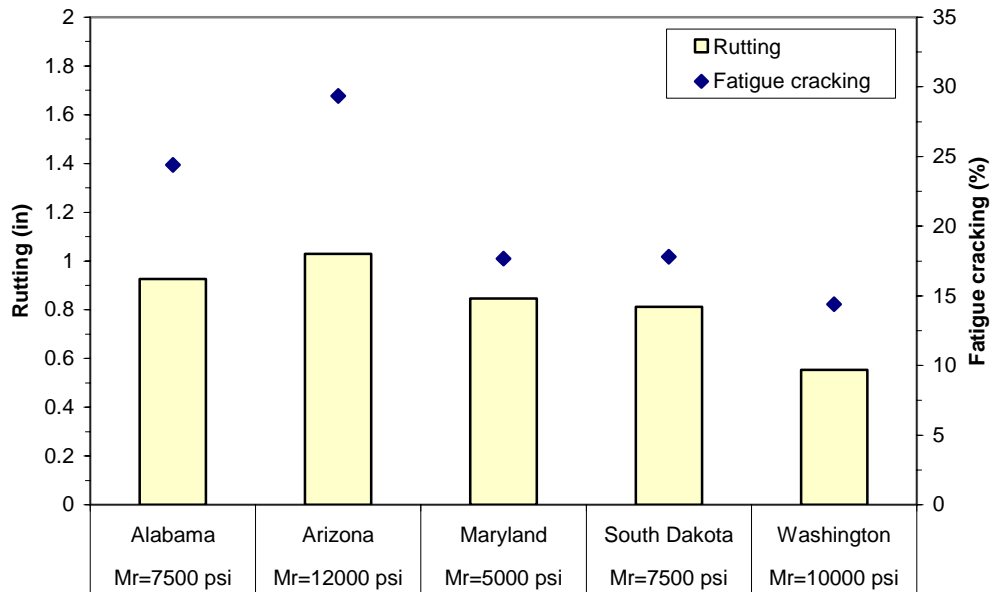


Figure 4.9. NCHRP 1-37A predictions for moderate traffic scenario.

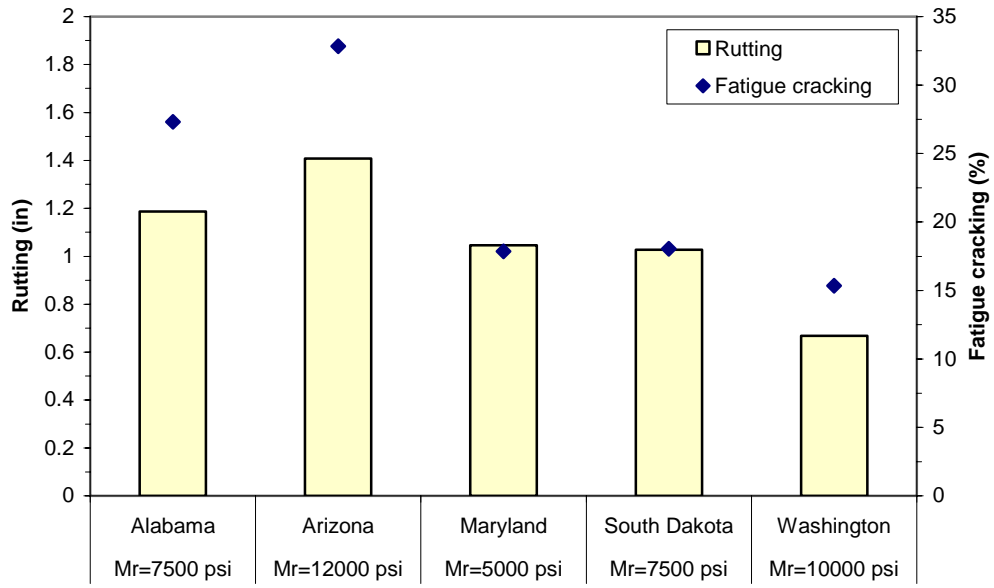


Figure 4.10. NCHRP 1-37A predictions for high traffic scenario.

The performance predictions for moderate and high traffic scenarios exceeded acceptable limits. In the case of rutting for example, a survey conducted by Witczak among pavement engineers in several state agencies suggests an acceptable total rutting limit of 0.5 inches on average, before adjustment for reliability (Witczak, 2004). The NCHRP 1-37A procedure recommends an acceptable total rutting limit of 0.75 inches after adjustment for reliability.

States located in the warmest zone (Alabama and Arizona) consistently had poorer performance than the other states located in mild to low temperature areas. The AASHO Road Test site, the data source for developing the 1993 AASHTO Guide, was located in Ottawa, IL, a low temperature region. The results here suggest that, at least according to the NCHRP 1-37A methodology, the 1993 AASHTO Guide overestimates the performance (or underestimates the required thickness) of pavement sections at locations having warmer temperatures than the original AASHO Road Test site.

It can also be noted from Figure 4.8 through Figure 4.10 that the performance consistently deteriorated as traffic increased in all five states. Figure 4.11 summarizes the NCHRP 1-37A predictions for the three traffic levels of all states in which it can be seen that performance consistently deteriorated for both rutting and fatigue cracking as traffic increased in all five states. These results suggest that the 1993 AASHTO guide overestimates pavement performance for traffic levels well beyond those experienced in the AASHTO Road Test (under 2 Million ESALs).

The alternate interpretation is that the NCHRP 1-37A methodology may be overestimating rutting and fatigue cracking, but this seems less likely given the larger set of field pavement sections incorporated in its calibration and the consistency within the predictions for the low traffic scenario at locations having moderate to low temperatures—i.e., for conditions similar to those in the original AASHTO Road Test results underlying the 1993 AASHTO guide.

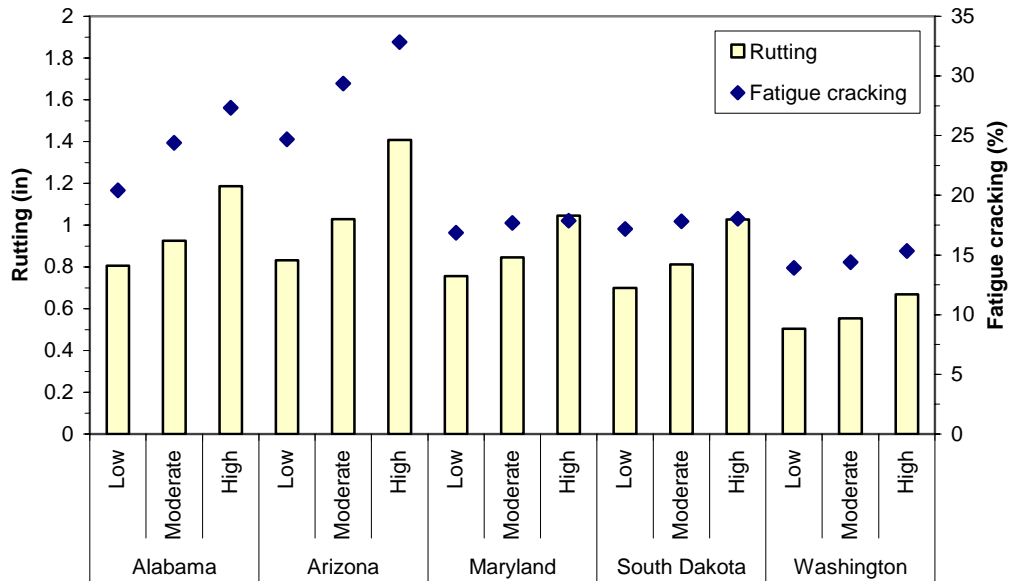


Figure 4.11. Summary of 1-37A predictions.

Traffic has always been a source of uncertainty in the 1993 AASHTO design procedure, especially for high traffic levels. The Figure 4.12 and Figure 4.13 respectively show the NCHRP 1-37A fatigue cracking and permanent deformation predictions versus traffic level for all states at a 95% design reliability level. The variability of the performance predictions increases as traffic level increases. According to the NCHRP 1-37A methodology, the variability observed in the Figure 4.12 and Figure 4.13 indicates that the 1993 AASHTO designs may be at least less reliable for high traffic levels than for low traffic. This observation is not entirely unexpected as the traffic level applied during the AASHO Road Test was a little less than two million ESALs. In addition, the perceived uncertainty of the 1993 AASHTO performance predictions for high traffic levels was arguably one of the main motivations for undertaking the development of the mechanistic-empirical alternative in NCHRP 1-37A project.

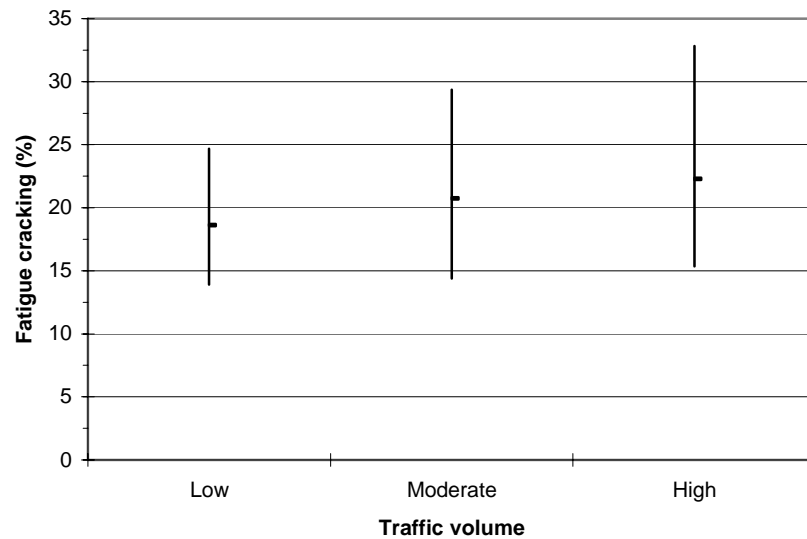


Figure 4.12. “Alligator” fatigue cracking predictions range.

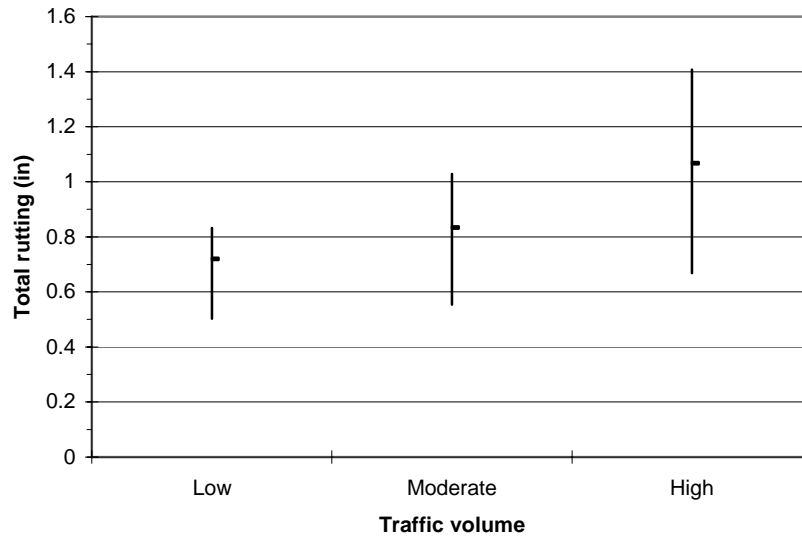


Figure 4.13. Permanent deformation predictions range.

The 1993 AASHTO guide and its earlier versions were developed from the AASHTO Road Test experiment data. As mentioned before, this experiment was conducted in one location with a small set of materials and limited traffic volumes. Since then, traffic has not only increased drastically in terms of volume, but it also has changed completely its configuration, with heavier and faster vehicles, different tires, tire pressures, and axle geometries.

In conclusion, different designs at the same serviceability in the 1993 AASHTO methodology had different performance predictions when evaluated using the NCHRP 1-37A procedure. The states with higher average temperatures had worse performance than those with mild to low average temperatures, indicating that the 1993 AASHTO Guide possibly overestimates the performance (or underestimates the required pavement thickness) for the warm locations.

When comparisons with traffic levels were made it was found that the performance predicted by the NCHRP 1-37A procedure deteriorated as traffic level

increased. The results also showed that performance prediction variability increased with increasing traffic level. The traffic analysis indicates that the 1993 AASHTO Guide may overestimate performance (or underestimate required pavement thickness) when traffic levels are well beyond those in the AASHTO Road Test.

The following chapter will concentrate on evaluating the NCHRP 1-37A procedure and the sensitivity of pavement performance to input parameters. The results are compared with field expectations for reasonableness.

Chapter 5: NCHRP 1-37A Performance Prediction Sensitivity to Parameters

Parametric studies are an important step in any implementation of the NCHRP 1-37A procedure as a new pavement design standard in highway agencies. The results and conclusions are useful for developing knowledge about the procedure, finding weaknesses and problems within the local agencies' practice that need to be addressed, and defining priorities for the implementation and calibration tasks.

The objective of the parametric study in this Chapter is to provide useful and relevant data analyses of performance prediction sensitivity to input parameters and to evaluate the results against engineering expectations of real field performance.

The pavement structure designed with the 1993 AASHTO guide for low traffic Maryland conditions (see Table 4.5) was the reference case for this parametric study. The variables selected for study were: asphalt and base layer thickness, traffic, environment, material properties, performance model parameters, and design criteria. Only level 3 inputs were used in this parametric study.

Parameters were varied by a percentage of their reference design values. When percentage variation was not possible, distinct cases were selected for comparison purpose (i.e., mixture type, vehicle class distribution, climate conditions, etc.).

5.1. Thickness

The thickness parametric study considered asphalt and base layers, with variations of 20% above and below the reference design – 6.7 inches and 18.6 inches respectively.

The results in Figure 5.1 indicate that base layer thickness has little influence on performance in the NCHRP 1-37A methodology. Alligator fatigue cracking slightly decreases with increased base thickness, while the permanent deformation variation was negligible. This result is significantly different from trends in the 1993 AASHTO guide, in which the base layer thickness has considerable influence on the structural number (SN) and consequently on PSI prediction.

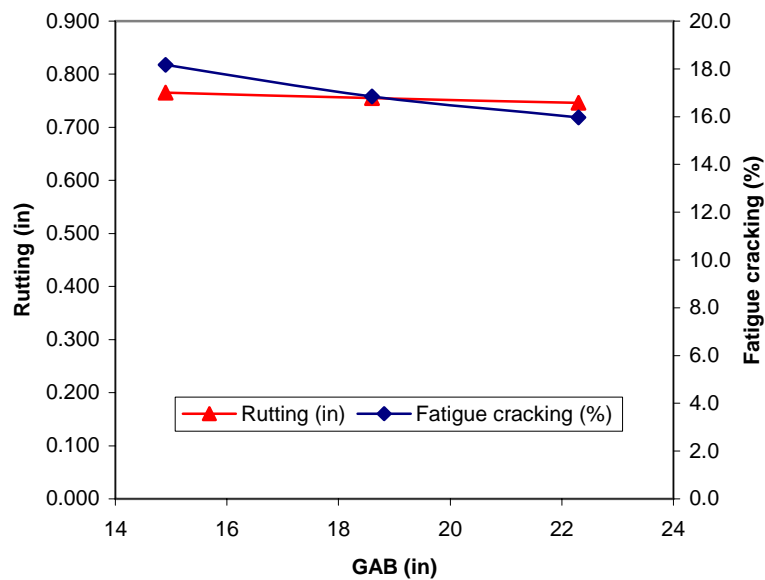


Figure 5.1. Sensitivity to base thickness.

The results shown in Figure 5.1 also contradict field expectations – it is believed that increasing the base layer thickness increases the overall pavement strength and consequently improves performance. However it can be shown that the NCHRP 1-37A results are a direct consequence of the multilayer linear elastic theory used for predicting stresses and strains within the pavement structure. For example, Figure 5.2 plots

horizontal tensile strains at the bottom of AC layer computed⁴ for the same structures analyzed in Figure 5.1. Only results at one set of elastic moduli are shown; similar results were also found for other moduli combinations corresponding to different months of the year. It can be seen in Figure 5.2 the variation in the tensile strains at the bottom of AC layer is negligible for variations up to 2 inches below and above the reference base thickness of 18.6 inches. The empirical model, described in Equation (3.21), shown again here as Equation (5.1), uses a power law correlating fatigue cracking and tensile strain (ϵ_t). Variation of the number of load applications to failure (N_f) is negligible for the very small tensile strain variations shown in Figure 5.2, which explains the small variation in the prediction of fatigue cracking observed in Figure 5.1.

$$N_f = \beta_{f1} k_1 (\epsilon_t)^{-\beta_{f2} k_2} (E)^{-\beta_{f3} k_3} \quad (5.1)$$

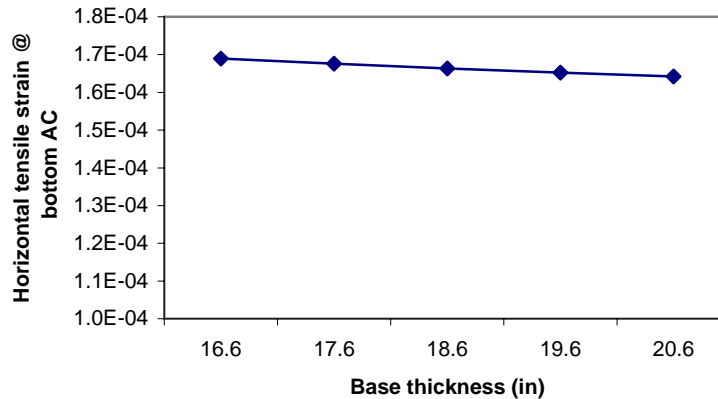
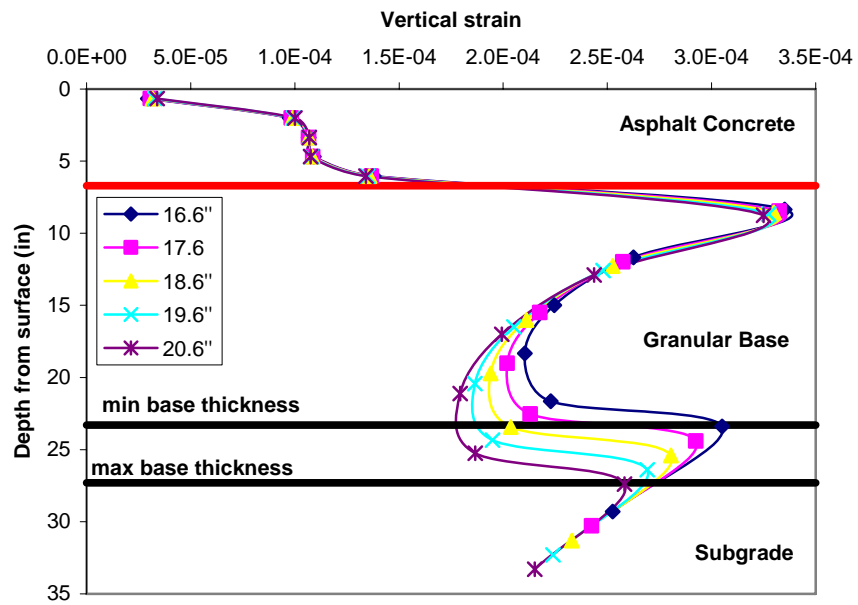


Figure 5.2. MLET calculated horizontal tensile strain versus base thickness.

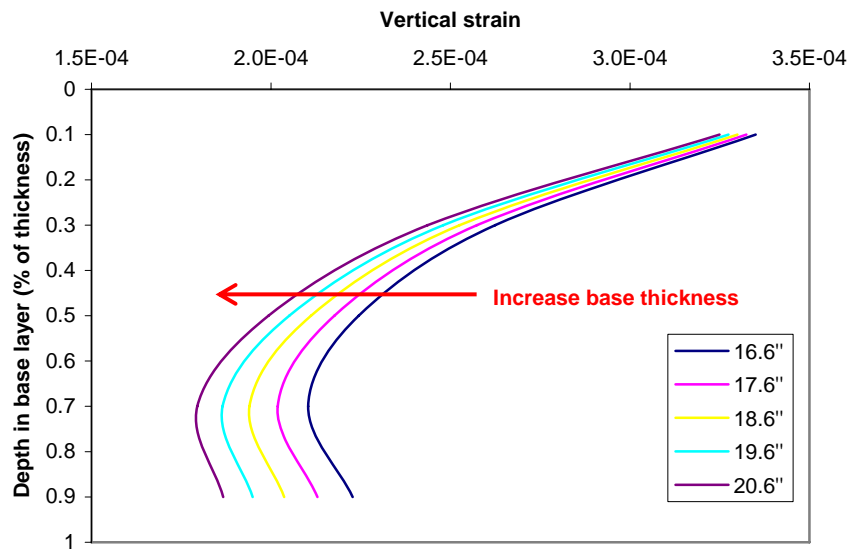
⁴ These strain calculations were done using the layer elastic analysis program LEAF, developed for use in the Federal Aviation Administration (FAA) airport pavement design and analysis application computer program (Hayhoe, 2002). LEAF code can be obtained in the internet for research use.

Following the same principle, Figure 5.3 shows (a) vertical compressive strain versus total pavement depth for base thickness variations up to 2 inches below and above the reference base thickness of 18.6 inches; and (b) vertical compressive strains in the base layer versus percentage depth of base thickness.

Figure 5.3(a) shows that the vertical compressive strain in the AC layer is insensitive to variations in base thickness. However, there is a reduction in strain levels within the base layer and at the top of the subgrade when the base thickness is increased. Figure 5.3(b) plots more clearly the effect of thicker base layers at normalized locations within the base layer. Figure 5.4 demonstrates that the NCHRP 1-37A rutting predictions are consistent with the strain trends in Figure 5.3. The compressive strains in the AC layer are essentially constant, and therefore the predicted rutting in the AC layer is also unvarying. The reduction in compressive strain in the base layer and the upper layers of the subgrade, showed in Figure 5.3(a), is counterbalanced by the nominal increase in base thickness. The net consequence is a reduction in subgrade rutting and a slight increase in base layer rutting.



(a)



(b)

Figure 5.3. MLET calculated vertical compressive strain versus pavement depth: (a) along the total thickness of the pavement; and (b) only base thickness, in percentage of total base thickness

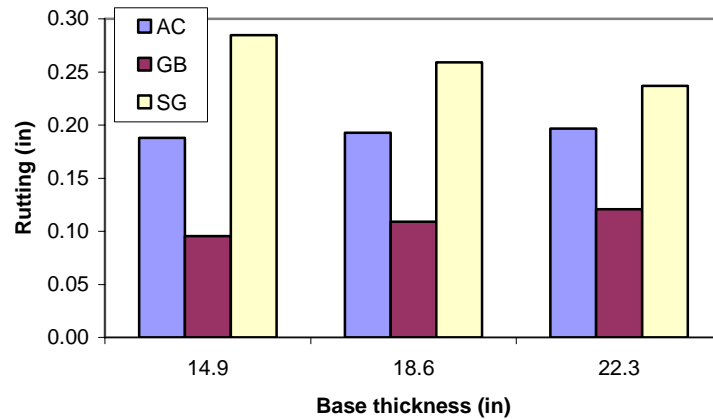


Figure 5.4. NCHRP 1-37A rutting predictions versus base thickness.

The same type of analysis was done varying the asphalt concrete layer thickness by 20% below and above the reference value of 6.7 inches. Figure 5.5 summarizes the results for fatigue cracking and rutting performance predicted by the NCHRP 1-37A procedure. In this case, the results are more consistent to what would be expected from the 1993 AASHTO guide and field performance.

The results showed in Figure 5.5 are also in agreement with MLET analysis. Increasing the AC thickness reduces the tensile strains at the bottom of the AC layer and consequently mitigates bottom-up fatigue cracking. The reduction in computed vertical compressive strains is much more pronounced in the case of AC thickness variation than in the case of base thickness variation. Increasing the thickness of the much stiffer asphalt layer reduces the vertical compressive strain in all layers underneath it, as oppose to what was observed in the base thickness scenario shown in Figure 5.3(a). Figure 5.6 shows that rutting is reduced in all layers when AC thickness increases.

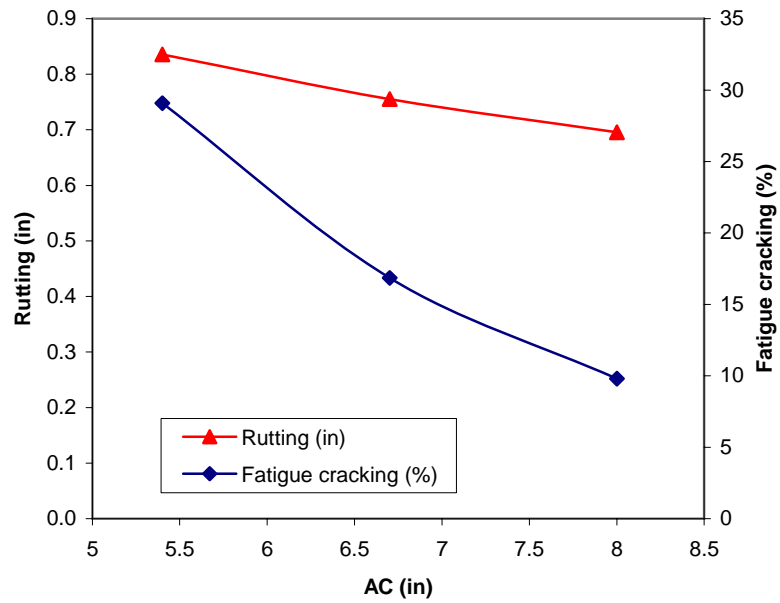


Figure 5.5. Sensitivity to AC thickness.

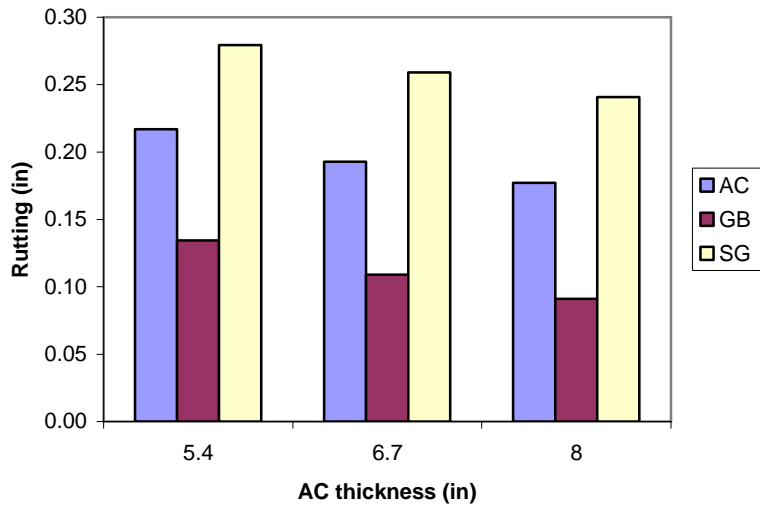


Figure 5.6. NCHRP 1-37A rutting predictions versus AC thickness.

The thickness analysis showed that NCHRP 1-37A M-E procedure emphasizes the structural contribution of the asphalt layer, a direct consequence of the multilayer linear elastic theory analysis. Das and Pandey (1999) found similar results. Using a

mechanistic-empirical design method for bituminous roads, they showed that large granular base layer thickness did not allow for much reduction in the asphalt layer thickness to meet the same performance criterion. Their results are in general agreement with NCHRP 1-37A predictions summarized in this study.

Evidently, when the base layer thickness is increased it is expected that the overall strength of the pavement will increase and performance will improve. The fact that this study showed a somewhat different trend with increasing base layer thickness may be a consequence of the simplifications implicit in linear elastic modeling of pavement materials.

5.2. Traffic

The comparison study presented in Chapter 4 demonstrated that performance predicted by the NCHRP 1-37A procedure deteriorated with increasing traffic levels for sections designed using the 1993 AASHTO guide (Figure 4.11). This section details traffic sensitivity and evaluates the influence of load spectra and vehicle class distribution on NCHRP 1-37A performance predictions.

The first exercise compared performance predictions using full load spectra and vehicle class distributions with simulations of ESALs. For the ESAL simulation, the default vehicle class distribution was modified to include only class 5 vehicles. This class of vehicle has only 2 single axles and is ideal to represent the standard single axle load of 18 kip. The load distribution was also modified so that only an 18 kip load level was considered in the axle load distribution. These two modifications guaranteed only a standard single axle would be used as the traffic loading.

The same 1993 AASHTO reference design for low traffic (3.8M ESALs) under Maryland conditions was used. The performance predictions from the regular axle load and vehicle class distributions for low volume roads were compared to the ESAL simulation. The annual average daily traffic (AADT) was adjusted to produce the target 3.8M ESALs at the end of the design period. Figure 5.7 shows predicted rutting for both cases. It can be seen that the full traffic load spectrum, although having the same equivalent number of ESALs, induces more rutting than the ESALs-only traffic (18 kip single axles only). Similar results were found during the development of the NCHRP 1-37A methodology; Figure 5.8 from El-Basyouny *et al.* (2005) shows that predicted AC rutting from traffic represented by standard 18 kip ESALs was less than that predicted using the full traffic load spectrum. Curiously, fatigue cracking sensitivity was negligible; Figure 5.9 shows almost identical results were found for the load spectrum and ESALs cases.

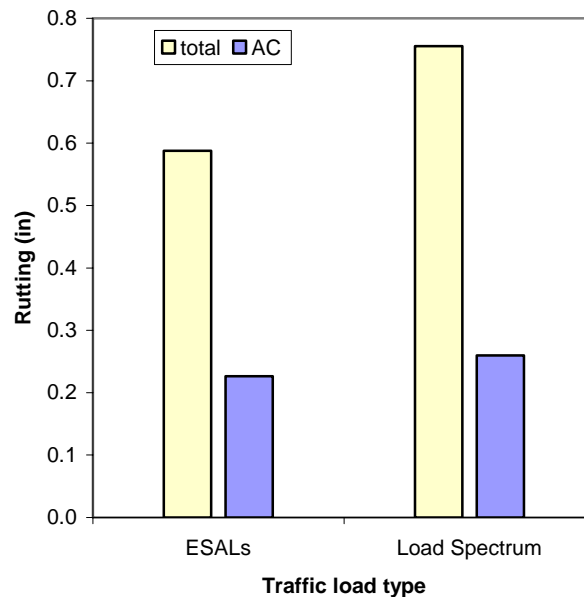


Figure 5.7. Rutting performance sensitivity to traffic load type at 15 years.

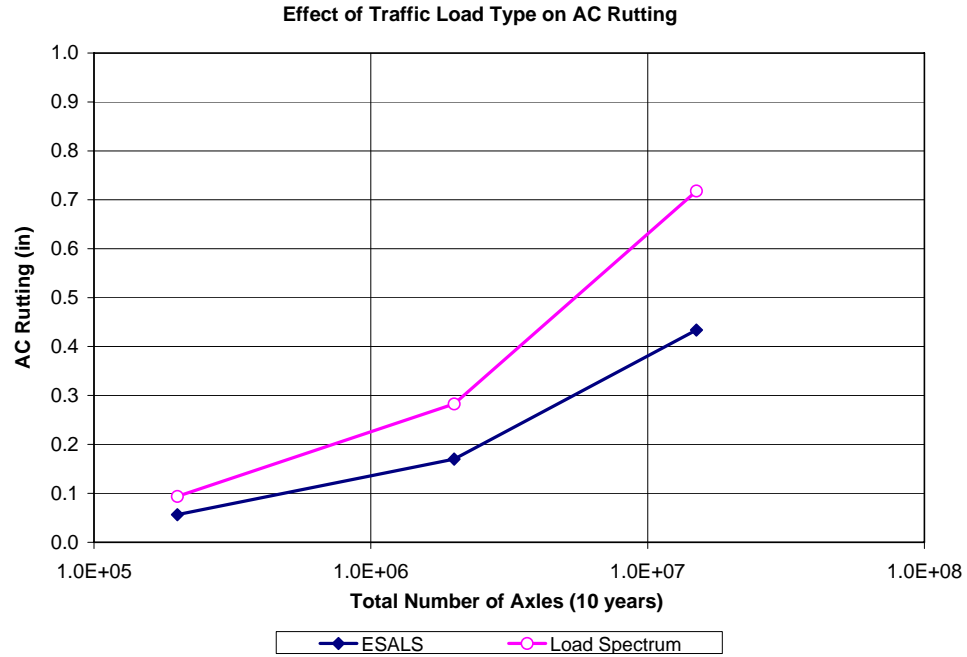


Figure 5.8. Effect of traffic load type on AC rutting (Basyouny et al., 2005).

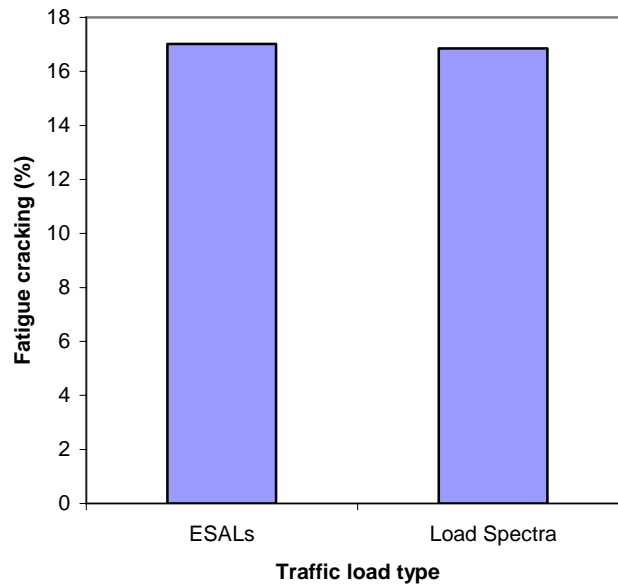


Figure 5.9. Fatigue cracking performance sensitivity to traffic load type at 15 years.

The sensitivity of performance predictions to vehicle class distribution was also evaluated. Traffic volume and other parameters (i.e., percentage in design direction and

lane, etc.) were kept constant. Only the distribution by vehicle class was altered. Three different default distributions from the NCHRP 1-37A software library were selected. The main difference between them was in vehicle classes 5 and 9, representing respectively single trucks and tractor-trailer combinations, the two most common truck types on highways in the U.S. Figure 5.10 summarizes vehicle class 5 and 9 distributions for the three different highway functional class used as examples in this study.

The predicted performance summarized in Figure 5.11 shows that rutting and fatigue cracking increased as the vehicle distribution changed from minor collector to principal arterial. This corresponds to an increase in the percentage of class 9 and a decrease in class 5 vehicles, and indicates that extra damage was caused by increasing the percentage of class 9 vehicles.

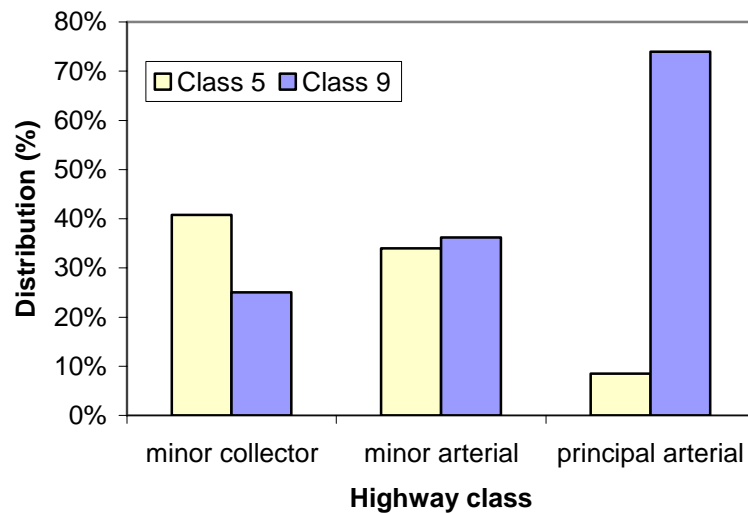


Figure 5.10. Class 5 and class 9 percentages for different vehicle distribution scenarios.

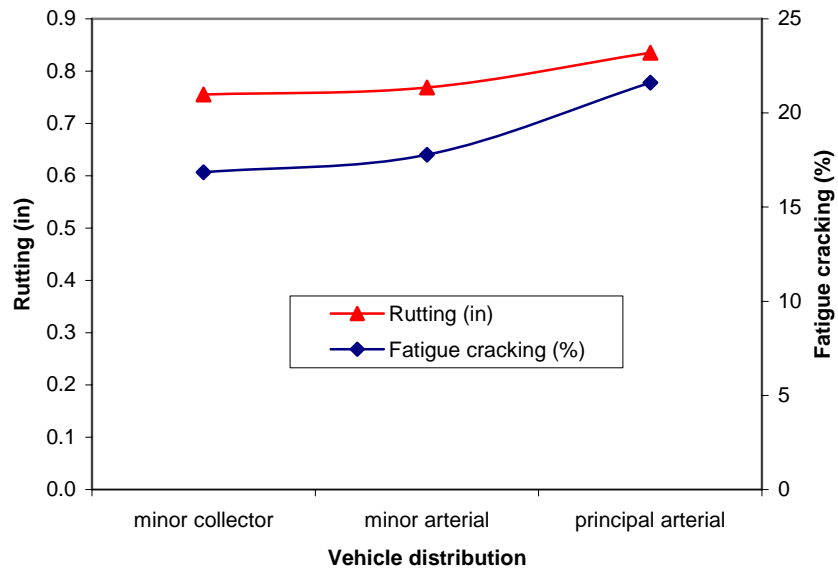


Figure 5.11. Performance for different vehicle class distributions.

Traffic data is a fundamental parameter for pavement design. Results shown earlier in Chapter 4 indicated that performance is very sensitive to traffic volume, as expected. In addition, the results from the present parametric study show the impacts that vehicle class and load distributions have on performance. The concept of equivalent traffic is not adequate for representing traffic loading in M-E designs for permanent deformation predictions. On the other hand, results for fatigue cracking predictions were very similar, which indicate that, for low traffic scenario and this environmental condition, equivalent traffic is suitable for this type of distress.

5.3. Environment

The climate effects were analyzed by simulating three different locations within the state of Maryland. These locations were chosen to represent the most significant local environmental variations. Although these locations are relatively close to one another,

their climate characteristics are sufficiently different to illustrate the effects of the Enhanced Integrated Climate Model (EICM) on a small region.

The climate condition on Maryland Eastern Shore is dominated by the Chesapeake Bay, its surrounding estuaries, and coastal plains. This region has on average warmer temperatures and more precipitation than the rest of the state – the annual average temperature is 56 °F and precipitation is on the order of 43 inches. As mentioned before in earlier chapters, temperature affects directly the stiffness of asphalt concrete mixtures, while moisture has impact on unbound material resilient modulus. These two effects combined affect the pavement performance.

The central region is characterized by the Piedmont Plateau; it is the intermediate climate condition, with annual average temperature in the order of 53 °F and precipitation around 40 inches. All Maryland designs in this parametric study were done for the central region location, unless otherwise stated.

The Blue Ridge Mountains and the Appalachian Mountains in the panhandle area of the west dominate the climate condition of the northwest region of the state. Annual precipitation is in the range of 36-38 inches (without considering snow precipitation) and average temperature around 51 °F. The temperature and precipitation ranges in the state are narrow, especially during the extreme seasons of winter and summer⁵.

All input variables in this exercise were kept constant. Only location and consequently environmental inputs were different, and the ground water table was 15 feet

⁵ Minimum and maximum average temperatures for the Eastern Shore region are respectively 25 and 88 °F; for the Central region are respectively 21 and 85 °F; and for the Mountains region, 19 and 85 °F. Source: U.S. Census Bureau Geography (www.census.gov) and Weather Base (www.weatherbase.com).

for all locations. According to LTPPBIND[®] software, the same binder grade was recommended for all three regions.

Figure 5.12 shows permanent deformation and fatigue cracking performance predictions for the reference design the in three different locations. The results agree with expectations. Performance is expected to decrease with increasing temperature and precipitation (for a fixed binder grade). The exception to this would be thermal cracking, which is not considered in this study

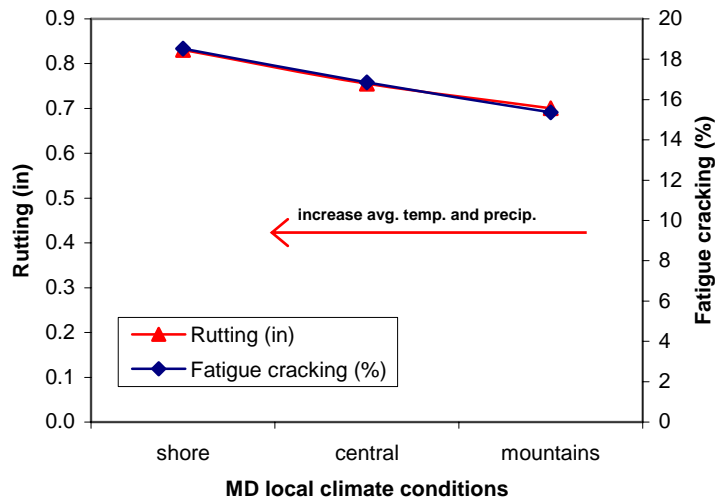


Figure 5.12. Sensitivity to local climate conditions.

Ground water table (GWT) depth is also a primary environmental input in the NCHRP 1-37A procedure, which is used along with the ICM file data (i.e., hourly observations of temperature, precipitation, wind speed, percentage sunshine, and relative humidity) by the environmental model (EICM) to predict temperature and moisture content variations within the pavement layers.

The GWT variations used for this sensitivity study were 3, 7 and 15 feet. The location was the Maryland central region. The results plotted in Figure 5.13 demonstrate that ground water table depth is not a significant parameter, at least for this particular

case in which frost/heave susceptibility is not an issue. Bottom-up fatigue cracking is slightly more sensitive than permanent deformation, but the overall trends are negligible. More conclusive research is required in locations where freeze/thaw cycles are more pronounced.

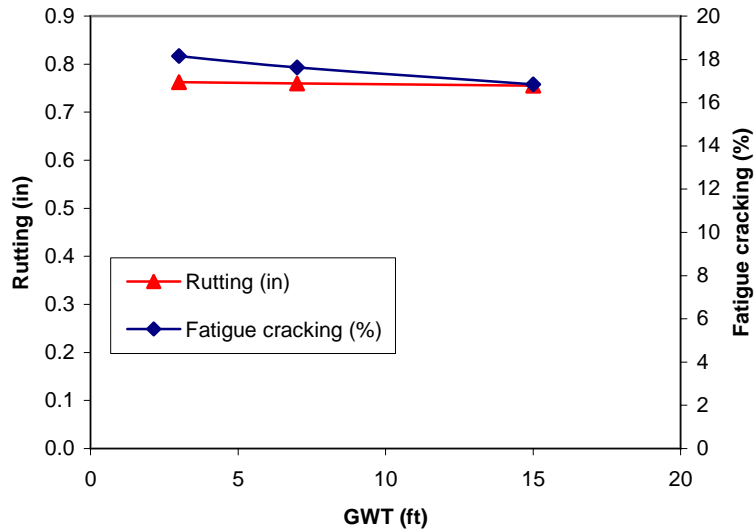


Figure 5.13. Sensitivity to ground water table.

5.4. Material Properties

Material characterization is one of the most significant input changes in the M-E design procedure. The pavement structural response models require more mechanical properties, as well as additional thermo-hydraulic properties for the climate models. This section describes the influence of basic material properties on performance prediction in the NCHRP 1-37A procedure. The main properties considered in this study are: volumetrics, gradation and binder type for asphalt concrete; and gradation, material classification, and resilient modulus for unbound base and subgrade. All analyses were done for level 3 inputs.

General properties, such as reference temperature and Poisson's ratio, were not included in this study and thus the values were kept equal to the default values provided by the NCHRP 1-37A software. Calculated/derived parameters typical of level 3 design for unbound materials (soil water characteristic curve, specific gravity, hydraulic conductivity, etc.) were also set to their default values.

5.4.1. Asphalt Concrete

Mix type, binder grade, and mix volumetrics (air voids and effective binder content) are the most important asphalt concrete mixture input properties. It has been demonstrated that mix type (represented by maximum aggregate nominal size), air voids, effective binder content and binder grade (through viscosity) are the most relevant parameters affecting the estimated dynamic modulus $|E^*|$ of an asphalt concrete mixture (Schwartz et al., 2006 – in preparation).

Figure 5.14 illustrates the sensitivity of dynamic modulus to different mixture parameters for three different temperature levels, in which NVE is the normalized variation of $|E^*|$ – the percentage variation in $|E^*|$ for 1% variation in the parameter. Viscosity is a function of binder grade and temperature. Percentage passing on sieve #4 (P4), #38 (P38), #34 (P34), and percentage retained on sieve #200 (P200) are the parameters representing the mixture aggregate gradation. Air voids (V_a) and effective binder volume (V_{beff}) completes the set of mixture parameters having the most influence on dynamic modulus.

Temperature is the parameter most affecting dynamic modulus of an asphalt concrete mixture. When temperature is fixed, as in Figure 5.14, viscosity then becomes

the leading factor affecting dynamic modulus. Volumetric parameters (V_{beff} and V_a) are the second and third, followed by aggregate gradation. These parameters were analyzed with the NCHRP 1-37A methodology to evaluate their influence on performance.

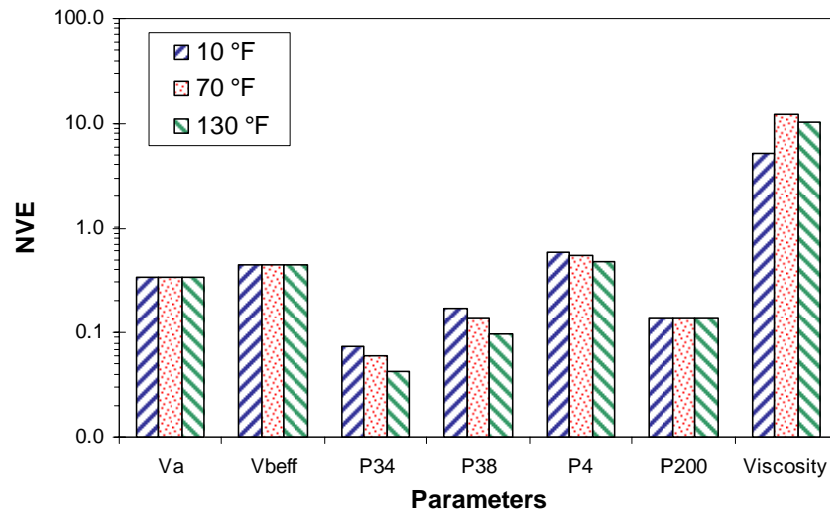


Figure 5.14. Sensitivity of predicted dynamic modulus to mixture inputs. (Schwartz et al., 2006 – in preparation)

Since the location and seasonal temperature variations are fixed for this exercise, the effects of binder viscosity were indirectly evaluated through variation of binder grade. Rutting and fatigue cracking performance was predicted for a 19mm dense graded asphalt mixture. Level 3 inputs are based on correlation between binder grade and A and VTS, the parameters describing the relationship between viscosity and temperature. These values are automatically selected in the software once the binder grade is chosen.

Figure 5.15 shows that fatigue cracking and rutting decrease with increasing binder grade (high temperature limit, in this case) – high grade binders are stiffer at high temperatures and have high viscosity values. These results agree with expectations. When binder grade increases, predicted rutting decreases.

In this particular example, fatigue cracking follows the same trend – it decreases with increasing binder grade. Although it is recognized that stiffer binders are more likely to experience cracking, this phenomenon is more pronounced in thin asphalt pavements. The pavement section used in this exercise consists of 6.7 inches of asphalt layer and 18.6 inches of granular base over the subgrade.

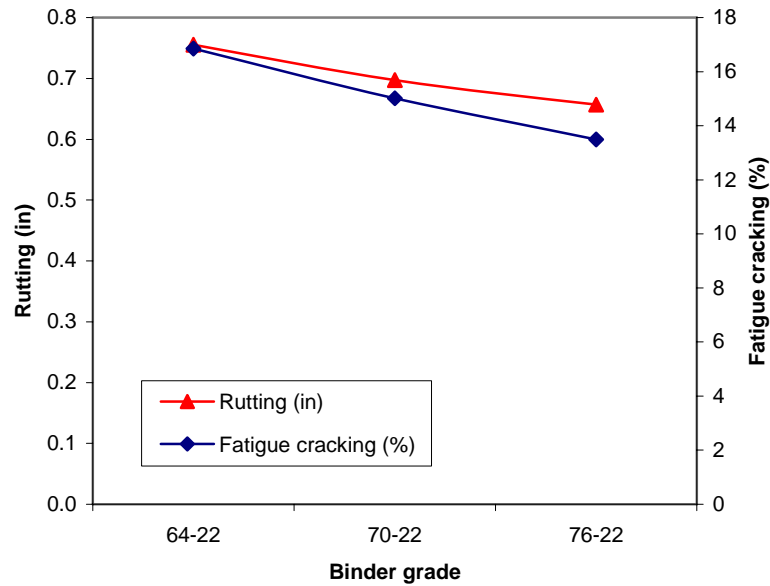


Figure 5.15. Sensitivity to binder grade.

Air voids and binder content are important sources of variability in construction and among the most influential parameters determining the mixture stiffness. One of the benefits of the M-E methodology is the ability to evaluate the effect of “as-constructed” conditions that are often different from the design assumptions. For this exercise, air voids and effective binder volume were each varied 10% above and below their base values. The performance predictions computed by the NCHRP 1-37A software versus variations of effective binder volume and air voids are shown in Figure 5.16 and Figure 5.17 respectively.

Figure 5.16 clearly shows that effective binder volume primarily affects fatigue cracking performance. The plot agrees with expectations. Mixtures rich in binder content have better tensile strength and better cracking performance. Conversely, it is expected that mixtures with high binder content have poor rutting performance. The dynamic modulus predictive equation, used in level 3 analysis in the NCHRP 1-37A procedure, captures the influence of excessive binder content by reducing the value of $|E^*|$. Low $|E^*|$ values applied in the MLET mechanistic model results in high compressive strain values and consequently more rutting. However this trend is not clearly observed in Figure 5.16.

Figure 5.17 illustrates the performance sensitivity to AC mixture air voids. The trends observed agree with expected field performance. Bottom-up cracks initiate at the voids under horizontal tensile stresses and propagate upwards following the stress path. Cracking initiation is more likely to occur when air voids increase in an asphalt mixture. The NCHRP 1-37A procedure is able to capture this behavior as observed in Figure 5.17.

Air voids are also expected affect permanent deformation. For example, lack of field compaction contributes to increased air voids in an asphalt concrete mat, and premature permanent deformation occurs as the mixture densifies. The expectation is that rutting increases with increasing air voids because the permanent deformations occurring at the earliest stage of loading are believed to be consequence of total or partial densification of the mixture. However, this trend is not evident in Figure 5.17.

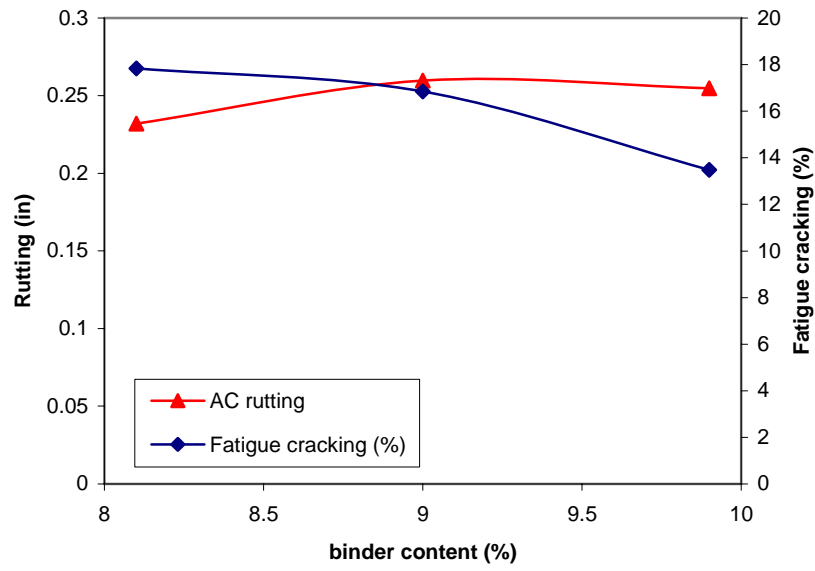


Figure 5.16. Sensitivity to effective binder content (% by volume).

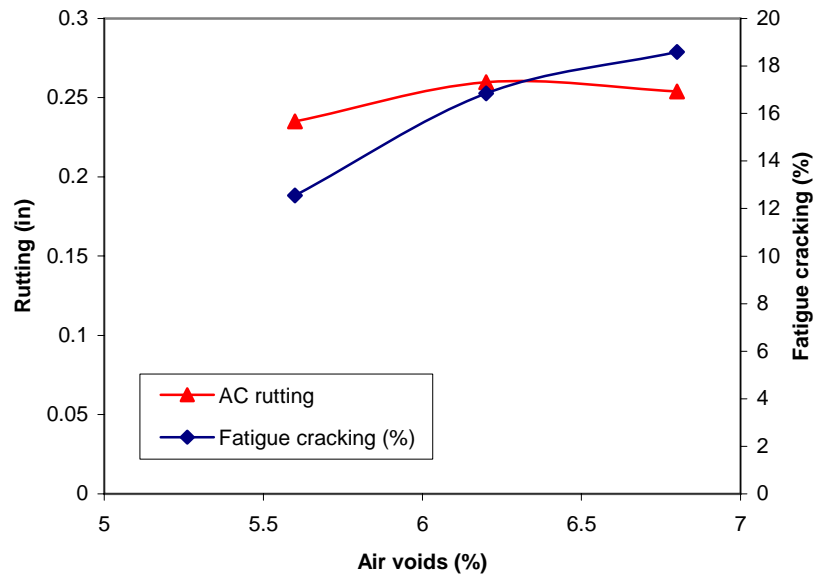


Figure 5.17. Sensitivity to air voids.

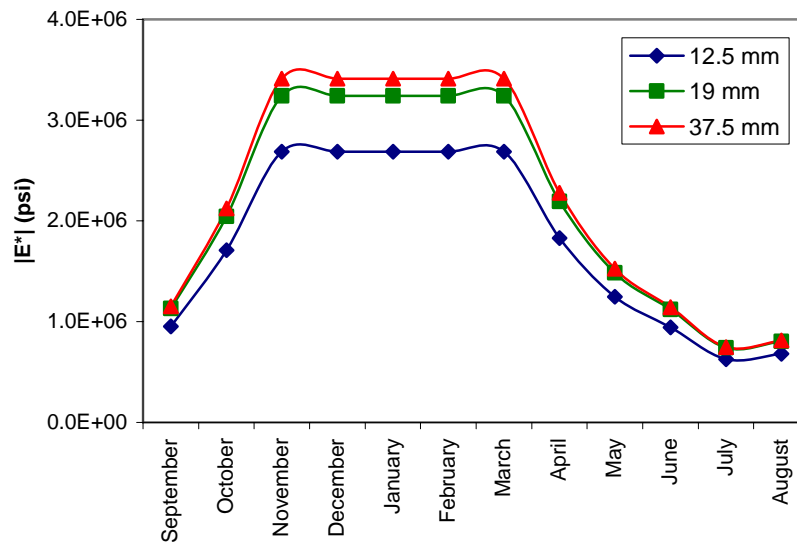
As indicated in Figure 5.14, mixture gradation influences stiffness and therefore performance. Gradation was evaluated for three dense graded mixtures plus one Stone Matrix Asphalt (SMA) mixture frequently used in the state of Maryland. The gradations

of these mixtures, summarized in Table 5.1, are representative of typical values commonly used in pavement projects throughout the state.

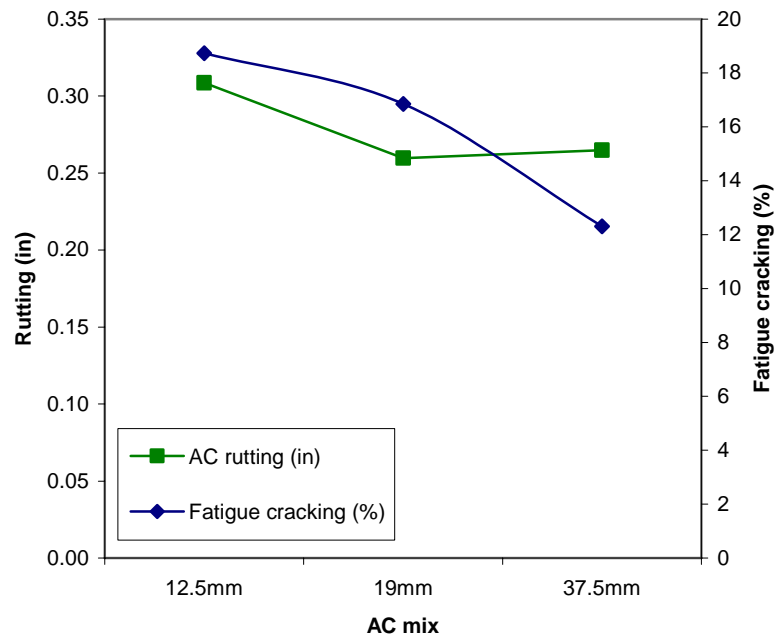
Table 5.1. AC mix properties.

	12.5 mm	19 mm (reference)	37.5 mm	19 mm SMA
Aggregate gradation				
% passing #34 (19mm)	100	96	78	100
% passing #38 (9.5mm)	83	73	55	63
% passing #4 (4.75mm)	46	44	27	27.4
% passing #200 (0.075mm)	3	6	4	8.5
Mix volumetrics				
Effective binder content, by volume (%)	9.1	9	10.1	12.1
Air voids (%)	6.2	6.2	5.8	3.6

All three dense graded mixtures were analyzed and compared. Figure 5.18(a) shows AC estimated dynamic modulus where it can be seen that stiffness increases with coarser mixtures—e.g., $|E^*|_{37.5}$ is higher than $|E^*|_{12.5}$ —implying better performance. Figure 5.18(b) shows that fatigue cracking performance follows this trend. The results were not as conclusive as for the rutting performance trends in Figure 5.18(b), although there is an improvement from the 12.5 mm mixture to the 19 mm.



(a)



(b)

Figure 5.18. (a) Year seasonal variation of predicted $|E^*|$; (b) Sensitivity to AC dense graded mixture type.

A comparison between a conventional dense graded mixture and Stone Matrix Asphalt (SMA) was also examined. The state of Maryland uses SMA in most of their high volume highway projects and the NCHRP 1-37A performance predictions for SMA mixtures are consequently of great importance. SMA is a gap-graded hot asphalt concrete mixture that has a large portion of coarse aggregates embedded in a rich mortar containing asphalt cement, filler, and additives (typically cellulose, mineral fibers, and/or polymers). The lack of intermediate aggregates is responsible for forming a stone-on-stone aggregate contact that provides strength, durability and rutting resistance (Brown and Cooley, 1999; Michael et al., 2003).

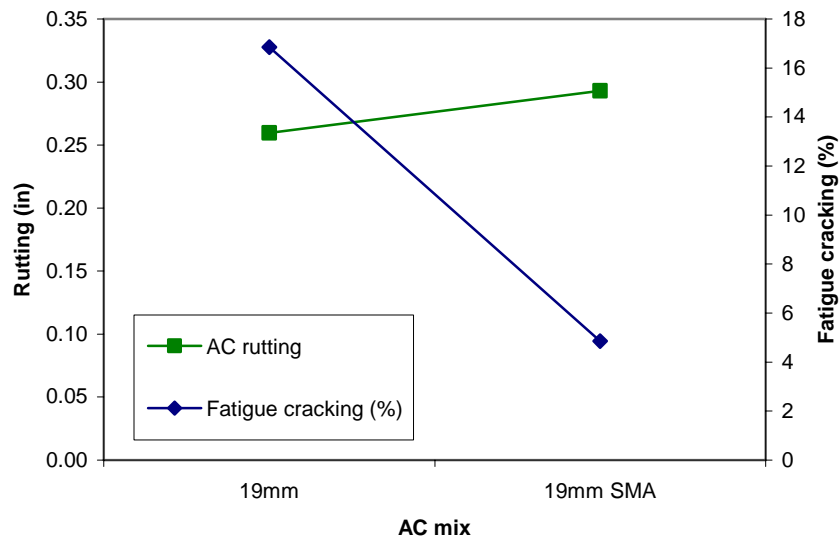
Examples of SMA's exceptional rutting performance can be found in the literature. Michael et al. (2003) summarized typical rutting performance of 86 Maryland

projects in service, with ages varying from 1 to 9 years, where measured total rut depth ranged from 0.05 to 0.20 inches – a good indication of SMA’s rut-resistance.

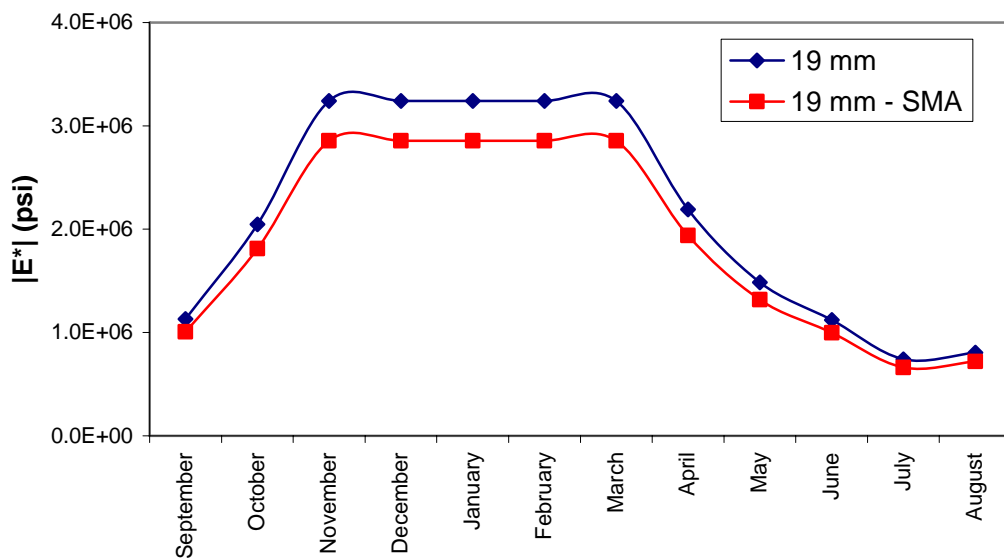
However, when SMA is analyzed using the NCHRP 1-37A procedure its rut-resistant benefits cannot be observed. Figure 5.19(a) illustrates the performance of a 19mm SMA mixture compared to an equivalent dense graded mixture. The SMA exhibits higher rutting than dense graded mixture, which contradicts field experience. Figure 5.19(b) shows seasonal variations of dynamic modulus for 19mm SMA and dense graded mixture. The dynamic modulus predicted in the NCHRP 1-37A methodology for SMA is lower than for the dense graded mixture, which is consistent with the lower rutting predicted for the dense graded mixtures.

The dynamic modulus of SMA mixtures measured in laboratory is lower than that of similar dense graded mixtures. One possible reason is the dynamic modulus testing protocol, in which the specimen is tested in unconfined conditions. Gap-graded mixtures like SMA depend more upon aggregate interlock derived from the stone-on-stone contact and as a consequence some researchers claim that testing under confined conditions is necessary to reflect realistically the true stiffness and strength of the material. The $|E^*|$ predictive model also has problems, as the database used for the model calibration includes only dense graded mixtures (see Section 3.2).

The principal conclusion drawn from this exercise is that the NCHRP 1-37A procedure in its present form cannot realistically predict the rutting performance of SMA mixtures. Continuing research on this subject includes the just-started NCHRP Project 9-30A to focus on improving the asphalt concrete rutting model in the NCHRP 1-37A procedure.



(a)



(b)

Figure 5.19. (a) Sensitivity to AC dense graded mixture and SMA; (b) year seasonal variation of predicted $|E^*|$.

From the parametric study of asphalt concrete properties, it can be concluded: (a) the NCHRP 1037A predicted performance trends agree with expected fatigue cracking performance for the variations in input parameters considered here; (b) the expected trends for permanent deformations could not be clearly observed in the NCHRP 1-37A

predictions; (c) NCHRP 1-37A rutting predictions do not capture the performance benefits of SMA mixtures; and (d) additional research is needed for the empirical asphalt concrete rutting model.

5.4.2. Unbound Materials

The fundamental unbound material property required for the NCHRP 1-37A procedure is the resilient modulus (M_R). For level 3 inputs, M_R is given as a default value at optimum density and moisture content for a given soil class.

Variations in the resilient modulus of the granular base and subgrade as well as different subgrade soil types were studied. The soil type also defines the default material properties required by the environmental model, including the soil-water characteristic curve, saturated hydraulic conductivity, and degree of saturation at equilibrium moisture conditions.

Base resilient modulus is intuitively expected to affect the overall pavement performance. Stiffer base layers reduce the tensile strains at the bottom of the asphalt layer, thus reducing fatigue cracking; vertical compressive strains are also reduced within the base layer and subgrade, consequently reducing permanent deformation. Figure 5.20 shows these trends for the NCHRP 1-37A predictions.

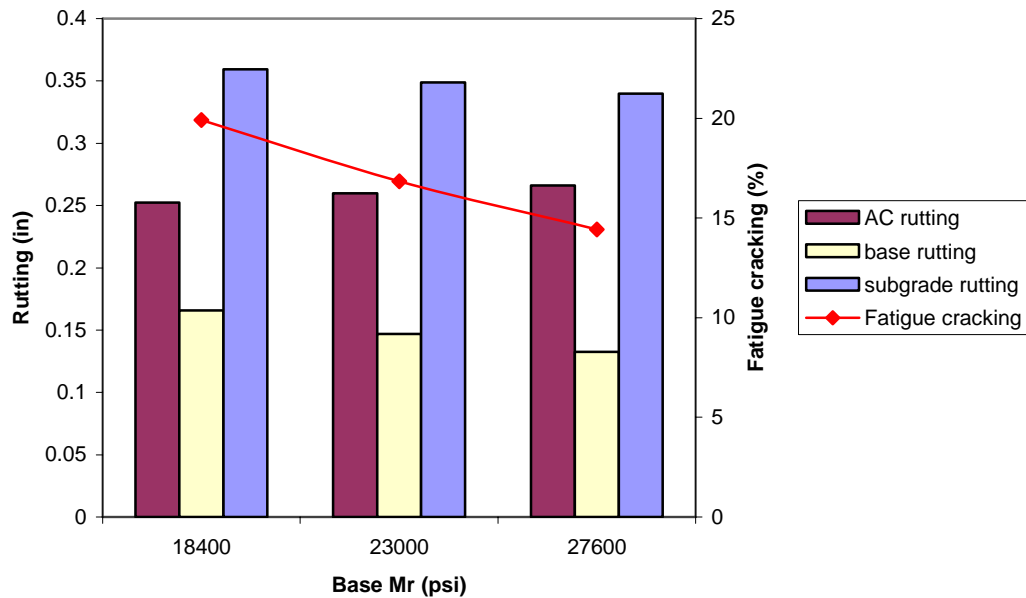


Figure 5.20. Sensitivity to granular base resilient modulus.

The reduction in permanent deformation is not as pronounced as in fatigue cracking. Figure 5.20 summarizes permanent deformation in each of the three layers. It is interesting to note the negligible reduction in AC rutting with variations in base layer resilient modulus. Due to the large $|E_{AC}|/M_{R,base}$ ratio, the influence of base layer modulus on the vertical compressive strains in the AC layer are only significant near its interface with the base layer. Figure 5.21 summarizes the vertical compressive strain profiles for different base resilient moduli for the reference case (Maryland – low traffic) computed using LEAF. The AC elastic deformations (vertical strains) are little affected by variations in base M_R , and thus the base M_R has little influence on rutting within the AC layer.

Conversely, horizontal tensile strains at the bottom of the asphalt concrete layer are more substantially affected by variations in the base resilient modulus, as

demonstrated in Figure 5.22 for the reference Maryland low traffic volume design. Variations in base resilient modulus therefore affects more fatigue cracking much more than AC permanent deformation as demonstrated in Figure 5.20.

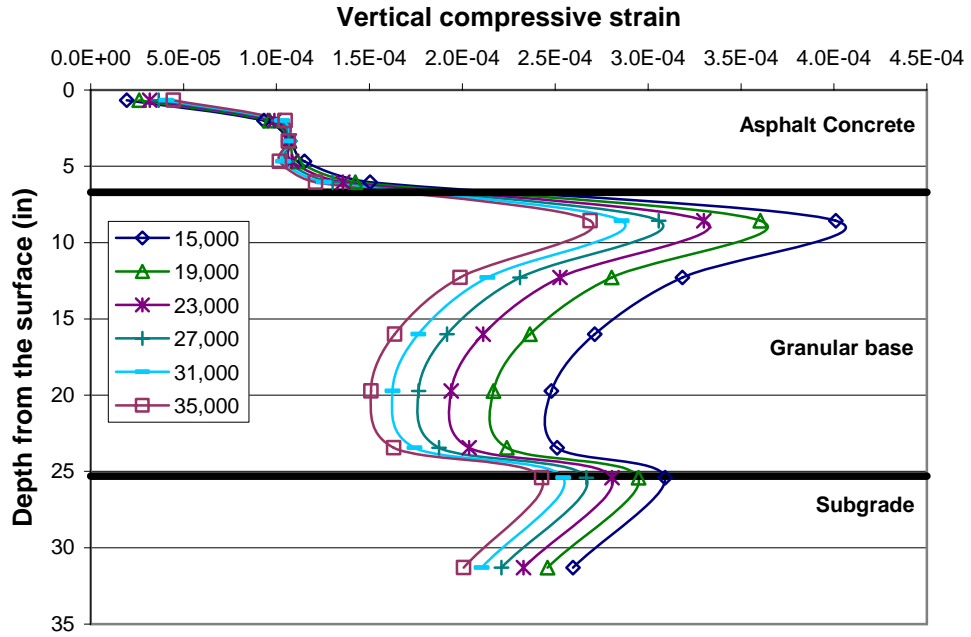


Figure 5.21. Multi-layer linear elastic computation of vertical compressive strains versus base M_R .

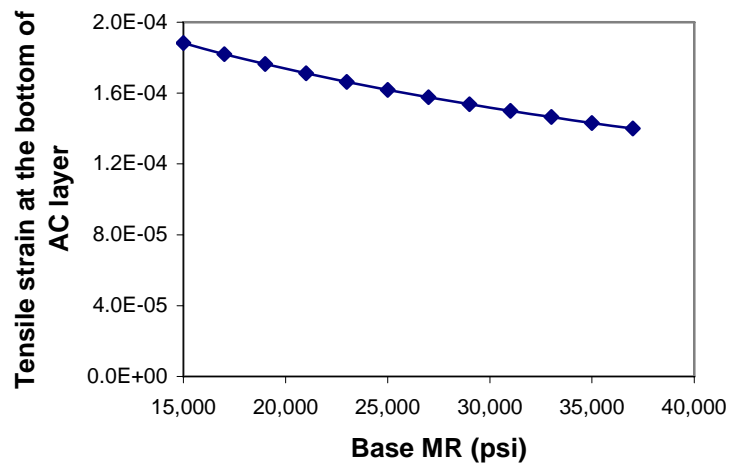


Figure 5.22. Multi-layer linear elastic computation of horizontal tensile strain at the bottom of AC layer versus base M_R .

Subgrade resilient modulus is also an important parameter affecting pavement performance. Figure 5.23 shows NCHRP 1-37A predicted performance for different subgrade M_R values. It can be seen that weaker subgrades, represented by low M_R values, are associated with poorer performance; fatigue cracking and rutting decrease with increasing subgrade stiffness, which agrees with expectations. The effect of subgrade stiffness on rutting is slightly larger than on fatigue cracking.

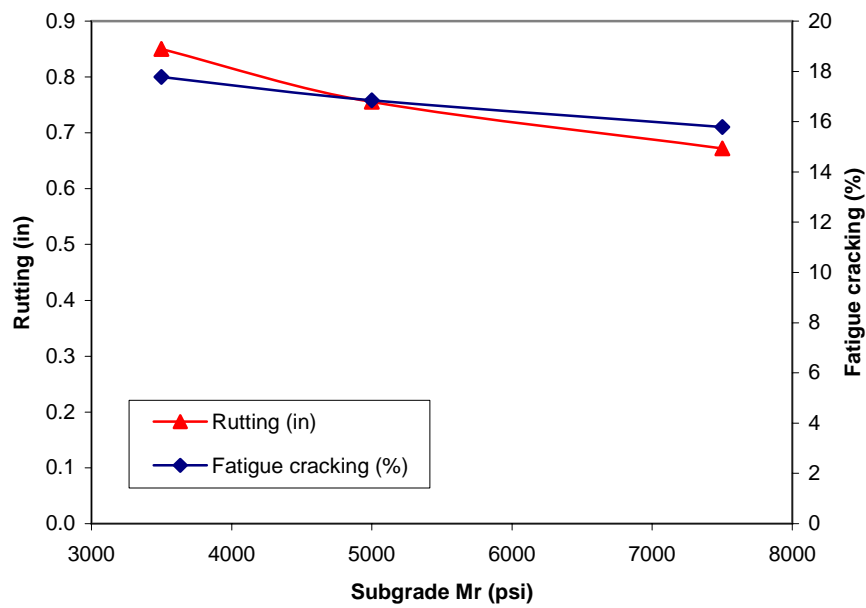


Figure 5.23. Sensitivity to subgrade resilient modulus.

The last unbound material property considered in this sensitivity study was soil type. Soil type affects default thermo-hydraulic properties and soil characteristics like specific gravity and equilibrium degree of saturation. Three subgrades were selected for this evaluation: (a) the default subgrade, an A-7-6 clay soil; (b) an A-5 silty soil, and (c) an A-2-4 silty-sand soil. The resilient modulus was kept constant at 5,000 psi for all 3 soil types. The results in Figure 5.24 show the sensitivity of permanent deformation and fatigue cracking to soil type. It is very difficult to evaluate reasonableness for these

results. There are no field studies where the same structure is evaluated over different subgrade types for the same subgrade stiffness and environmental conditions.

Nevertheless, the results show that the NCHRP 1-37A procedure is capable of capturing some influence of different subgrade types beneath the pavement section.

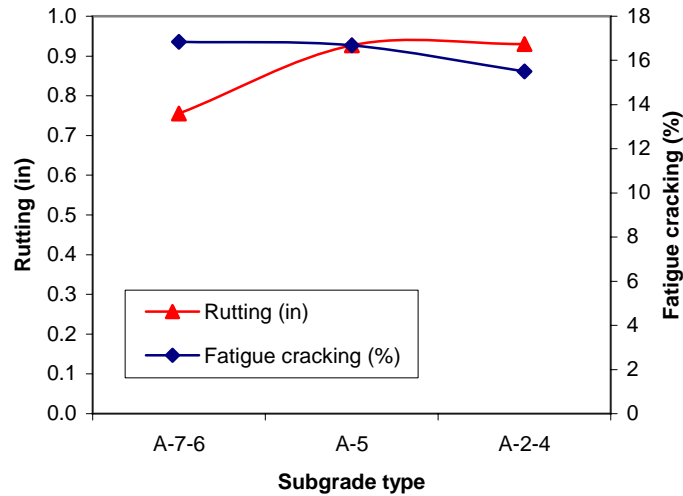


Figure 5.24. Sensitivity to subgrade type.

The parametric study of unbound material properties shows that the NCHRP 1-37A performance predictions are generally consistent with expectations. The results are also consistent with the implications of multi-layer linear elastic theory for pavement responses. The NCHRP 1-37A performance predictions are sensitive to basic unbound material properties.

5.5. Empirical Performance Model Calibration

The empirical models in the NCHRP 1-37A procedure are based on laboratory simulations of field conditions. This work was done prior to NCHRP 1-37A, and the existing models from the literature were evaluated and adapted for the NCHRP 1-37A

needs. Once calibrated in the laboratory (“as-published” in the literature), field calibrations were required to adjust the predictions to measured performances.

The field calibration was done using LTPP sections with performance measurements of several distresses commonly found in flexible pavements. This national calibration used sections selected throughout the country to cover all climatic zones and a wide variety of pavement sections.

The empirical performance prediction models are the weak link in any M-E design methodology. They are developed from field performance measurements and normally are based on nonlinear regression formulations. Results from empirical models are strictly adequate only for similar conditions and materials as used for the calibration.

The calibration coefficients of the models used for predicting permanent deformation and bottom-up fatigue cracking are evaluated in this section with the objective to assess the overall sensitivity of predicted performance to the calibration coefficients.

Rutting

The permanent deformation empirical models, described earlier on in Section 3.2.4, are reproduced here in Equations (5.2) to (5.5). The rut depth for an asphalt layer is computed as:

$$RD_{AC} = \sum_{i=1}^N (\varepsilon_p)_i \cdot \Delta h_i \quad (5.2)$$

in which:

RD_{AC} = rut depth at the asphalt concrete layer

N = number of sublayers

$(\varepsilon_p)_i$ = vertical plastic strain at mid-thickness of layer i

Δh_i = thickness of sublayer i

The plastic strain within each sublayer is determined from the following empirical equation:

$$\frac{\varepsilon_p}{\varepsilon_r} = \beta_{\sigma_3} \left[\beta_1 10^{-3.4488} T^{1.5606} \beta_2 N^{0.4791} \beta_3 \right] \quad (5.3)$$

in which:

ε_p = vertical plastic strain at mid-thickness of sublayer i

ε_r = computed vertical resilient strain at mid-thickness of sublayer i for a given load

β_{σ_3} = function of total asphalt layers thickness and depth to computational point, to correct for the confining pressure at different depths.

$\beta_1, \beta_2, \beta_3$ = field calibration coefficients

T = temperature

N = number of repetitions for a given load

The depth correction factor is determined using the following empirical expression:

$$\beta_{\sigma_3} = (C_1 + C_2 \cdot depth) \cdot 0.328196^{depth} \quad (5.4a)$$

$$C_1 = -0.1039 \cdot h_{AC}^2 + 2.4868 \cdot h_{AC} - 17.342 \quad (5.4b)$$

$$C_2 = 0.0172 \cdot h_{AC}^2 - 1.7331 \cdot h_{AC} + 27.428 \quad (5.4c)$$

in which:

$depth$ = depth from the pavement surface to the point of strain calculation

h_{AC} = total thickness of the asphalt layers

The permanent deformation for the unbound base layer is determined using the following empirical relation:

$$\delta = \beta_1 \cdot 1.673 \cdot \left(\frac{\varepsilon_0}{\varepsilon_r} \right) e^{-\left(\frac{\rho}{N}\right)^\rho} \varepsilon_v h \quad (5.5)$$

in which:

δ = permanent deformation for sublayer i

β_1 = field calibration coefficient

$\varepsilon_0, \beta, \rho$ = material properties (NCHRP 1-37A report, 2004)

ε_r = resilient strain imposed in laboratory test to obtain the above material properties, ε_0, β , and ρ

N = number of repetitions of a given load

ε_v = computed vertical resilient strain at mid-thickness of sublayer i for a given load

h = thickness of sublayer i

For both asphalt and base layer models, the field national calibration values are equal to 1. They were varied 10% above and below these values for this parametric study. Figure 5.25 and Figure 5.26 show percentage of rutting variation versus percentage of calibration coefficient variation for the asphalt concrete and base layer calibration coefficients, respectively. Each coefficient was varied separately from the others and the results reflect the percentage change in performance compared to the unchanged condition.

According to Figure 5.25, a small variation in any one of the calibration coefficients in the asphalt concrete rutting model has a substantial impact on the

performance predictions. Conversely, Figure 5.26 illustrates that the unbound rutting model is less sensitive to calibration coefficient variation. Moreover, the calibration of the unbound rutting model is only able to shift the values, but there is no possibility for adjusting the rate of deformation over the design period.

This exercise had the objective of evaluating the sensitivity of the rutting models to the field calibration coefficients, as defined in the NCHRP 1-37A report. It is important to observe that, not only are the predictions sensitive to the field calibration coefficients, the calibration process itself is also very difficult.

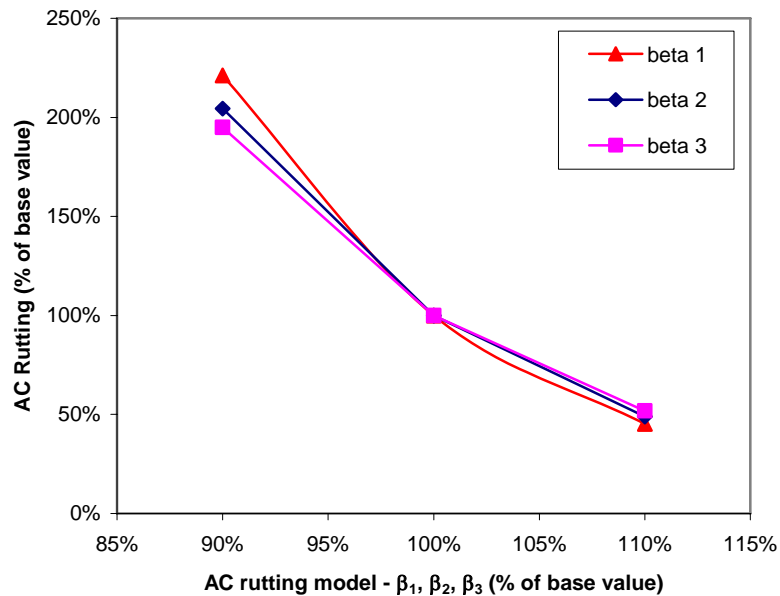


Figure 5.25. Sensitivity to AC rutting model calibration coefficients.

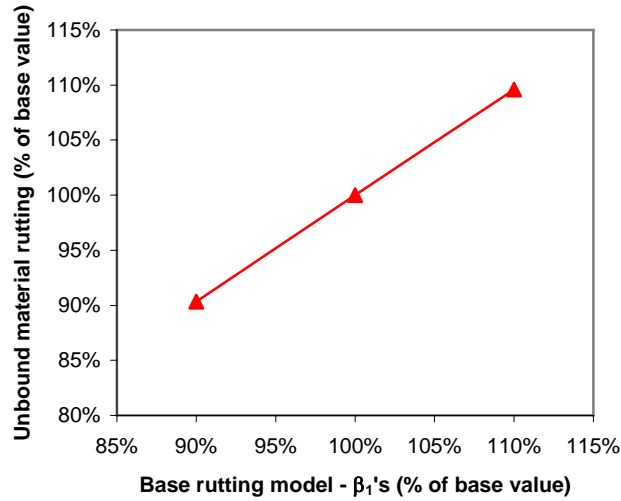


Figure 5.26. Sensitivity to base layer rutting model calibration coefficient.

Alligator Fatigue Cracking

The fatigue cracking model is defined in terms of number of load repetitions to failure as given by Equation (3.21), described earlier in Section 3.2.4, and reported here as Equation (5.6):

$$N_f = k_t \left[0.00432 \cdot \beta_1 C (\varepsilon_t)^{-\beta_2 \cdot 3.9492} (E)^{-\beta_3 \cdot 1.281} \right] \quad (5.6)$$

in which:

N_f = number of repetitions of a given load to failure

k_t = correction factor for different asphalt layer thickness effects

$\beta_1, \beta_2, \beta_3$ = field calibration coefficients

C = laboratory to field adjustment factor

ε_t = tensile strain at the critical location within asphalt concrete layer

E = asphalt concrete stiffness at given temperature

The thickness correction factor for fatigue cracking is computed using the following equation:

$$k_t = \frac{1}{0.000398 + \frac{0.003602}{1 + e^{(11.02 - 3.49 * h_{AC})}}} \quad (5.7)$$

in which:

h_{AC} = total AC thickness

The number of load repetitions is converted into damage using the Miner's Rule:

$$D = \sum_{i=1}^T \frac{n_i}{N_{fi}} \quad (5.8)$$

in which:

D = damage

T = total number of seasonal periods

n_i = actual traffic for period i

N_{fi} = traffic repetitions of a given load to cause failure at period i

And finally damage is converted into cracking area using the following equation:

$$FC = \left(\frac{C_4}{1 + e^{(C_1 C_1' + C_2 C_2' \log(D-100))}} \right) \cdot \left(\frac{1}{60} \right) \quad (5.9a)$$

$$C_2' = -2.40874 - 39.748(1 + h_{AC})^{-2.856} \quad (5.9b)$$

$$C_1' = -2C_2' \quad (5.9c)$$

in which:

FC = "alligator" fatigue cracking (% of total lane area)

C_1, C_2, C_4 = constants

D = damage

h_{AC} = total AC thickness

The fatigue model in its current configuration can only be calibrated through Equation (5.6). The coefficients β_1 , β_2 , and β_3 were varied 10% above and below the default value, which is 1 for the national calibration.

The results in Figure 5.27 show percentage of fatigue cracking variation versus percentage of calibration coefficient, and except for β_1 the predictions are very sensitive to calibration coefficients. The observed distress is fatigue cracking expressed as a percentage of total lane area, and the calibration is done on the number of loads to failure – Equation (5.6). This calibration process requires an optimization algorithm to obtain satisfactory results.

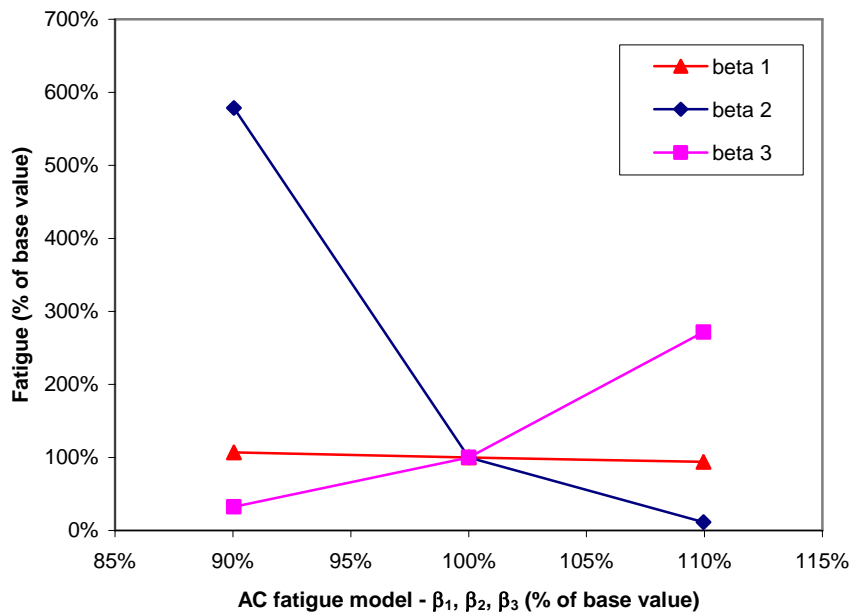


Figure 5.27. Sensitivity to fatigue cracking model calibration coefficients.

The parametric study shown in this section was an attempt to evaluate the influence of field calibration coefficients on performance predictions. The asphalt

concrete rutting model, in its current version, is very sensitive to field calibration coefficients. Adjustments in these coefficients modify not only the rutting prediction value but also the rate of rutting over time. Conversely, the rate of base rutting performance over time cannot be modified, but only shifted which limits its practicality. It is also important to emphasize that regardless the calibration process used, trench data are essential. Without trench data, total rutting must be allocated over the layers based on *ad hoc* assumptions, which introduces substantial uncertainties to the calibration process.

The fatigue cracking model is calibrated by adjusting the predictive equation for the number of given loads to failure. However, cracking is measured as a percentage of total lane area. This incompatibility requires an optimization process for calibrating the relationship between damage and cracked area in the fatigue cracking model.

In addition to field calibration, laboratory testing can be used to calibrate the models for different asphalt concrete mixtures or granular base materials. A database of calibrated coefficients can be constructed for routine design purposes.

5.6. Service Life

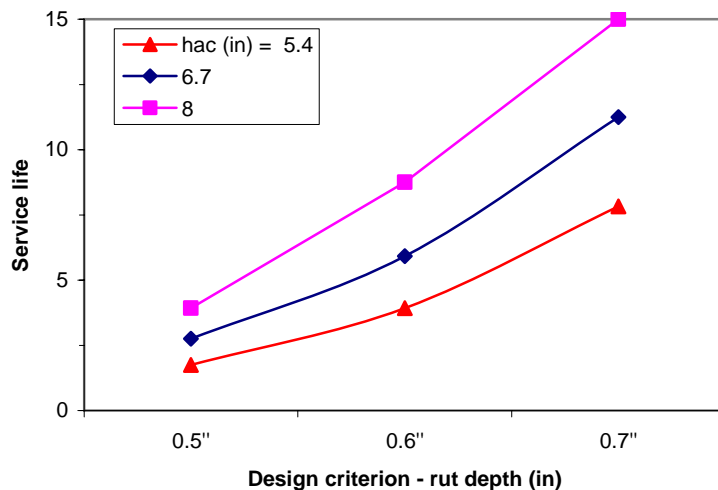
The parametric study in the previous sections had demonstrated the sensitivity of predicted performance to some of the parameters required for the NCHRP 1-37A methodology. Most of the results agree with field expectations and followed trends that were justifiable based on strain trends predicted by multi-layer linear elastic theory. However, there were a few results that were inconclusive and/or did not follow field expectations. The objective of this section is to show some of the results presented in

previous sections in terms of their predicted service life at specified design criteria rather than in terms of absolute distress magnitude

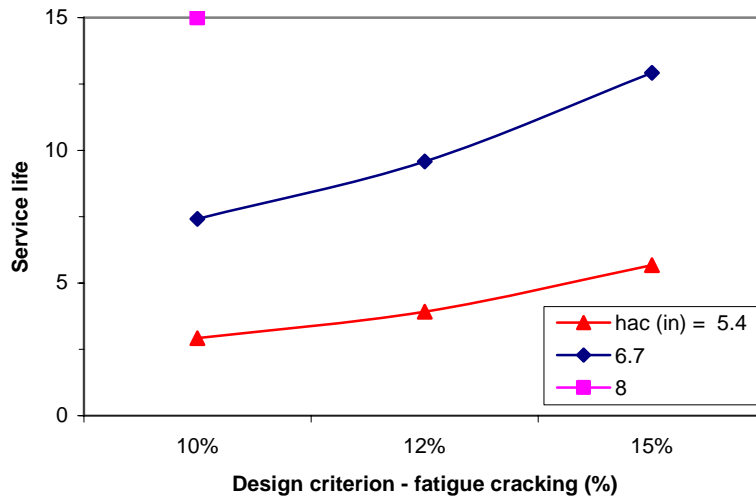
Different design criteria for permanent deformation and fatigue cracking were selected. For permanent deformation, total rut depths of 0.5, 0.6 and 0.7 inches were used to calculate service life for some of the parametric studies reported in previous sections. For fatigue cracking, the criteria were 10, 12 and 15% of total lane area.

The impact of the most significant parameter in each group on service life was evaluated: thickness design (asphalt concrete thickness), traffic (vehicle distribution), environment (Maryland local climate regions), and material properties (binder grade, mixture gradation, and base and subgrade resilient modulus).

Figure 5.28 shows predicted service life versus design criterion for three different asphalt thicknesses. The results for both permanent deformation and fatigue cracking demonstrate that service life is more sensitive in absolute terms—i.e., number of years of service life—at higher design criterion values.



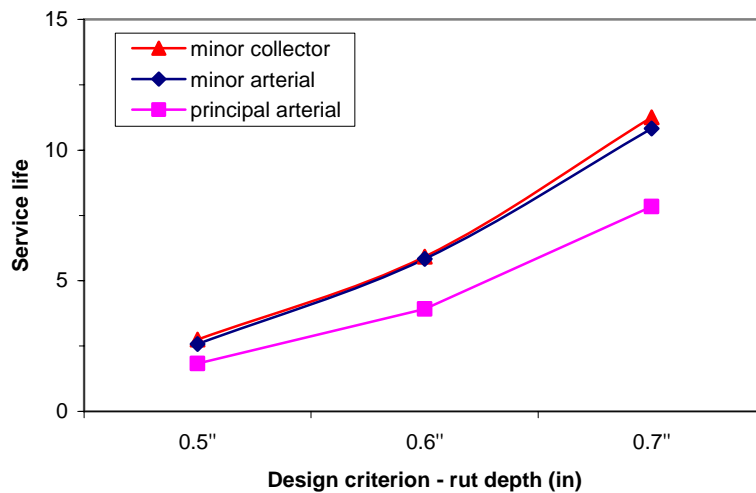
(a)



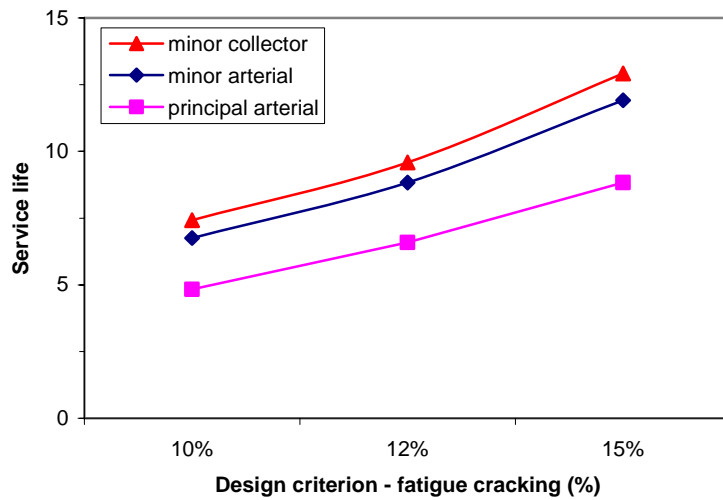
(b)

Figure 5.28. Service life sensitivity to design criterion for different AC thickness: (a) rutting; (b) fatigue cracking.

Figure 5.29 shows the plots of predicted service life versus design criterion for different vehicle distributions. Vehicle distributions commonly used for minor collectors and minor arterials had equivalent impact on service life independent from the design criterion chosen. The impact on service life of vehicle distributions typical of principal arterial roads was more substantial.



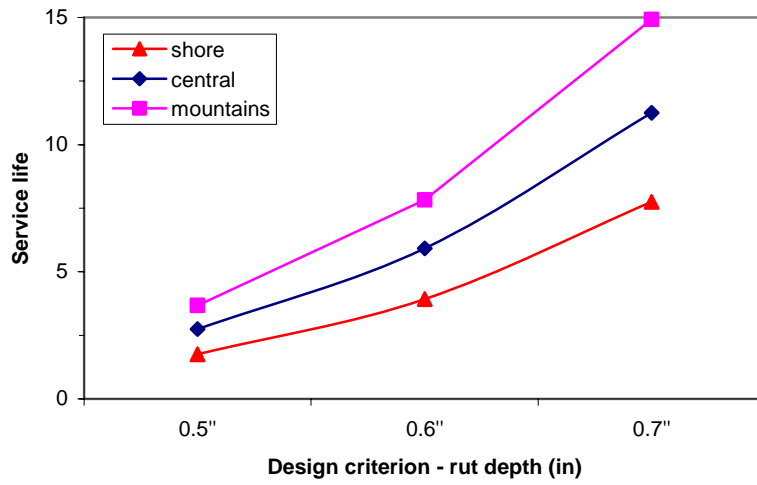
(a)



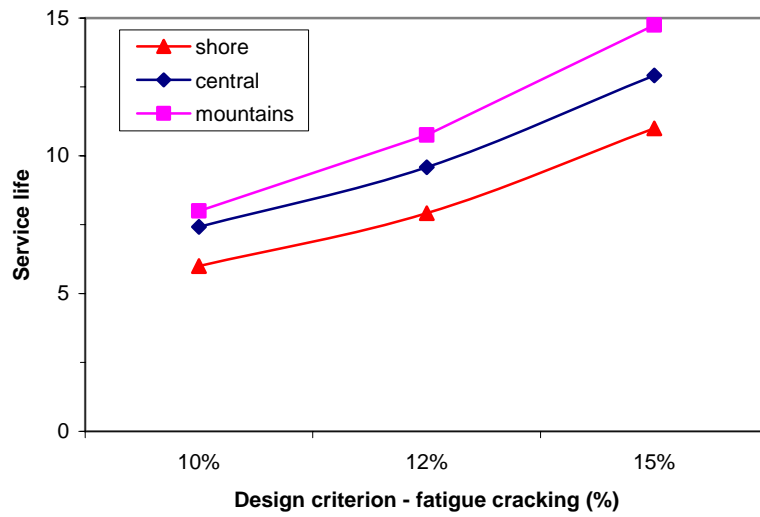
(b)

Figure 5.29. Service life sensitivity to design criterion for vehicle distribution: (a) rutting; (b) fatigue cracking.

Figure 5.30 emphasizes the impact of project location on service life. Three distinct Maryland regions were evaluated and the region with highest average temperature and precipitation (Eastern Shore) had poorer performance than the other two with lower average temperature and precipitation. Because of the common concave-downward asymptotic nature of the predicted distress vs. time curve, especially for rutting, it is easier to observe the sensitivity of project location to performance prediction by plotting service life than the actual distress values. Figure 5.31 shows predicted service life versus design criteria for different binder grades.

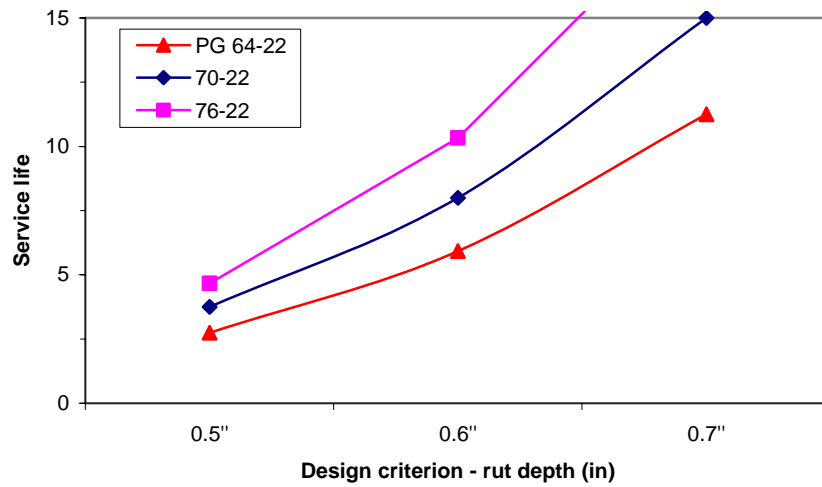


(a)

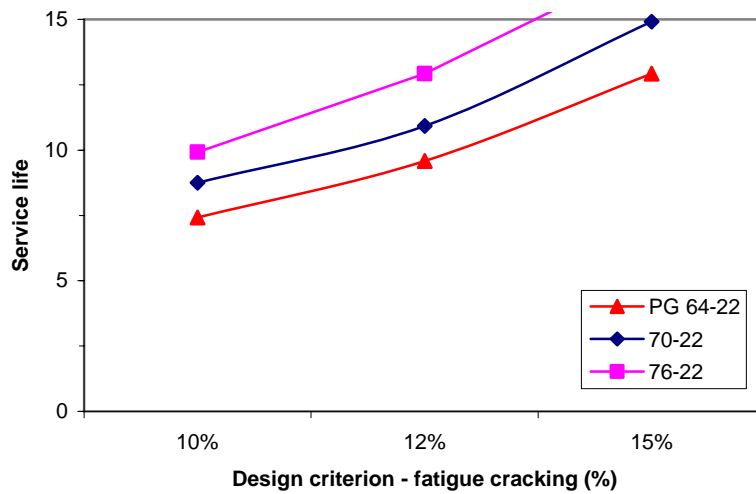


(b)

Figure 5.30. Service life sensitivity to design criterion for MD climate conditions: (a) rutting; (b) fatigue cracking.



(a)

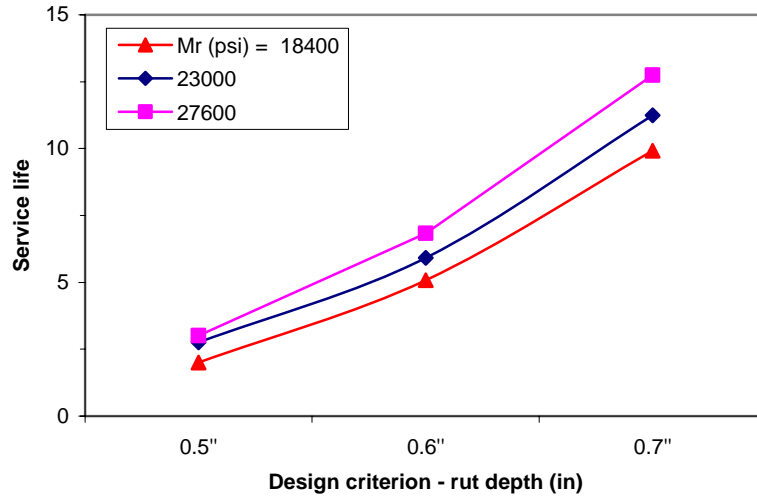


(b)

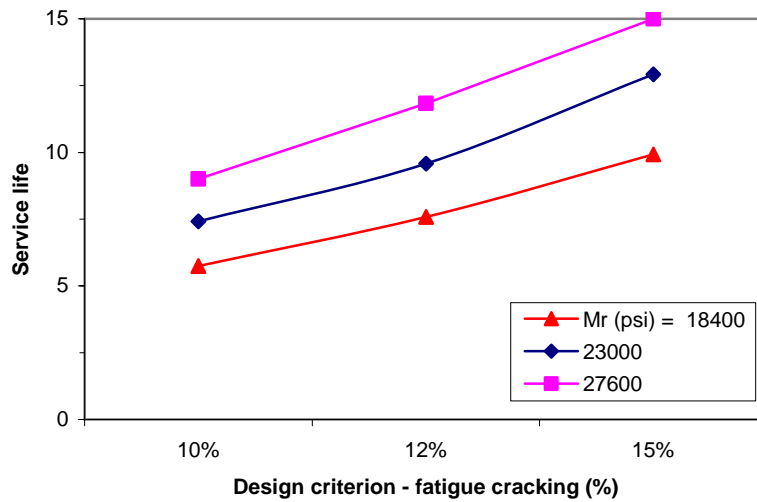
Figure 5.31. Service life sensitivity to design criterion for different binder grade: (a) rutting; (b) fatigue cracking.

Plots of service life versus base and subgrade resilient moduli are shown respectively in Figure 5.32 and Figure 5.33. The plots emphasize the conclusions established in earlier sections. The base resilient modulus has little impact on service life for permanent deformation and significant impact on service life for fatigue cracking. On

the contrary, subgrade resilient modulus has more influence on rutting than fatigue cracking service life, as would be expected.

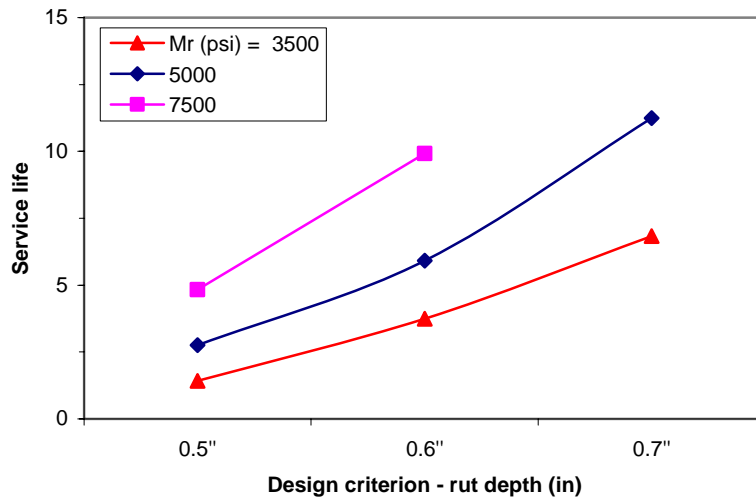


(a)

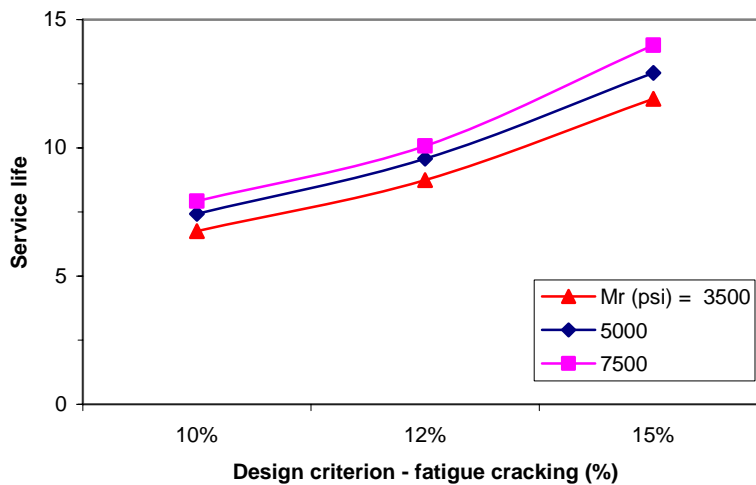


(b)

Figure 5.32. Service life sensitivity to design criterion for different base resilient modulus: (a) rutting; (b) fatigue cracking.



(a)



(b)

Figure 5.33. Service life sensitivity to design criterion for different subgrade resilient modulus: (a) rutting; (b) fatigue cracking.

The results shown in this section simply re-emphasize the conclusions from the previous sections. Due to the shape of the trends of predicted rutting and fatigue cracking, the sensitivity of service life to variations in input parameters is more pronounced than the sensitivity of the absolute distress magnitudes. The design criteria must be selected carefully as they have a direct and significant impact on service life. The NCHRP 1-37A

procedure can be used as an effective tool to evaluate the impact of different input data sets on performance and service life of pavement structures. It can also be used to assess the impact of different design criteria for different road classes and environmental conditions.

Chapter 6: Case Study: Maryland Designs

The application of the NCHRP 1-37A methodology is demonstrated in this chapter. Three Maryland projects provided by the Maryland State Highways Administration (MSHA) were selected for this exercise:

- I-95 at Contee Road
- US-219
- ICC – Inter-County Connector

The objective is to evaluate the NCHRP 1-37A flexible pavement design procedure for typical Maryland conditions and policies. A rehabilitation project was intended as a 4th design that consisted of a new asphalt concrete overlay over a rigid pavement with previous asphalt concrete layers already in place. However, it was not possible to get the NCHRP 1-37A software to run, probably due to the semi-rigid nature of the pavement structure.

The iterative M-E design process shown in Figure 6.1 is divided into 3 distinct parts. Only the input data and analysis were evaluated in this exercise. The input data was provided by MSHA based on their typical data acquisition survey. The initial trial design was defined as the 1993 AASHTO design proposed by the MSHA design team. The pavement structures were all simple 3-layer flexible pavements. Based on findings from the sensitivity study, it was decided that the iterative process would only consider variations in the asphalt concrete thickness.

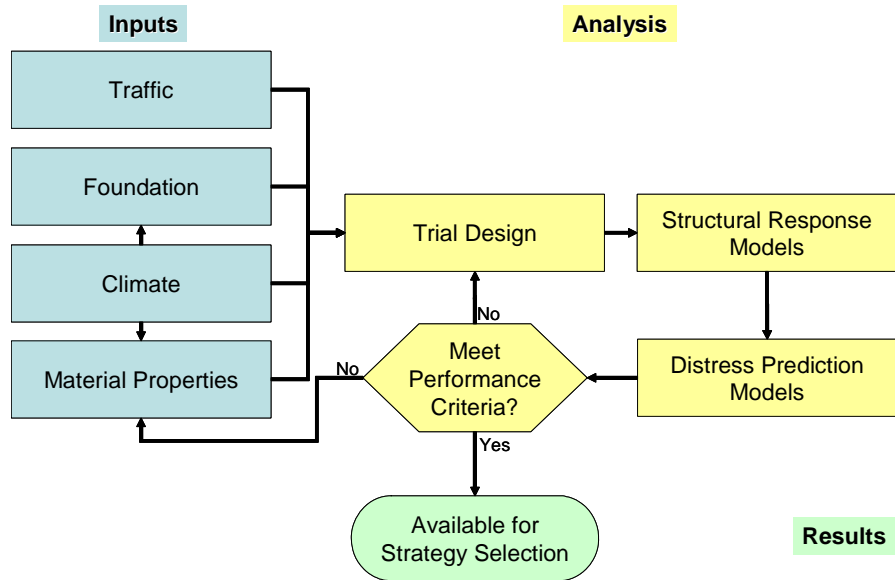


Figure 6.1. M-E flexible pavement design flow chart.

Traffic

Traffic data was provided for all three projects. The I-95 and US-219 projects are expansions of existing alignments and therefore traffic data specifically for these projects were available. The ICC project is a new alignment; measured traffic data was therefore not available. The MSHA provided their best estimates of traffic distribution and growth for the ICC project.

Traffic information included: annual average daily truck traffic (AADTT), trucks in design direction and lane, operational speed, and traffic growth. For the projects with measured data availability, AADTT was obtained from Automated Vehicle Classification (AVC). MSHA default values were used for percentage of trucks in the design direction and lane. The operational speed was adopted as the design operational speed for the project. Table 6.1 presents the general traffic inputs for the three projects.

Table 6.1. Traffic data for case study.

	I-95	US-219	ICC
AADTT	5781	864	7362
Trucks in design direction (%)	50	50	50
Trucks in design lane (%)	80	90	80
Operational speed (mph)	60	60	65
Traffic growth (%)	1.15	2.49	0.07

Weigh-in-motion (WIM) data were provided by MSHA for all three projects. Vehicle class and load distributions were extracted from WIM data. In the case of the ICC project, a WIM station close to the project location was used as reference for the typical load distribution expected for the traffic in that region. The vehicle class distribution for the ICC project was chosen as the default distribution for principal arterials provided in the NCHRP 1-37A procedure. Hourly truck distribution was only available for the US-219 project. For the I-95 and ICC projects, the NCHRP 1-37A default values were used instead.

Figure 6.2 summarizes the vehicle class distribution for the three projects. Since the WIM data were collected for a limited period of time, the load distributions were assumed to be constant throughout the year. Figure 6.3 to Figure 6.5 show the load distribution input for each project.

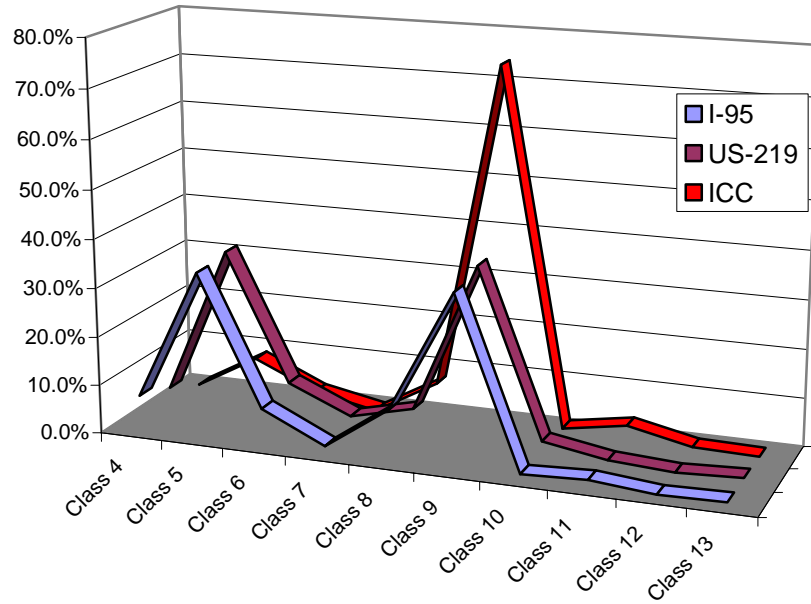


Figure 6.2. Vehicle distribution by project.

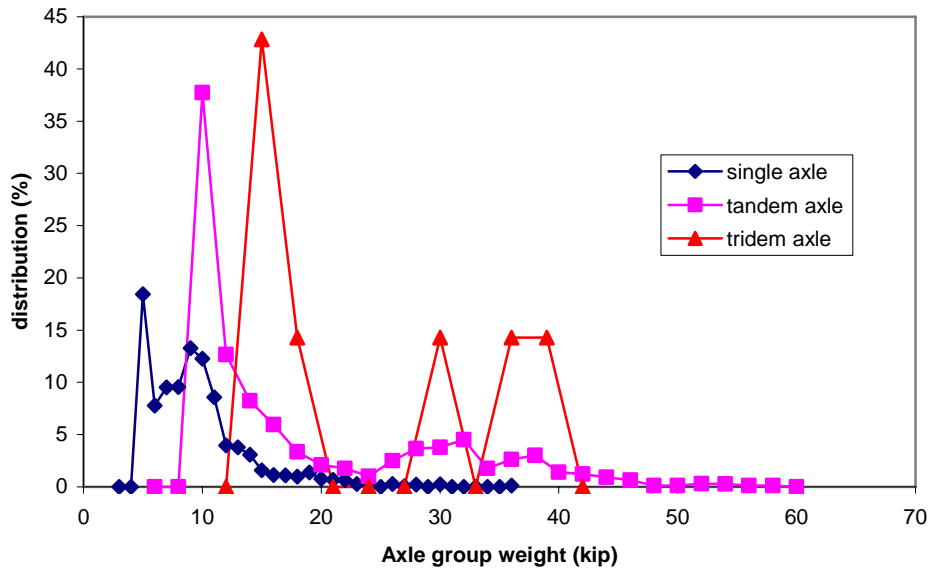


Figure 6.3. Load distribution for the I-95 project.

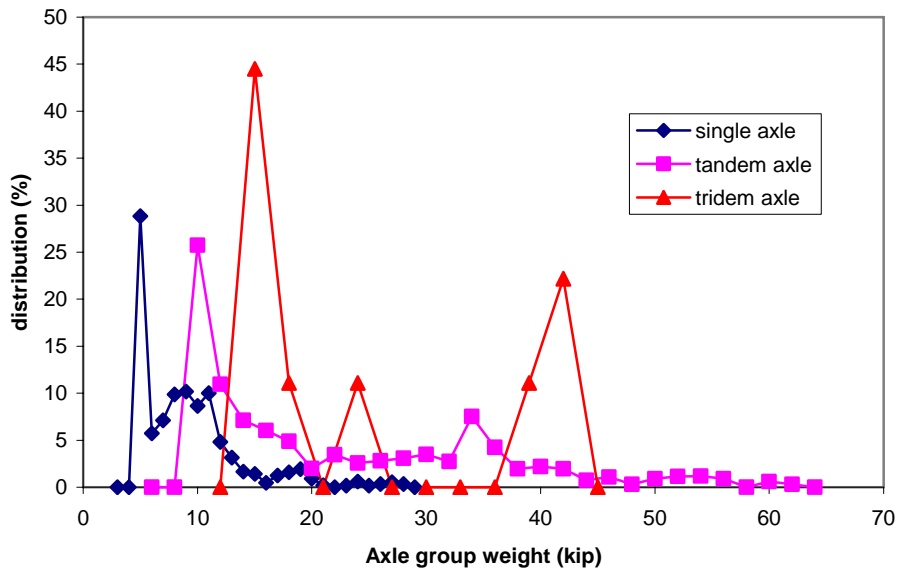


Figure 6.4. Load distribution for the US-219 project.

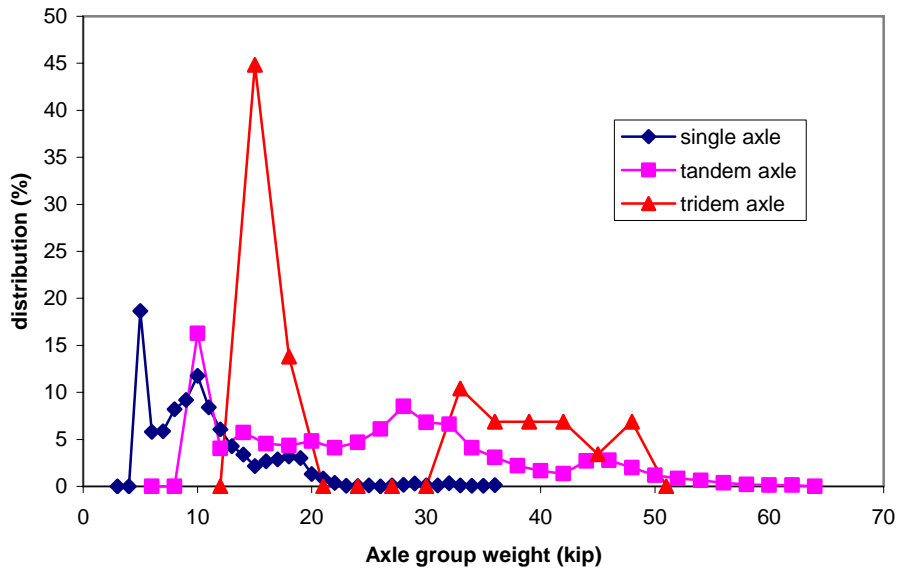


Figure 6.5. Load distribution estimated for the ICC project.

The equivalent traffic volume for the 15-year design period was calculated as input for the 1993 AASHTO designs. The number of ESALs for the I-95, US-219, and ICC projects are, respectively, 11.1 Million, 2.8 Million, and 31.5 Million.

Structure and material properties

All three projects were designed to have the same type of structure: a three-layer flexible pavement system consisting of asphalt concrete surface (AC), granular aggregate base (GAB), and subgrade. The AC and GAB material properties were assumed the same in all projects for simplification and equal to the properties used in the Maryland case presented in the comparison study in section 4.2. Only the subgrade resilient modulus varied from project to project based on data provided by MSHA:

- I-95 at Contee Road Mr = 7,500 psi
- US-219 Mr = 5,000 psi
- ICC – Inter-County Connector Mr = 5,000 psi

Environmental conditions

Three integrated climate model files were generated based on global coordinates of the three projects. The Enhanced Integrated Climate Model (EICM) interpolates climate data from weather stations near the location of the project. The ground water table depth was assumed to be 15 ft.

Reliability and performance criteria

The reliability level for all projects was set at 95% to be consistent to what was used for the 1993 AASHTO designs provided by MSHA. Permanent deformation and “alligator” fatigue cracking were evaluated. The other predicted distresses did not show any significant level of predicted deterioration and were not considered.

Fatigue cracking predictions were very low, varying from 1 to 5% of the total lane area. The fatigue cracking design criterion recommended by the NCHRP 1-37A methodology is 25%. Permanent deformation was the controlling distress for all the designs. The rutting design criterion recommended by the NCHRP 1-37A is 0.75 inches. Two alternative rutting design criteria were considered in this study, 0.5 and 0.6 inches.

Designs

The 1993 AASHTO designs provided by MSHA for the three projects were as follows:

- I-95 at Contee Road
 - Asphalt concrete: 12 inches
 - Granular base: 12 inches
- US-219
 - Asphalt concrete: 9 inches
 - Granular base: 18 inches
- ICC
 - Asphalt concrete: 15 inches
 - Granular base: 15 inches

The state of Maryland has been using Stone Matrix Asphalt (SMA) in its projects for a long time. In all three projects studied, MSHA designed the upper 2 inches of the asphalt concrete to be a SMA mixture. As discussed in Chapter 5, the NCHRP 1-37A methodology is not able to fully capture the benefits of gap-graded mixtures in its current formulation. The alternative adopted to overcome this limitation was to consider the asphalt concrete layer as a full 19mm dense mixture with the same binder grade normally used with SMA mixtures in Maryland (PG 76-22).

Figure 6.6 shows rutting and fatigue cracking predictions for the I-95 project at the end of the design period as a function of asphalt concrete thicknesses. The 1993 AASHTO design (with 12 inches of AC) exhibits a 15-year permanent deformation of approximately 0.6 inches, below the 0.75-inch threshold of the NCHRP 1-37A procedure. If a design criterion of 0.5 inches is to be achieved, a 16-inch asphalt concrete layer would be required. It can be seen from Figure 6.6 that there is not a lot of improvement in performance going from 14 to 16 inches, Fatigue cracking was already at very low levels, so little additional benefit would be expected from additional AC thickness. Most contribution of rutting comes from top 4" of the asphalt concrete layer; in thicker pavements, increasing 2" going from 14 to 16", is not likely to affect rutting much.

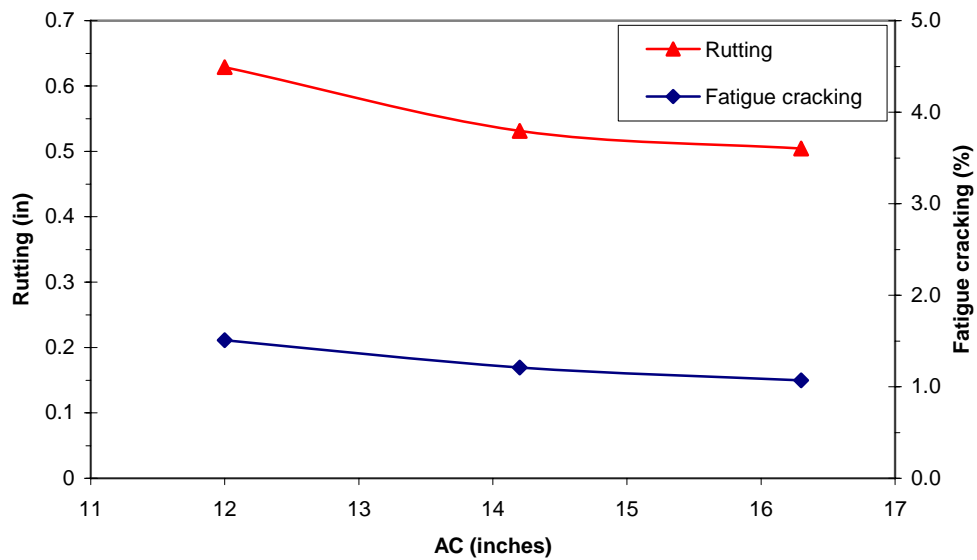


Figure 6.6. I-95 project performance predictions.

Figure 6.7 illustrates the performance predictions for the US-219 project. The rutting prediction for the 1993 AASHTO design (with 9 inches of AC) is 0.6 inches. The design criterion of 0.5 inches can be met with a 12-inch asphalt concrete layer. Figure 6.8 shows the results of rutting and fatigue cracking predictions for the ICC project. The design criterion of 0.6 inches obtained by the 1993 AASHTO design for the two previous projects was only achieved with an AC layer of 19 inches (4 inches more than the AASHTO original design). The threshold of 0.5 inches could not be reached within reasonable variation of the AC thickness. Other techniques—e.g., increasing the mixture stiffness through use of modified binders—would need to be employed to reduce rutting to these low levels under the heavy traffic volume projected for the ICC.

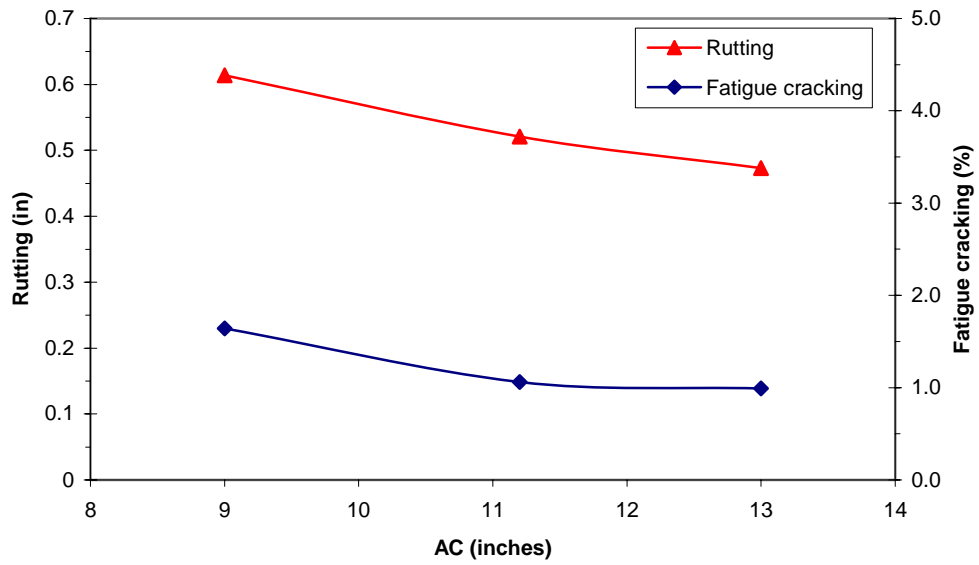


Figure 6.7. US-219 project performance predictions.

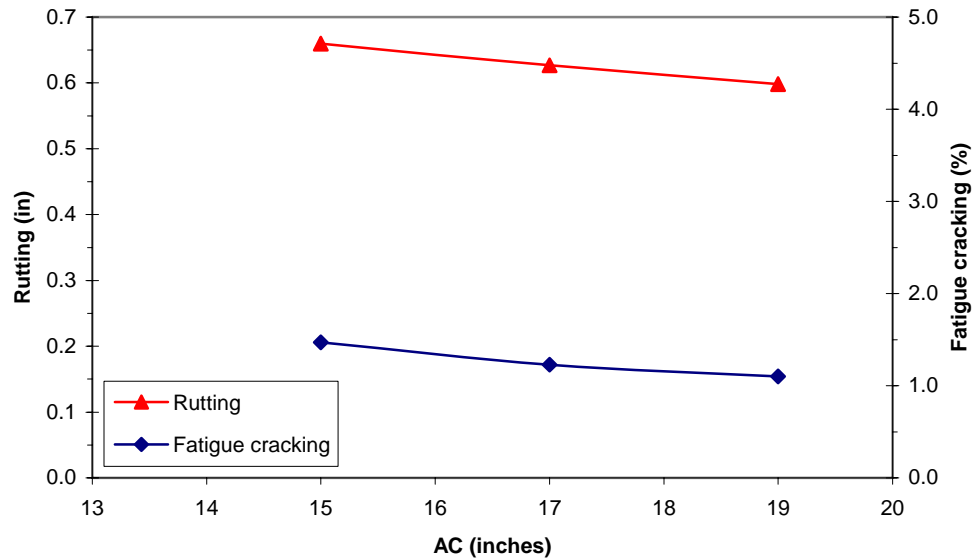


Figure 6.8. ICC project performance predictions.

Additional improvements that could improve performance include improving the quality and strength of the base layer, use of stabilized cement base, or reinforced

subgrade. These alternatives were not attempted so to keep the 3-layer structures comparable to the 1993 AASHTO designs.

Results

The results above confirm the findings of Chapter 4. According to the NCHRP 1-37A methodology, 1993 AASHTO designs are less conservative for high traffic levels (e.g., the ICC project). The number of ESALs of the I-95 project is over 11 million. This result also reinforces one of the findings of Chapter 5 that vehicle class distribution has considerable effect on predicted performance; the vehicle class and load distributions were equivalent of major arterials or interstates (considerable high volume of vehicles class 9). The results indicate that, for this type of road class, ESALs alone may not be a good variable representing traffic for pavement designs.

Based on the results of the I-95 and US-219 projects, it is fair to state that the 1993 AASHTO Guide, for conditions that resemble the traffic characteristics of the AASHO Road Test, provides designs that are compatible with a rutting criterion of 0.6 inches. Table 6.2 to Table 6.4 show a comparative analysis of AC thickness for the two rutting limits.

Table 6.2. I-95 structural designs.

	1993 AASHTO	NCHRP 1-37A	
		0.5''	0.6''
AC	12''	16''	12''
GAB	12''	12''	

Table 6.3. US-219 structural designs.

	1993	NCHRP 1-37A	
	AASHTO	0.5''	0.6''
AC	9''	12''	9''
GAB	18''	18''	

Table 6.4. ICC structural designs.

	1993	NCHRP 1-37A	
	AASHTO	0.5''	0.6''
AC	15''	NA*	19''
GAB	15''	15''	

NA* - Not achievable within reasonable AC thickness variation

The results observed in this exercise using three Maryland projects agree with the findings of the comparative and the sensitivity analysis studies. There seems to be good agreement between the 1993 AASHTO Guide and the NCHRP 1-37A methodology for a rutting criterion of 0.6 inches, when structures are designed for environmental conditions and traffic characteristics that resemble the AASHO Road Test. The 1993 AASHTO designs for high traffic levels are likely to experience premature permanent deformation, according to the NCHRP 1-37A methodology.

Chapter 7: Conclusions

7.1. Summary

This thesis has focused on comparisons between the empirical 1993 AASHTO guide and the mechanistic-empirical NCHRP 1-37A pavement design methodology for flexible pavements. The comparisons were made over a span of different regions around the country. Local input variables were obtained from a survey conducted with State DOTs. This thesis also focused on analyzing the NCHRP 1-37A performance prediction sensitivity to input parameters. The most important variables were considered in the three major groups: traffic, environmental conditions, and material properties. A simple application of the new mechanistic-empirical pavement design guide was also performed via evaluation of three typical pavement projects provided by the Maryland State Highway Administration (MSHA). Solutions from the NCHRP 1-37A methodology were compared with 1993 AASHTO solutions. Throughout the thesis, the implicit assumption is made that “The NCHRP 1-37A predictions are closer to true values than those from the 1993 AASHTO guide.” All observations and conclusions are made in the context of this assumption. The NCHRP 1-37A software version used in all calculations was the version 0.7, released in April, 2004.

7.2. Principal Findings

The evaluations of pavement designs for different regions in the U.S. found that pavement sections designed with the 1993 AASHTO guide for warm temperature states exhibited inferior performance as predicted using the NCHRP 1-37A methodology when

compared to those designed for cold/mild temperature states. This result indicates that, at least according to the NCHRP 1-37A methodology, the 1993 AASHTO Guide overestimates the performance of pavement sections at locations having temperatures warmer than the original AASHTO Road Test site, the basis of the 1993 AASHTO guide.

It was also found that performance predictions deteriorated consistently in all states as traffic levels increased. These results suggest that, according to the NCHRP 1-37A methodology, the 1993 AASHTO guide overestimates pavement performance for traffic levels significantly beyond those experienced in the AASHTO Road Test.

Traffic has always been a source of uncertainty in the 1993 AASHTO design procedure, especially for traffic levels beyond those experienced during the AASHTO Road Test. The AASHTO Road Test was trafficked with fewer than 2 million ESALs, a traffic volume considerably lower than actual traffic on many highways today. The comparison between the AASHTO guide and the NCHRP 1-37A procedure found that, although the pavement structures were designed for the same serviceability loss under the 1993 AASHTO procedure, the variability of performance predictions increased as traffic level increased when these structures were analyzed using the NCHRP 1-37A methodology. This result indicates that, at least according to the NCHRP 1-37A methodology, the 1993 AASHTO designs are less reliable for high traffic and exhibit more uncertainties than those for low traffic levels.

The parametric study of the mechanistic-empirical NCHRP 1-37A methodology provided useful and relevant insights into performance prediction sensitivity to input parameters. Maryland design conditions at low traffic levels were the reference case for the parametric study.

It was found that variations in base thickness had little influence on fatigue cracking and permanent deformation. These results, although surprising from the practical application standpoint, were found to be a direct consequence of the linear elasticity assumption for the pavement materials. Due to the much higher asphalt concrete stiffness, varying the base thickness did not affect the horizontal tensile strain at the bottom of the asphalt concrete layer that controls fatigue cracking. There were small vertical strain reductions in the base layer, but they were counterbalanced by the increase in thickness, which kept the total rutting fairly constant. Overall, the NCHRP 1-37A procedure attributes much less structural capacity contribution to the unbound pavement layers than does the 1993 AASHTO procedure.

Variations of asphalt concrete thickness, on the other hand, were found to have a much more significant impact on performance prediction, which agrees with field expectations. These results suggest that, in the NCHRP 1-37A methodology, the design process is dominated by the asphalt concrete layer.

Traffic data is a fundamental input for pavement design. Results from the comparison study (Chapter 4) indicated that NCHRP 1-37A performance prediction is very sensitive to traffic volume, as expected. In addition, the results from the parametric study (Chapter 5) demonstrated the impacts that vehicle class and load distributions have on performance. The results from the parametric study clearly show that the concept of equivalent traffic is not adequate for representing traffic loading in the NCHRP 1-37A framework for permanent deformation predictions. Results for fatigue cracking predictions were less sensitive to the details of the traffic distribution, suggesting that equivalent traffic may be more suitable for this type of distress, at least for low traffic and

mild environmental conditions. A major advantage of the more sophisticated characterization of traffic in the NCHRP 1-37A methodology is that it can be successfully used to evaluate the impact of overloaded trucks and seasonal traffic on performance; these insights can be used to help define overload penalties and seasonal maximum weight limits.

The evaluation of environmental effect on performance indicated that the NCHRP 1-37A methodology is very sensitive to climate zone. This agrees with field expectations; pavements in warm locations typically exhibit more rutting and, to a lesser extent, more conventional fatigue cracking than do pavements in mild/cold locations⁶. When within-region weather conditions were simulated (i.e., evaluation of three geographical areas in the state of Maryland), the results confirmed that the NCHRP 1-37A methodology remains sensitive to local climate variations. These results agree with expectations.

The most common input variables used to characterize asphalt concrete mixtures (i.e., binder grade, air voids and binder content) and granular base materials (i.e., base and subgrade resilient modulus and subgrade soil type) were also investigated in the parametric sensitivity study. The expected fatigue cracking performance trends agree with the NCHRP 1-37A predictions for the variations in the asphalt concrete material input parameters considered. However, the trends for permanent deformation were not quite so clear, which is less consistent with engineering experience. The effect of mixture volumetrics was also investigated by comparing performance predictions for dense graded against gap-graded (i.e., Stone Matrix Asphalt) mixtures. The NCHRP 1-37A

⁶ Thermal cracking was not considered in this study because it is not an issue at all the locations analyzed. Thermal cracking is important only in cold climates.

performance predictions did not realistically capture the behavior of SMA mixtures. This is particularly problematic for the state of Maryland, which is one of the national leaders in SMA production and placement.

The NCHRP 1-37A fatigue cracking predictions were sensitive to the base layer resilient modulus but relatively insensitive to subgrade resilient modulus. These results agree with physical expectations and with the elastic theory, in which the asphalt concrete/base stiffness ratio is an important factor defining the strain magnitude at the interface between the two layers. Conversely, subgrade resilient modulus had more impact on permanent deformation than the base resilient modulus. Rutting variations with subgrade stiffness are expected; soft subgrades are more likely to experience higher rutting levels than stiff subgrades. These results reinforce the earlier observation that the NCHRP 1-37A methodology is less sensitive to base layer properties than is the 1993 AASHTO procedure.

The parametric sensitivity study suggests how the NCHRP 1-37A methodology can be valuable for determining pay factors for quality control/quality assurance programs in state agencies. As-built construction data can be used as input data to assess post-construction performance as compared to design expectations.

The sensitivity of performance predictions to the empirical model calibrations was also evaluated in the parametric sensitivity study. Predicted performance was found to be very sensitive to small variations of the permanent deformation and fatigue cracking empirical model calibration coefficients. This result suggests the importance of local calibration of the performance prediction models. It is expected that, even within small

regions, different material types (e.g., different asphalt concrete mixtures, subgrade soil types) may have different calibration coefficients.

The sensitivity of service life to the specified design criteria was also investigated. Due to the concave-downward asymptotic shape of the two distress predictions evaluated, the sensitivity of service life to variations in input parameters is quite significant. The use of tolerance levels on acceptable service life should be considered to mitigate the effects of the shape of the prediction models considered in here. With that being stated, it was found that the NCHRP 1-37A procedure can be used as an effective tool to evaluate the impact of different design criteria on performance and service life of pavement structures. This type of evaluation is useful to agencies when defining the design criteria for different road classes and environmental conditions.

The results of the three Maryland projects agreed with the findings of the comparative and the sensitivity studies. The 1993 AASHTO Guide provided structures that satisfied a rutting criterion of 0.6 inches on average, based on NCHRP 1-37A predictions. Similar results were found in pavement sections designed for low traffic and mild/cold climate conditions in the comparative study (South Dakota and Washington State). No significant fatigue cracking was observed in any of the three Maryland designs. This is consistent with reality; cracking is not frequently observed in major Maryland roads, except for reflection cracking in Portland cement concrete pavements having asphalt concrete overlays.

7.3. Implementation Issues

The implementation of the NCHRP 1-37A methodology is a challenging task to state agencies. In addition to the local calibration needed to enhance the effectiveness and accuracy of the empirical performance models, large amounts of input data are required for routine designs. Traffic characterization needs careful assessment; Automated Vehicle Counters (AVC) and Weigh-in-motion (WIM) stations can be used to provide the data required in the NCHRP 1-37A procedure. A database of regional load spectra data by road functional class can be developed as an alternative to project-specific traffic data collection, particularly for less important projects.

Material characterization inputs can also be placed in a database for use in routine designs. As shown consistently in this study, the impact of unbound materials on performance as predicted by the NCHRP 1-37A methodology is less pronounced than the impact of asphalt concrete. Continuing research is needed to better model the behavior of unbound materials in the pavement structure.

To reduce the burden of level 1 material characterization (i.e., laboratory-specific data) at early stages of implementation, level 3 (i.e., correlated material properties or selected from range of typical values) should be considered for all materials, especially for the unbound materials. Asphalt concrete level 3 inputs are easily obtained from mixture volumetrics and gradation. However, given the sensitivity of performance predictions to the asphalt concrete properties, level 1 characterization of typical mixes should be a high implementation priority. Improved asphalt testing equipment (e.g., the Simple Performance Tester developed in NCHRP Project 9-29) will make it easier for agencies to collect level 1 laboratory measured asphalt concrete dynamic moduli in the

future. Unbound resilient modulus can be estimated from material type, at least during the early stages of implementation. For major projects and/or as more expertise is accumulated, samples of granular base materials and subgrade can be tested in the laboratory to determine resilient modulus at optimum density and moisture content, or field FWD data can be used to backcalculate resilient modulus. Databases of material property inputs can be developed for routine design applications.

Continuing research to enhance the NCHRP 1-37A's empirical models is definitely required. Based on engineering judgment of the reasonableness of predictions shown in this thesis and predictions computed by different authors presented in conferences over the past two years, the rutting model was considered the weakest of the two distress models investigated. The rutting model was calibrated without a full set of appropriate field data. Trench data was not available in the LTPP database; consequently, the distribution of rutting over the pavement layers must be estimated in the NCHRP 1-37A software based on limited available trench data from the original AASHTO Road Test, from the MnRoad field experiment, and engineering judgment. Considerable additional research is required to enhance the rutting model; this is currently underway in NCHRP Project 9-30A. The ideal for a more robust rutting model is one based more completely on advanced theory of mechanics that can better capture the deterioration and permanent deformation response of the asphalt concrete and other flexible pavement materials.

Chapter 8: References

- AASHTO. (1972). *AASHTO Interim Guide for Design of Pavements Structures*, American Association of State Highway and Transportation Officials, Washington, DC.
- AASHTO. (1986). *AASHTO Guide for Design of Pavements Structures*, American Association of State Highway and Transportation Officials, Washington, DC.
- AASHTO. (1993). *AASHTO Guide for Design of Pavements Structures*, American Association of State Highway and Transportation Officials, Washington, DC.
- Asphalt-Institute. (1982). *Research and Development of the Asphalt Institute's Thickness Design Manual (MS-1), 9th ed. Research Report 82-2ts*, Asphalt Institute, Lexington, KY.
- Asphalt-Institute. (1991). *Thickness Design - Asphalt Pavements for Highways and Streets. Manual Series No.1 (MS-1)*, Asphalt Institute, Lexington, KY.
- Attoh-Okine, N. O. (2002). "Uncertainty Analysis in Structural Number Determination in Flexible Pavement Design - A Convex Model Approach," *Construction and Building Materials*, Vol. 16, No. 2, pp. 67-71.
- Ayres, M. (1997). *Development of a Rational Probabilistic Approach for Flexible Pavement Analysis*, Ph.D. Dissertation, University of Maryland, College Park, MD.
- Baladi, G. Y., and A. Thomas. (1994). "Mechanistic Evaluation of AASHTO Flexible Pavement Design Equations," *Transportation Research Record 1449*, Washington, DC, pp. 72-78.
- Basma, A. A., and T. I. Al-Suleiman. (1991). "Climatic Considerations in New AASHTO

- Flexible Pavement Design," *Journal of Transportation Engineering*, Vol. 117, No. 2, pp. 210-223.
- Brian, M., and D. G. Zollinger. (1995). "Sensitivity Analysis of Input Parameters for Pavement Design and Reliability," *Transportation Research Record 1482*, Washington, DC, pp. 111-122.
- Claussen, A. I. M., J. M. Edwards, P. Sommer, and P. Udge. (1977). "Asphalt Pavement Design - The Shell Method," *Proceedings of the 4th International Conference on the Structural Design of Asphalt Pavements*, pp. 39-74.
- Coree, B. J., and T. D. White. (1990). "AASHTO Flexible Pavement Design Method: Fact or Fiction," *Transportation Research Record 1286*, Washington, DC, pp. 206-216.
- El-Basyouny, M. M., M. W. Witczak, and S. El-Badawy. (2005). "Verification for the Calibrated Permanent Deformation Models for the 2002 Design Guide," *Proceedings of the Association of Asphalt Pavement Technologists*, Long Beach, CA, pp.
- FHWA. (2001). "Guide to LTPP Traffic Data Collection and Processing," Federal Highway Administration, Washington, DC.
- Gharaybeh, F. A., H. R. Al-massaeid, and M. T. Obaidat. (1998). "Parametric Sensitivity Study of the AASHTO Flexible Pavement Design Equation," *Journal of the Institution of Engineers (India)*, Vol. 78, No. 4, pp. 175-179.
- Haas, R., W. R. Hudson, and J. Zaniewski. (1994). *Modern Pavement Management*, Krieger Publishing Company, Malabar, FL.
- Hajek, J. J. (1995). "General Axle Load Equivalency Factors," *Transportation Research Record 1482*, Washington, DC, pp. 67-78.

- HRB. (1961). "The AASHO Road Test. Special Report 61A - The History and Description of the Project," Highway Research Board, National Academy of Sciences - National Research Council, Washington, DC.
- HRB. (1962). "The AASHO Road Test. Report 5 - Pavement Research," Highway Research Board, National Academy of Sciences - National Research Council, Washington, DC.
- HRB. (1962). "The AASHO Road Test. Report 7 - Summary Report," Highway Research Board, National Academy of Sciences - National Research Council, Washington, DC.
- Huang, Y. H. (2004). *Pavement Analysis and Design*, Prentice-Hall, Upper Saddle River, NJ.
- Kaloush, K. E. (2001). *Simple Performance Test for Permanent Deformation of Asphalt Mixtures*, Ph.D. Dissertation, Arizona State University, Tempe, AZ.
- Kansas-State-Highway-Commision. (1947). "Design of Flexible Pavement Using the Triaxial Compression Test," *Highway Research Board*, Vol. Bulletin 8, No., pp.
- Lavin, P. (2003). *Asphalt Pavements*, Spon Press, New York, NY.
- Leahy, R. B. (1989). *Permanent Deformation Characteristics of Asphalt Concrete*, Ph.D. Dissertation, University of Maryland, College Park, MD.
- NCHRP. (2004). *Mechanistic-Empirical Design of New and Rehabilitated Pavement Structures*, National Cooperative Highway Research Program, NCHRP Project 1-37A, National Research Council, Washington, DC.
- Newcomb, D. A., and B. Birgisson. (1999). "Measuring In Situ Mechanical Properties of Pavement Subgrade Soils," NCHRP Synthesis 278, Transportation Research Board, Washington, D.C.

- Noureldin, A. S., R. B. Leahy, and J. R. Lundy. (1996). "Development of Temperature Coefficients for the AASHTO Flexible Pavement Design Equation," *Proceedings of the Association of Asphalt Paving Technologists*, St. Louis, MO, pp. 300-320.
- Richardson, D. N. (1996). "AASHTO Layer Coefficients for Cement-Stabilized Soil Bases," *Journal of Materials in Civil Engineering*, Vol. 8, No. 2, pp. 83-87.
- Richardson, D. N. (2001). "AASHTO Drainage Coefficients for Flexible Pavements," *Transportation Research Record 1778*, Washington, DC, pp. 73-80.
- Saraf, C. L., G. J. Ilves, and M. Kamran. (1995). "Effect of Heavy Vehicle Weights on Pavement Performance," *4th International Symposium on Heavy Vehicle Weights and Dimensions*, Ann Arbor, MI, pp. 253-261.
- Sebaaly, P. E., and N. Tabatabaee. (1992). "Effect of Tire Parameters on Pavement Damage and Load-Equivalency Factors," *Journal of Transportation Engineering*, Vol. 118, No. 6, pp. 805-819.
- Shook, J. F., F. N. Finn, M. W. Witzak, and C. L. Monismith. (1982). "Thickness Design of Asphalt Pavements - The Asphalt Institute Method," *Proceedings of the 5th International Conference on the Structural Design of Asphalt Pavements*, pp. 17-44.
- Tseng, K., and R. Lytton. (1989). "Prediction of Permanent Deformation in Flexible Pavement Materials. Implication of Aggregates in the Design, Construction, and Performance of Flexible Pavements," *ASTM*, Vol. STP 1016, No., pp. 154-172.
- Witzak, M. W. (2004). "Assessment of the Allowable Threshold Rut Depths by Layers in Asphalt Pavement Systems," Transportation Research Board, NCHRP 9-19, National Cooperative Highway Research Program, Washington, D.C.
- Zaghloul, S., and T. White. (1994). "Load equivalency Factors for Asphalt Pavements,"

Proceedings of the Association of Asphalt Paving Technologists, St. Louis, MO, pp. 481.

Zhang, Z., J. P. Leidy, I. Kawa, and W. R. Hudson. (2000). "Impact of Changing Traffic Characteristics and Environmental Conditions on Flexible Pavements," *Transportation Research Record 1730*, Washington, DC, pp. 125-131.